**An In Vitro Model of the Brain Tissue Reaction to Chronically Implanted Recording Electrodes Reveals Essential Roles for Serum and bFGF in Glial Scarring**

by

Vadim Steven Polikov

Department of Biomedical Engineering
Duke University

Date:_____

Approved:

_____
William "Monty" Reichert, PhD, Committee Chair

_____
Jau-Shyong Hong, PhD

_____
Bruce Klitzman, PhD

_____
Sidney Simon, PhD

_____
Patrick Wolf, PhD

Dissertation submitted in partial fulfillment of
the requirements for the degree of Doctor
of Philosophy in the Department of
Biomedical Engineering in the Graduate School
of Duke University

2009

ABSTRACT

An In Vitro Model of the Brain Tissue Reaction to Chronically Implanted Recording Electrodes

Reveals Essential Roles for Serum and bFGF in Glial Scarring

by

Vadim Steven Polikov

Department of Biomedical Engineering
Duke University

Date:_____
Approved:

_____
William "Monty" Reichert, PhD, Committee Chair

_____
Jau-Shyong Hong, PhD

_____
Bruce Klitzman, PhD

_____
Sidney Simon, PhD

_____
Patrick Wolf, PhD

An abstract of a dissertation submitted in partial
fulfillment of the requirements for the degree
of Doctor of Philosophy in the Department of
Biomedical Engineering in the Graduate School
of Duke University

2009

# Abstract

Chronically implanted recording electrode arrays linked to prosthetics have the potential to make positive impacts on patients suffering from full or partial paralysis [1;2]. Such arrays are implanted into the patient's cortical tissue and record extracellular potentials from nearby neurons, allowing the information encoded by the neuronal discharges to control external devices. While such systems perform well during acute recordings, they often fail to function reliably in clinically relevant chronic settings [3]. Available evidence suggests that a major failure mode of electrode arrays is the brain tissue reaction against these implants (termed the glial scar), making the biocompatibility of implanted electrodes a primary concern in device design. Previous studies have focused on modifying the form factor of recording arrays, implanting such arrays in experimental animals, and, upon explantation, evaluating the glial scarring in response to the implant after several weeks in vivo. Because of a lack of information regarding the mechanisms involved in the tissue reaction to implanted biomaterials in the brain, it is not surprising that these in vivo studies have met with limited success. This dissertation describes the development of a simple, controlled in vitro model of glial scarring and the utilization of that model to probe the cellular and molecular mechanisms behind glial scarring.

A novel in vitro model of glial scarring was developed by adapting a primary cell-based system previously used for studying neuroinflammatory processes in neurodegenerative disease [4]. Midbrains from embryonic day 14 Fischer 344 rats were mechanically dissociated and grown on poly-D-lysine coated 24 well plates to a confluent layer of neurons, astrocytes, and microglia. The culture was injured with either a mechanical scrape or foreign-body placement (segments of

50 mm diameter stainless steel microwire), fixed at time points from 6 h to 10 days, and assessed by immunocytochemistry. Microglia invaded the scraped wound area at early time points and hypertrophied activated astrocytes repopulated the wound after 7 days. The chronic presence of microwire resulted in a glial scar forming at 10 days, with microglia forming an inner layer of cells coating the microwire, while astrocytes surrounded the microglial core with a network of cellular processes containing upregulated GFAP. Neurons within the culture did not repopulate the scrape wound and did not respond to the microwire, although they were determined to be electrically active through patch clamp recording.

This initial model recreated many of the hallmarks of glial scarring around electrodes used for recording in the brain; however, the model lacked the reproducibility necessary to establish a useful characterization tool. After the protocol was amended to resemble protocols typically used to culture neural stem/precursor cells, an intense scarring reaction was consistently seen [5]. To further optimize and characterize the reaction, six independent cell culture variables (growth media, seeding density, bFGF addition day, serum concentration in treatment media, treatment day, and duration of culture) were varied systematically and the resulting scars were quantified. The following conditions were found to give the highest level of scarring: Neurobasal medium supplemented with B27, 10% fetal bovine serum at treatment, 10 ng/ml bFGF addition at seeding and at treatment, treatment at least 6 days after seeding and scar growth of at least 5 days. Seeding density did not affect scarring as long as at least 500,000 cells were seeded per well, but appropriate media, bFGF, and serum were essential for significant scar formation.

The optimized in vitro model was then used to help uncover the underlying molecular and cellular mechanisms behind glial scarring. A microwire coating that mimics the basal lamina present within glial scars was developed that allows cells responding to the coated microwire to be isolated and evaluated (i.e. through cell counting or cell staining). A panel of soluble factors known to be involved in glial scar formation was added to the media and the cellular response was recorded. The extent of cell accumulation on the coated microwires was significantly increased by titration of the culture with serum, the pleotropic growth factor bFGF, the inflammatory cytokines IL-1β and IL-1α, and the growth factors PDGF and BMP-2. The other fourteen soluble factors tested had little to no effect on the number of cells that attached to the coated microwires, although a specific blocker of the bFGF receptor was able to abrogate the effect of bFGF. This study proposes essential roles in glial scarring of serum, which infiltrates brain tissue upon disruption of the blood-brain barrier, and bFGF, which is a necessary growth and survival factor for the neural precursor cells that respond to injury. These insights suggest repeated rounds of implant micromotion-induced cellular damage, with the resultant neuronal death, serum release, and bFGF deposition may thicken the glial scar and lead to recording signal loss.

# Dedication

*To my parents and grandparents. I would not have finished without you.*

# Contents

# List of Tables

# List of Figures

# List of Terms and Abbreviations

| | |
|---|---|
| A2B5 | Antigen expressed on the surface of one population of neural precursor cells |
| ANOVA | Analysis of Variance |
| BBB | Blood-Brain Barrier |
| BDNF | Brain Derived Neurotrophic Factor |
| bFGF | Basic Fibroblast Growth Factor |
| BMP-2 | Bone Morphogenic Protein 2 |
| BMP-4 | Bone Morphogenic Protein 4 |
| CNS | Central Nervous System |
| CNTF | Cilliary Neurotrophic Factor |
| DAPI | 4',6-diamidino-2-phenylindole |
| DAPT | N-[(3,5-Difluorophenyl)acetyl]-L-alanyl-2-phenyl]glycine -1,1-dimethylethyl ester |
| db-CAMP | N6,2'-0-dibutyryladenosine 3'5'-cyclic monophosphate sodium |
| Dex | Dexamethasone |
| DMEM | Dulbecco's Modified Eagle Medium |
| ECM | Extracellular Matrix |
| ED-1 | Antibody that recognizes CD68 protein in microglia |
| FBS | Fetal Bovine Serum |
| GFAP | Glial Fibrillary Acidic Protein |
| H&E | Hemotoxylin and Eosin |
| HFM | Hollow Fiber Membranes |
| HS | Horse Serum |
| IBA-1 | ionized calcium-binding adaptor molecule 1 (Molecule expressed in microglia) |

| | |
|---|---|
| IFN-γ | Interferon Gamma |
| IL-10 | Interleukin-10 |
| IL-1α | Interleukin-1 alpha |
| IL-1β | Interleukin-1 beta |
| IL-6 | Interleukin-6 |
| LIF | Leukemia Inhibitory Factor |
| LPS | Lipopolysaccharide |
| MAC-1 | Integrin antigen on microglia, also called CD11b/CD18, recognized by the OX-42 antibody |
| MAP-2 | Microtubule associated protein 2, a stain for mature neuron processes |
| MCP-1 | Monocyte chemoattractant protein-1 |
| MEM | Minimal Essential Medium |
| MIP-1α | Macrophage inflammatory protein-1 alpha |
| NB | Neurobasal |
| NCAM | Neural Cell Adhesion Molecule |
| NeuN | Marker for Neuron Soma |
| NF | Neurofilament |
| NG2 | Chondroitin Sulphate proteoglycan expressed on the surface of one population of neural precursor cells |
| NGF | Neural Growth Factor |
| NPC | Neural Precursor Cell |
| NT-3 | Neurotrophin 3 |
| OX-42 | Antibody recognizing the MAC-1 integrin antigen on microglia, also called |

| | |
|---|---|
| | CD11b/CD18 |
| PBS | Phosphate Buffered Saline |
| PDGF | Platelet Derived Growth Factor |
| PNS | Peripheral Nervous System |
| RGD | Arginine-Glycine-Aspartic acid |
| SNR | Signal to noise ratio |
| TGF-β | Transforming Growth Factor Beta |
| TNF-α | Tumor Necrosis Factor Alpha |
| UEA | Utah Electrode Array |
| Vim | Vimentin |

# Acknowledgements

Sincere thanks to my committee for their feedback and support. Special thanks to Monty for giving me the freedom to pursue my interests, even when they were different than his own. I could not have asked for a better advisor. None of this could have happened without the support of Dr. Hong, who opened up his lab to me for five years without asking for anything in return. I hope I was able to contribute in some way to your lab. My teacher and guide at the bench was Dr. Michelle Block, without whom I would have never attempted primary cell culture. I hope VCU realizes what kind of extraordinary researcher they added to their faculty. Thank you to my labmates, who put up with my annoying questions at lab meetings, my friends at grad school, who made grad school fun, and Hannah, who makes life fun. Finally, thank you to my family, without whom I would have quit on the Ph.D. a long time ago.

# Chapter 1: Specific Aims

## *1.1 Significance*

Chronically implanted recording electrode arrays linked to prosthetics have the potential to make positive impacts on patients suffering from full or partial paralysis [1;2]. Such arrays are implanted into the patient's cortical tissue and record extracellular potentials from nearby neurons, allowing the information encoded by the neuronal discharges to control external devices. While such systems perform well during acute recordings, they often fail to function reliably in clinically relevant chronic settings [3]. Available evidence suggests that a major failure mode of electrode arrays is the brain tissue reaction against these implants (termed the glial scar), making the biocompatibility of implanted electrodes a primary concern in device design. Previous studies have focused on modifying the form factor of recording arrays, implanting such arrays in experimental animals, and, upon explantation, evaluating the glial scarring in response to the implant after several weeks in vivo. Because of a lack of information regarding the mechanisms involved in the tissue reaction to implanted biomaterials in the brain, it is not surprising that these in vivo studies have met with limited success. By developing a simple, controlled in vitro model of glial scarring and utilizing the model to probe the cellular and molecular mechanisms behind glial scarring, electrode designers will be able to more effectively engineer chronically stable implantable recording electrodes.

## *1.2 Hypothesis*

It is proposed that an in vitro model can be developed that 1) mimics many of the hallmarks of glial scarring observed in vivo and 2) provides useful mechanistic information to better understand this biological response to implanted materials in the brain.

## *1.3 Experimental Approach*

Primary cell cultures derived from embryonic day 15 (E15) rat midbrain were used as the basis for an in vitro model of glial scarring. The cell culture can re-create many of the stereotypical tissue reactions to implanted recording electrodes after a scrape wound, where a portion of the confluent layer of cells is scraped off and cells are allowed to migrate back in, or after a mock microwire implantation, where small segments of stainless steel microwire are placed on top of the cell layer. The cellular reaction can be visualized by staining for cell-specific markers to identify the neurons, astrocytes, microglia, and precursor cells reacting to either the scrape or the microwire "injuries" in culture. The density of astrocyte protein GFAP (upregulated within wounds) around the microwire, or the number of cells migrating to and accumulating on an ECM-hydrogel coating around the microwire, can be quantified to obtain a quantitative measure of scarring in the culture. The effects of various culture conditions and bioactive molecules on the size of the scar are examined to probe the molecular and cellular signals that affect glial scar formation.

## *1.4 Specific Aims*

**Specific Aim 1: Develop and characterize an in-vitro model of glial scarring**

A set of stereotypical characteristics of the in vivo reaction to recording electrodes implanted chronically in the brain was used as a basis for designing an in vitro system. Because the in vivo environment contains a variety of cell types participating in the deleterious tissue reaction, a primary culture with physiologically relevant proportions of astrocytes, microglia, and neurons was used. Cultures were evaluated by immunocytochemistry to identify the relative proportions, locations, and behavior of the various cell types in culture. Neuronal health was evaluated with patch clamp recordings. The culture's reaction to a scraping off of a portion of the confluent cellular layer over the course of several days generated a model of mechanical injury in the brain. The culture's reaction to short segments of stainless steel microwire generated a model of glial scarring around a foreign body.

**Specific Aim 2: Optimize the glial scarring model developed in Specific Aim 1 to consistently generate a glial scar in vitro**

The various parameters involved in generating the in vitro model were modified to obtain the greatest amount of scarring around a microwire in the highest possible proportion of experiments. This was necessary to develop a strong, reliable positive control to then allow further exploration of the mechanisms leading to glial scarring. Parameters optimized included the growth media, the seeding density, bFGF (a growth factor) added to the media, the serum concentration in the treatment media, the treatment day, and the duration of the culture. Because the glial scar is defined by an upregulation of GFAP in "activated" astrocytes around an implant, the relative amount of scarring around each microwire was quantified with a Matlab program that sums the higher-than background amount of GFAP staining around the microwire in culture.

**Specific Aim 3: Investigate the effect of various soluble factors on glial scar formation within the in vitro model of glial scarring optimized in Specific Aim 2.**

The in vitro model developed in Specific Aim 1 and optimized in Specific Aim 2 was used to help uncover the underlying molecular and cellular mechanisms behind glial scarring. A microwire coating that mimics the basal lamina present within glial scars was developed that allows cells responding to the coated microwire to be isolated and evaluated (i.e. through cell counting or cell staining). This coating can be used to incorporate and elute active proteins, as well as investigate the effect of various extracellular matrix components on glial scar formation. A panel of soluble factors known to be involved in glial scar formation was added to the media and the cellular response was recorded, allowing mechanistic insights into glial scar formation.

# Chapter 2: Background

## *2.1 Introduction*

Reports that monkeys accurately and reproducibly controlled a robotic arm via chronically implanted cortical electrodes rekindled the hope of approximately 200,000 patients suffering from full or partial paralysis in the U.S. [6-8]. The implants, made out of dozens of wire electrodes, sampled extracellular potentials from portions of the monkeys' cortex (Figure 1). The potentials recorded from neurons adjacent to the electrodes were correlated to observed physical motion, eventually allowing the researchers to translate the neuronal activity directly into robotic arm movements. Because of the length of time required for training and the eventual clinical necessity of a long-term brain-machine interface, the implants were chronic, that is they were permanently implanted into the monkeys' brains.

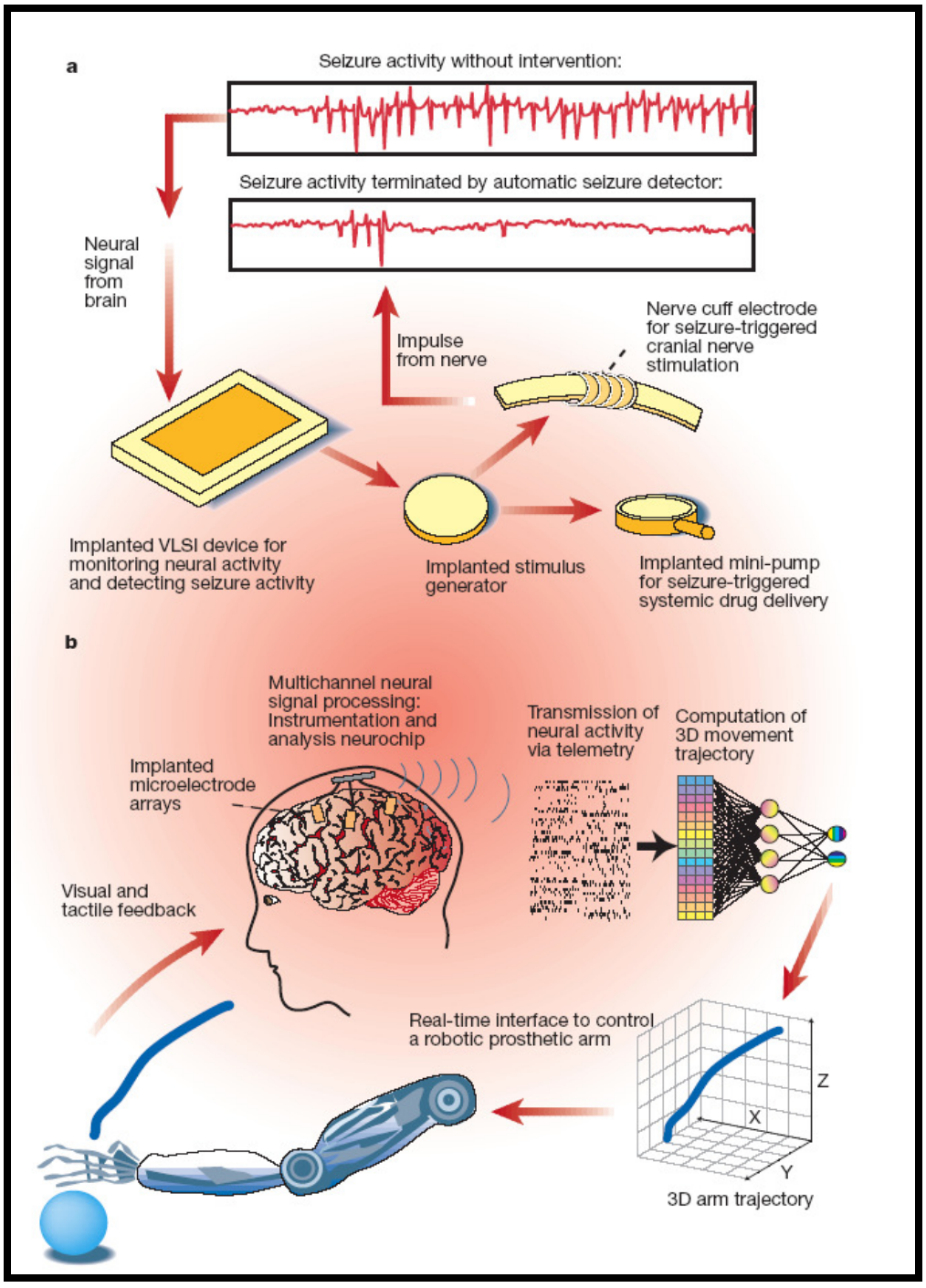


**Figure 1: Applications of Brain-Machine Interfaces. Schematic description of two potential applications of brain-machine interfaces. a, A "brain pacemaker" that monitors neural activity to detect seizures. When seizures activity is detected, the implant sends a signal to a nerve cuff electrode or a mini-pump for drug delivery to stop the seizures. b. Electrode arrays sample the activity of large populations of neurons to control the movements of a prosthetic arm. From [7]**

The purpose of these implanted devices is to record signals with high signal to noise ratios (SNR) from as many individual neurons, termed single units, as possible. Single units must be separated from the background electrical noise and from the overlapping signals, or multi-unit potentials, of other nearby neurons. Principle component analysis and other signal processing techniques can be used to separate single units from noise and multi-unit potentials [9], with a target SNR for recordings around 5:1 [10;11].

With the successes reported in the both the scientific literature[6-8] and the popular press (e.g. http://msnbc.msn.com/id/6989239/) of thought-controlled arm motion in primates it would appear anecdotally that the technology is close to broad human implementation [12]. A number of engineering groups have developed multi-channel recording electrode arrays for chronic applications. These designs span several different technologies, including microwires [13;14], polymers [10] and different types of silicon micromachined implants [15;16]. The basic sensor and instrumentation requirements of such neural implant systems are well established, and in general the present designs perform as intended in short term studies.

However, to those familiar with the problems encountered by the different laboratories implanting animals with these electrode arrays, it is clear that the instability of the brain-electrode interface is the single most important barrier between experimental animal work and human clinical application. The basic strategy is to implant multiple electrodes in a single procedure in the hope that enough of them remain functional for the required period of time. In 2004, University of Pittsburgh neurobiologist Andrew Schwartz published a frank and comprehensive

assessment of the state of thought-controlled robotics research [17]. Therein, he noted that each laboratory reporting successful results can point to an "all-star" animal that provided the prolonged stable neuronal signals needed to complete the necessary training. Schwartz further estimated that 40-60% of electrodes are capable of recording a signal upon implantation, and few, if any, maintain those recordings for more than a few months. Although failures are hardly ever reported, in general, current recording electrode designs do not perform consistently in clinically relevant chronic implantations. In June 2007, Cyberkinetics, Inc stopped funding the only clinical study initiated to date to evaluate the use of recording arrays for paralyzed patients after the company experienced significant signal stability problems in each of the four patients enrolled in the study [12;18]. This failure was a powerful reminder of the different requirements of a chronic brain implant suitable for use in basic research and the reliability threshold needed for clinically relevant neuroprosthetics. For clinical applications, implanted microelectrode arrays intended as control and communication interfaces need to record unit activity for time periods on the order of decades [19] and must have a substantially high performance reliability.

While this is a well known problem in the field, recording stability problems are seldom reported in the literature because data from the "all-star animal" or "all-star electrode" is easier to publish. Still, evidence of the issue can be found in several published studies. Nicolelis et al. reported a 40% drop in the number of functional electrodes between 1 and 18 months [20]. Only 7 of 11 electrode shafts in Rousche and Normann's implanted array recorded signals at implantation, and the number of electrodes recording signals dropped to 4 of 11 after 5 months [21]. In a study by Williams et al., 8 cats were implanted with microwire electrode arrays and electrical activity was recorded over time [13]. Three of the electrode arrays failed within the first 15 weeks, presumably due to the tissue reaction and loosening of the skull cap used to keep the electrode in

place. The other electrode arrays remained active until the cats succumbed to unrelated medical complications between 15 and 25 weeks post implantation. Liu et al. found a large amount of variation in the stability of neural recordings between different electrode shafts on the same array and between arrays implanted in different cats [22]. Most neuronal recordings in the study either grew in stability until day 80 post implantation, after which the recording remained stable, or degenerated from a high stability to nearly no signals around 60 days post implantation.

## *2.2 Tissue Response to Electrode-Like Implants in the Brain*

Available studies suggest that the greatest challenge to obtaining consistent or stable intracortical recordings is the biological response that the brain mounts against implanted electrodes. In order to design recording electrodes that minimize or evade the tissue response of the central nervous system (CNS), it is necessary to understand the biological mechanisms involved. The following section provides an overview of the CNS tissue response to implanted needle-like materials, a topic that has been reviewed in other contexts previously in [23] and [24].

### 2.2.1 How the Tissue Response is Measured

The literature reflects a concerted effort to identify and characterize the changing temporal characteristics of the foreign body response in the CNS. The most common method to assess the tissue response is to implant model probes into test animals and sacrifice the animals at various time points to evaluate the probe and adjacent neural tissue. Direct evidence linking tissue response to device performance, however, has not been studied extensively. The majority of available evidence is derived from studies that examine the brain tissue response to passive or

non-functional implants. Because biocompatibility is a functional characteristic, which strictly speaking requires an analysis of tissue response using an electrically functional implant, the effect of the tissue response on device function is mostly inferred.

In general, electrodes are removed following tissue fixation and the excised tissue surrounding the implant is sectioned and stained to identify cell numbers, locations, types, and byproducts. For the most part, the results are subjective, consisting of a description of a particular stain in comparison to adjacent, uninjured tissue from a few selected sections with the number of animals per time point and number of sections analyzed varying considerably from study to study. A few studies have examined the explanted electrodes with histological methods [25-27]. Most of the histological studies have focused on the astrocyte response, and less so on the microglial, neural precursor cell, or neuronal response.

Early studies relied on Hemotoxylin and Eosin (H&E) to determine the location of neurons and other relevant cell types relative to the implant [28], although H&E is not a cell type specific stain. To gain more specificity, immunostaining for cell type specific proteins such as GFAP for astrocytes, and NeuN or MAP-2 for neurons is used to localize cells and to determine their state of activation [29]. Following activation, microglial cells exhibit increased expression of certain leukocyte-associated molecules, including CD68 (recognized by the ED1 antibody) and Mac-1/CD11b (recognized by the OX-42 antibody), or of various lectins [30]. A stain for vimentin, an intermediate filament expressed in reactive astrocytes, immature cells, microglia, and perivascular cells, can also be employed [31] although specificity is lost. To test the brain's response to acute injury, as opposed to chronic implantation, the implant can be removed soon

after implantation, or merely used to create the initial insertion injury without actual implantation [25;32].

Although staining allows for the identification of reactive cells around an implant, other methods have been used to examine the extracellular environment. Microdialysis sampling allows the user to assess the chemical environment surrounding the implant without the presence of confounding cells [33]. The dialysis membrane can be adjusted to pass only certain molecular weight compounds, and the collected dialysate is then tested (often through an immunoassay) to determine the presence of different compounds in question. In a modification of the microdialysis sampling paradigm, hollow fiber membranes (HFM) of poly(acryloniterile-vinyl chloride) (PAN-PVC) have been implanted to mimic electrodes [34]. The foreign body response around an HFM implant is then characterized by immunostaining for cells and testing extracellular milieu collected from the hollow inner compartment. Finally, others have studied the neural tissue response to implants using hippocampal slice cultures grown on porous membranes or on silicon chips with recording capabilities with variable success [35;36].

### 2.2.2 Cells Involved In the Brain Tissue Response

There are several distinct cell populations involved in the inflammatory and wound healing response to materials implanted in the CNS, also referred to as the "foreign body response." The cell most commonly associated with brain tissue is the neuron. The location of the neuron soma and its cellular processes relative to the electrode recording sites determines the strength and quality of the recorded electrical signal. Theoretical models predict that action potentials cannot be observed above noise farther than approximately 130 microns from a recording site and that

the neuron soma contributes the majority of the recorded signal [37]. Direct measurements suggest however, that the maximum distance is much less, somewhere between 50-100 microns [38-41]. Thus, the distance required to maintain a recording between an electrode site and a neuron cell body is on the order of cell dimensions.

Although neuronal networks are responsible for information processing and ultimate control of bodily functions, neurons make up less than 25% of the cells in the brain [42]. The remaining tissue consists of the glial cells (oligodendrocytes, astrocytes, microglia, and neural precursor cells) and vascular-related tissue. Oligodendrocytes are the myelin forming cells of the CNS, while astrocytes, microglia, and neural precursor cells are the main effectors of the brain's response to injury.

Astrocytes make up 30-65% of the glial cells in the CNS [43]. They contain an elaborate set of cellular extensions, giving them a star-like appearance in histological preparations of brain tissue sections and in cell culture. They provide growth cues to neurons during CNS development, mechanically support the mature neuronal circuits, help control the chemical environment of the neurons, buffer the neurotransmitters and ions released during neuronal signaling, and even modulate the firing activity of neurons [42;44;45]. Specialized astrocytic extensions, termed “end feet,” abut capillary walls and aid in the transfer of nutrients across the blood-brain barrier (BBB). Similar processes weave together to form the 15 μm thick glia limitans, the glial boundary between CNS and non CNS structures that can be clearly seen even between the CNS and the peripheral nervous system (PNS) [43;46]. Astrocytes are characterized by 8-10 nm diameter intermediate filaments of polymerized glial fibrillary acid protein (GFAP), which is considered an astrocyte specific cell marker [47]. Astrocytes at the site of injury express a

"reactive" phenotype characterized by enhanced migration, proliferation, hypertrophy, upregulation of GFAP, changes in the number and distribution of cellular organelles and glycogen deposits, and increased matrix production [23]. Immunostaining for GFAP is the most common method for astrocyte identification and for determining the extent of “reactive gliosis”, a term used to describe the activation, hypertrophy and proliferation of astrocytes in response to injury [47;48].

Microglia are the second major glial cell type involved in the brain’s wound healing response, constituting 5-10% of the total number of glial cells in the brain [49]. These cells appear to arrive in the brain via a prenatal infiltration of the CNS by blood-borne hematopoetic cells and remain thereafter as the resident macrophages in neural tissue. Primarily, they act as cytotoxic cells killing pathogenic organisms or as phagocytes secreting proteolytic enzymes to degrade cellular debris and damaged matrix after injury or during regular cell turnover [42;50]. Microglia reside in an inactive or ramified, highly branched state until "activated" via injury mediated mechanisms. Upon activation, they begin to proliferate, assume a more compact “amoeboid” morphology, phagocytose foreign material, and upregulate the production of lytic enzymes to aid in foreign body degradation [49]. When CNS damage severs blood vessels, microglia are indistinguishable from the blood borne, monocyte-derived macrophages that are recruited by the degranulation of platelets and the cellular release of cytokines. Macrophage-like cells arriving from damaged blood vessels, those present as perivascular resident cells, and microglia seem to perform the same functions in response to injury and will not be distinguished hereafter in this dissertation.

Microglia are also known to secrete multiple soluble factors that affect a variety of processes and signaling pathways, which makes it difficult to understand their precise role in the brain tissue

response to implanted materials [51]. They are a potent source of MCP-1, a chemokine that recruits macrophages and activated microglia [52], and of pro-inflammatory cytokines such as IL-1 [53], IL-6 [54], and TNF-α [55-57]. Furthermore, microglia are known to secrete, either constitutively, or in response to pathological stimuli, neurotrophic factors that aid in neuronal survival and growth [58], including NGF [58;59], BDNF [58], and NT-3 [59]. Finally, microglia produce various cytotoxic and neurotoxic factors (reviewed by [58]) which can lead to neuronal death in vitro [53] and in vivo following traumatic injury [60;61]. These cytotoxic factors include excitatory amino acids, such as glutamate, reactive oxygen intermediates (ROIs) generated as a result of the microglial "respiratory burst" [62] such as hydrogen peroxide ($H_2O_2$) or superoxide anion ($O^{2-}$) [63], and reactive nitrogen intermediates such as nitric oxide (NO) [64;65]. It has been suggested that the presence of insoluble materials in the brain may lead to a state of "frustrated phagocytosis," or an inability of macrophages to remove the foreign body, which results in a persistent, constitutive release of neurotoxic substances [66].

More recently, neural precursor cells (NPC's) have been identified as part of the brain's response to injury. NPC's had been overlooked entirely until only recently because they are an undifferentiated cell type that does not express unique cell markers such as GFAP (astrocytes), MAP-2 (neurons), CNPase or GalC (oligodendrocytes), or OX-42 (microglia) and are therefore difficult to find in stained tissue sections. However, recent evidence suggests they are equally if not more numerous than astrocytes, are found distributed all throughout the brain, and do express certain unique markers such as NG2, A2B5, and Olig2 [67-69]. Because the neural stem cell field is so new and is growing so rapidly, there are different classifications and nomenclature adopted by different researchers for NPC's including neural stem cells (NSC's), neural stem/precursor cells (NSPC's), oligodendrocyte precursor cells (OPC's), glial precursor cells (GPC's), astrocyte

precursor cells (APC's), NG2 cells, NG2/A2B5 cells, O2A precursors, polydendrocytes, and synantocytes. Many overlapping populations of neural stem cells exist, but there seems to be a clear distinction between (1) the multipotent neural stem cells found in small specific niches in the brain that can generate new neurons (as well as astrocytes and oligodendrocytes) and (2) the more widely distributed and more differentiated NPC's responding to injury which have lost the ability to form new neurons at injury sites (although this ability is found in some areas of the brain [70] and can be recovered in vitro through a specific de-differentiation protocol [71]). For the remainder of this dissertation, only the second, more numerous type will be referenced, and will be referred to as NPC's, although that designation likely describes a large, heterogeneous population of cells.

Upon injury and the subsequent breakdown of the BBB, large numbers of NPC's migrate to the site of injury within the first few days and begin to proliferate [72-74]. The majority of cells proliferating at the site of injury are NPC's (with the remainder being microglia) and this proportion increases over time as microglia stop proliferating after the first week [75;76]. The local environment determines the differentiation of NPC's [77], so over the course of weeks in the wound environment, many of the NPC's lose their NG2 staining and acquire GFAP staining, thus turning into the reactive astrocytes observed within the glial scar [73;76;78]. However, there may still remain a thin, dense layer of GFAP-negative NPC's commonly found within the glial scar in between the layer of microglia attached to an electrode and the layer of GFAP+ reactive astrocytes farther away from the implant. Differentiation at the site of injury from NPC's to astrocytes is accomplished through the IL-6 cytokines (IL-6, CNTF, LIF), which function through the gp130 membrane receptor and the STAT3 pathway, and through the BMP cytokines (BMP-2, BMP-4), which function through the SMAD pathway [79-84]. These two pathways also interact

through P300 to induce astrogliotic genes [85;86]. Both IL-6 and BMP cytokines are produced by microglia, astrocytes, and NPC's at the site of injury and direct a reactive astrocyte fate (as opposed to an oligodendrocyte or neuronal fate) for the large mass of proliferating NPC's that migrate to respond to injury [87-91]. Because an astrocytic fate can be induced by either the members of the BMP family or the members of the IL-6 family, blocking just one pathway will not block reactive astrocyte formation [92]. The Notch pathway, serum, and bFGF have also been implicated in the differentiation of NPC's into astrocytes at the expense of other cell types [79;80;93-101]. Exploration of the intracellular signaling pathways that stimulate astrocyte differentiation has found that the translocation of the repressor transcription factor Olig2 out of the NPC nucleus, induced by serum, BMP's, the STAT3 pathway, and the Notch pathway, results in the downregulation of NPC markers like NG2 and the upregulation of astrocyte markers like GFAP [78;102].

### 2.2.3 Cytokines and Growth Factors Involved in the Brain Tissue Response

A large number of soluble and ECM-presented factors are released by cells responding to CNS injury. Some factors, like chemokines MIP-1α and MCP-1 and certain inflammatory cytokines like TNF-α, IL-1β, IL-6, and CNTF are released immediately, as dying cells release intracellular stores, or within 2-4 hours as early response genes are transcribed into protein [103-106]. Other factors like IL-10, bFGF, and IFNγ are released at later time points, either by cells that respond to injury or those that respond to the initial wave of factors [107;108]. Over time extracellular matrix is laid down that sequesters and presents more cytokines and growth factors such as TGF-β, BMP-2, BMP-4, and bFGF near the injury site.

The first factors released are inflammatory factors that call in immune cells from the damaged vasculature and from the surrounding brain. Infiltrating leukocytes and resident microglia release TNF-α, IL-1β and IL-6 which kill invading pathogens, activate nearby cells, and stimulate proliferation of cells near the injury site [88]. IL-6 and IL-1β cause their own upregulation so they are also produced by neurons and astrocytes [88]. IL-1β often acts as a "master cytokine" orchestrating inflammation and inducing the production of wound healing factors like bFGF [108], although it may initially inhibit wound healing during the early inflammatory phase [109]. IL-1β injected directly into the brain by itself was able to cause astrogliosis [110] and it has been shown to induce basal lamina production in astrocytes [111].

The IL-6 cytokines CNTF, LIF, and IL-6 act through a common membrane receptor gp-130 and lead to STAT3 movement to the nucleus, which turns on the genes that convert astrocytes and NPC's into reactive, GFAP expressing astrocytes [81;83;85;89;93;94;112]. Gp130 is essential for the normal developmental differentiation of astrocytes in the brain and STAT3 enables reactive astrocytes to close up the BBB after injury [113-115]. After a mechanical injury to a layer of astrocytes in vitro, LIF and CNTF were found to be released in the media and the conditioned media from the lesioned astrocytes differentiated NPC's into astrocytes [116]. Administration of CNTF directly into the brain increased GFAP and vimentin expression, and doubled the rate of proliferation [117;118]. IL-6 releasing microcapsules implanted in the brain caused a massive proliferation and activation of astrocytes and microglia [119]. This effect on proliferation may stem from the ability to provide cells with the competence to respond to growth factors like EGF for re-entry into the cell cycle [120]. Because of the overlapping functions of the different IL-6 cytokines, the removal of just one still allows the glial scarring process to proceed and makes blocking this process with an antibody treatment difficult [121].

Like IL-6 cytokines, BMP cytokines also induce NPC's to differentiate into astrocytes, and the natural inhibitor and regulator of BMP's in wound sites, noggin, blocks this process [122;123]. Both BMP-2 and BMP-4 are upregulated after brain injury, as is noggin [123]. Serum released at the site of injury also contains BMP's, which may be an initial trigger after injury [92].

The pleotropic growth factor bFGF has many roles throughout the body and during development, but it has a central role in the tissue response to brain injury. bFGF is essential for the survival and growth of NPC's, is upregulated in injury, and induces cell migration [97;98;124-130]. bFGF is also a mitogen for NPC's and astrocytes, helping generate the large mass of new cells that must repopulate the wound [126] and improves neuronal survival and functional recovery after injury, likely through its actions on glia [98;108;128;131], although it may have direct pro-apoptotic effects on neurons as well [132]. By itself it can initiate [133] and enhance [98] glial scarring in vivo, possibly by serving to de-differentiate cells into a more plastic phenotype so that they are competent to receive and act on signals from other cytokines (i.e. CNTF) [84;97;101]. The bFGF induced signal for cells to stay undifferentiated and to proliferate is mediated through the nuclear factor NCoR, which is removed from the nucleus and degraded after a cell is exposed to CNTF [134]. bFGF is sequestered by the ECM deposited within the basal lamina and must be presented by heparan sulfate proteoglycans to function appropriately [135;136].

### 2.2.4 Insertion Trauma

Few studies have examined the initial impact of insertion, and it appears that the first encounter of cortical tissue with a needle-like electrode is a violent one [137]. As the electrode is inserted

into the cortex, its path severs capillaries, extracellular matrix, glial and neuronal cell processes. The electrode may pull and snap extracellular matrix materials as it progresses deeper into tissue, push aside tissue that had once occupied the electrode space, and induce a high-pressure region surrounding the electrode.

This mechanical trauma initiates the CNS wound healing response, a response that shares similarities to wound healing responses of other tissues. Disruption of blood vessels releases erythrocytes, activates platelets, clotting factors, and the complement cascade to aid in macrophage recruitment and initiate tissue rebuilding. Insertion induced accumulation of fluid and necrotic nervous tissue causes edema, further adding to the pressure surrounding the implant. When a 10x10 array of silicon probes was implanted in feline cortex, 60% of the needle tracks showed evidence of hemorrhage and 25% showed edema upon explantation of the probes after 1 day [138]. Although a large number of the tracks were affected, only 3-5% of the area was actually covered by hemorrhages and edema, suggesting the actual magnitude of the damage to blood vessels may have been relatively minor. Alternatively, this may have been underestimated by the analytical methods employed.

Activated, proliferating microglia appear around the implant site as early as 1 day post-implantation [26;139;140]. Edema and erythrocytes remain after 4 days post-implantation, although excess fluid and cellular debris diminishes after 6-8 days due to the action of activated microglia and re-absorption [141]. The presence of erythrocyte breakdown products (but not hemorrhages) and necrotic tissue can still be seen after 6 weeks time [27;141]. At later time points some report that typical inflammatory cells or hemorrhaging can not be seen [32], while others have reported observing macrophages at the device brain tissue interface at up to 16 weeks

[25-27;141]. As testament to the transitory nature of this mechanically induced wound healing response, electrode tracks could not be found in animals after several months when the electrode was inserted and quickly removed [10;25;32;142], indicating that the persistent presence of the implant augments the brain tissue response.

### 2.2.5 Long Term Microglial Reaction

The brain tissue response of chronically implanted electrodes would be less of an issue if the foreign body response disappeared a few weeks after implantation as observed with stab wounds. However, once the acute inflammatory response declines, a chronic foreign body reaction is observed. This reaction is characterized by the presence of both reactive astrocytes, which form a glial scar (detailed in the next section), and activated microglia [25-27;141].

In many studies a significant portion of cells in damaged neural tissue do not stain for GFAP, suggesting the presence of large numbers of activated microglia or neural precursor cells at the surface of implanted biomaterials long after the initial wound healing response is complete, and perhaps as long as the material remains in contact with brain tissue [26;28;29;35;141;143-147]. For example, nearly 25% of electrode tracks in a multi-pronged silicon probe array showed macrophage-like cells present 6 months after implantation [138]. Activated microglia will attempt to phagocytose foreign matter for eventual degradation. When 25 μm polymeric microspheres were implanted into rat cortex, they were all phagocytosed by the activated microglia within 2 months and remained internalized throughout the remainder of the 9 month study [29]. Immunostaining around a needle-like implant revealed scattered reactive microglia in the initial wound healing response, clustering of microglia in a reactive tissue sheath forming around the

implant after 2 weeks, and continued presence of microglia in a tight cellular sheath at 12 weeks post-implantation [26]. Cells not staining for GFAP had adhered to the implant upon its extraction in the same study.

When macrophages outside the CNS encounter a foreign object, they surround it and begin secreting lytic enzymes. If individual macrophages cannot degrade the object, these cells often fuse into multinucleated foreign body "giant" cells characteristic of chronic inflammation. This closely parallels the activated microglial reaction to electrode implants in the CNS. Needles made out of a plastic used for tissue mounting (Araldite) implanted into rabbit cortex attracted variably sized multinucleated “giant” cells as early as 18 days post implantation [141]. These cells were separated from other cortical tissue by a basal lamina and were mostly found adjacent to degraded regions of the plastic needles, suggesting the action of hydrolase activity. A similar layer of tightly coupled multinucleated giant cells was observed by Edell et al. with cortically implanted silicon electrodes [28].

A recent study observed persistent ED-1 immunoreactivity around silicon microelectrode arrays implanted in rat cortex at two and four weeks following implantation that was not observed in microelectrode stab wound controls, indicating that the phenotype was not the result of the initial mechanical trauma induced by probe insertion but was associated with the foreign body response [25]. In addition, electrodes explanted at 1, 2 and 4 weeks after implantation were covered with ED-1/OX-42 immunoreactive cells that released MCP-1 and TNF-$\alpha$ in vitro, indicating that inflammation mediated neurotoxic mechanisms may be occurring at the microelectrode brain tissue interface.

### 2.2.6 Glial Scar Formation

The most common observation of the long-term CNS response to chronically implanted electrodes is the formation of an encapsulation layer referred to as the "glial scar" [11;25;27;28;148]. Studies have demonstrated that reactive glial tissue surrounds and progressively isolates implanted arrays in a process similar to the fibrotic encapsulation reaction that is observed with non-degradable implants in soft tissues of the body. The development of this encapsulation tissue is limited to higher vertebrates and has been implicated in the resistance of the spinal cord and the brain to nerve regeneration after injury [149].

The purpose of the glial scar remains unclear, but it is thought to play a role in separating damaged neural tissue from the rest of the body to maintain the BBB and to prevent lymphocyte infiltration [23;43]. Although the glial scar is blamed for neuroelectrode failure and the failure of neurons to re-grow CNS injuries, the glial scar can be seen as the brain's beneficial attempt to recreate the boundary between "brain" and "non-brain" regions as it normally does through the glia limitans [46;73]. When glial scar formation is inhibited through ablation of proliferating cells or GFAP+ astrocytes, the BBB is not restored, long-term healing is blocked, leukocyte infiltration is increased, and functional deficits are higher [150-152]. The inflammatory environment that initially kills cells allows for long-term recovery [153]. When STAT3, the IL-6 cytokine-driven transcription factor that allows for the activation and differentiation of NPC's into the "reactive" astrocyte phenotype, is knocked out, injury results in less cellular migration, more inflammation, and worse deficits after injury [114], while overexpression of IL-6 allows faster healing [154]. The reactive astrocytes blamed for a loss in recordings are important for the maintenance of the BBB [114].

Unlike soft tissue encapsulation, which involves fibroblasts and a thick secreted collagenous matrix, NPC's and reactive astrocytes are the major components of CNS encapsulation tissue [26-28;155-160]. Current theories hold that glial encapsulation insulates the electrode from nearby neurons, thereby hindering diffusion and increasing impedance [22;27;155;161;162], extends the distance between the electrode and its nearest target neurons [22], or creates an inhibitory environment for neurite extension, thus repelling regenerating neural processes away from the recording sites [163-165].

The time course of NPC migration to the injury site and the differentiation of those cells into astrocytes is not well established because the involvement of NPC's is a relatively new finding. However, studies that have looked at this cell type find it to be highly motile and migration to the injury site seems to occur in the first 24-48 hours, with NPC's concentrating in the 1mm region adjacent to the injury through migration and proliferation over the first 2 weeks [4;73;76]. Differentiation of NPC's into GFAP+ astrocytes occurs approximately 4-5 days after injury until large numbers of GFAP+ cells are seen by 7 days after injury to fill in the astrocyte depletion (presumably through cell death) seen after injury [73;76;78].

After the initial NPC migration, proliferation, and differentiation into GFAP expressing astrocytes over the first week after implantation, the GFAP-positive glial scar matures (assuming the tissue is stable with no further damage due to micromotion). Turner and colleagues used confocal microscopy to show the time course of GFAP-positive astrogliosis [27]. Passive silicon electrodes were implanted in the rat cerebral cortex and explanted at 2, 4, 6, and 12 week time points (Figure 2). At two weeks, GFAP staining revealed a reactive astrocyte region surrounding

the implants that extended out 500-600 µm. This region decreased over time, but the layer of cells immediately adjacent to the implant became denser and more organized suggesting contraction around the implant. At 2 and 4 weeks, activated astrocytes around the implant had extended their processes toward the insertion site. The mesh of astrocytic processes became stronger and more compact at 6 and 12 weeks, as suggested by the fact that removal of the implant did not result in the collapse of cellular processes into the implantation tract. Both visual and mechanical inspection of the glial sheath suggested that its formation was complete as early as 6 weeks post-implantation and remained intact as long as the implant remained *in situ*.

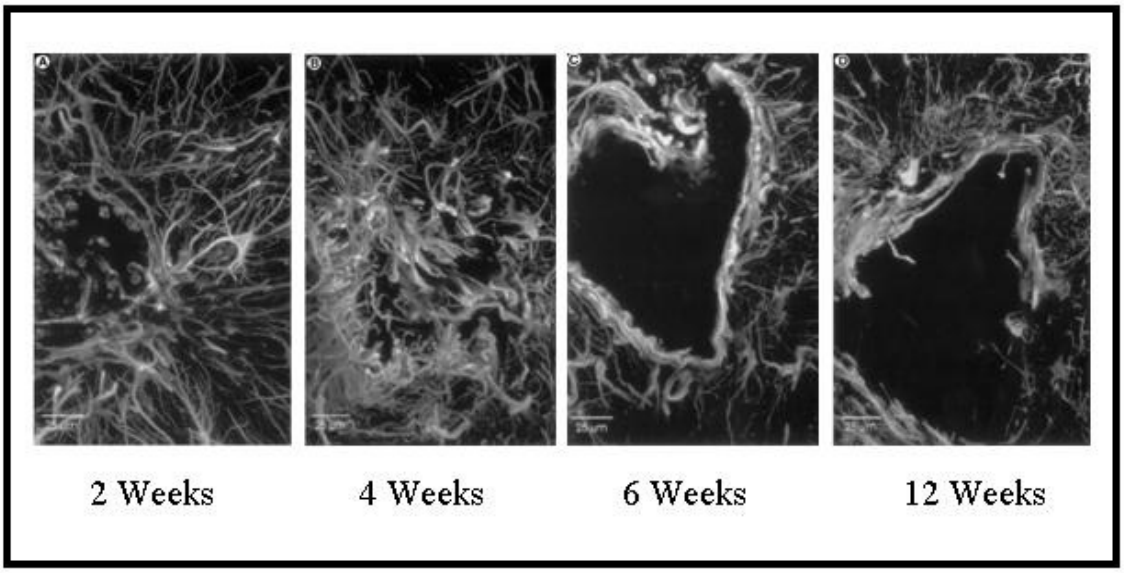


**Figure 2: Time course of glial scar formation at four time points as imaged by GFAP staining. At 2 and 4 week time points, the astrocytic processes fall back into the void left by the probe extraction before tissue processing. By 6 weeks, the processes have interwoven to form a stronger, more dense sheath surrounding the implant. Minimal changes between the 6 and 12 week time points indicate the glial scar completion within 6 weeks. From [27].**

A later study by the same group confirmed this time course [26]. This study found a region of diffuse glial activation as imaged by GFAP staining 100-200 µm away from the implant site after

day 1, and a steady increase of astrocyte activation to 500 µm away from the implant through 1, 2, and 4 weeks. A more compact sheath formed by 6 weeks and remained constant at 12 weeks, with the actual sheath extending only 50-100 µm around the insertion site. The investigators also stained for vimentin, which is expressed in reactive astrocytes or immature cells (such as NPC's) but not mature astrocytes. Vimentin expression followed a time course similar to GFAP, but revealed fewer positive cells, a spatial distribution closer to the implant (25-50 µm thick layer), and a completed sheath at 4 weeks post-implantation. It is important to note that in each of the aforementioned studies the electrodes were not functional, that is, they were not connected to an external electrical connector externalized through and attached to the skull. Such untethered electrodes may underestimate the actual reactivity caused by electrically active implants that may transmit forces to the implanted electrode [166]. A glial scar forms around every adult CNS implant, regardless of implant type or size. To date, only studies employing non-specific H&E staining have not observed glial scar formation [22;32;141], and in a report where both H&E and GFAP were used on the same samples, it was noticed that H&E staining revealed little gliosis, but GFAP staining clearly showed the development of a brightly stained astrocytic scar around the implant [11].

However, there is a clear difference between embryonic and adult mammalian CNS responses to injury, with only adult animals forming a glial scar [167-170]. Embryonic cells regenerate readily from mechanical insults and do not produce a typical glial scarring response[171;172]. Neurites can grow across a tissue explant modeling the glial scar from newborn animals but does not grow across the tissue explant from adult animals [173]. One line of experiments has pointed to a critical period of development around postnatal week two or three after which a mature glial scar is capable of forming [171;174]. Differentiation of precursors in pre-critical period cortical slices

was in the neuronal direction while postnatal cells differentiated into astrocytes [80] and it has been shown that the upregulation of bFGF and its receptor is much higher after the developmental onset of the scarring response [128;129;133]. Inflammatory cytokines, including IL-1β and IL-6, delivered directly into the fetal brain can induce the type of glial scar formation seen in adult animals, suggesting the lack of appropriate cytokines and growth factors is the cause of this non-scarring phenotype [170].

Other factors and cell types may also contribute to the formation of the glial scar. Several investigators have reported the presence of connective tissue inside this scar similar to the extracellular matrix (ECM) encapsulation seen in wound healing models outside of the CNS [22;141]. Meningeal fibroblasts, which also stain for vimentin, but not for GFAP, may migrate down the electrode shaft from the brain surface and form the early basis for the glial scar [31;46;164]. Support for this fibroblastic role in glial scar formation comes from experiments by Kim et al. who compared the cellular response to implants completely surrounded by cortical tissue (a less realistic model) to transcranial implants that also contacted the skull and the meninges (a more accurate model of functional recording electrode arrays) [34]. They found a significant increase in ECM and connective tissue in the transcranial probes, as well as a thin layer of GFAP negative/vimentin positive cells (possibly NPC's, or meningeal cells) surrounding the transcranial probes that was not present in the implants completely surrounded by brain tissue. Staining for ED1, a microglial marker, confirmed that microglia were present within this 1-2 cell thick layer, and the authors also concluded that the presence of ECM suggested meningeal fibroblasts had migrated down the probe from the top of the cortex. An alternative explanation however may be that tethering to the skull created more intense micromotion forces, leading to a

larger scar with more ECM [166]. BBB breakdown is also associated with increased ECM deposition in the glial scar [175].

Although the glial scar is primarily a cellular scar of microglia, astrocytes, NPC's and cellular processes, ECM does play a role in organizing the scar and creating a chemical barrier to neurons[176;177]. A basal lamina (often also referred to as a basement membrane) is often seen (and may be present each time but just not stained for) in the glial scar, typically between the microglia coating the implant and the cellular layers of NPC's and GFAP+ cells in the scar, or between the astrocyte and the meningleal layer that helps reform the glia limitans after a stab injury [178-183]. Meningeal-like cells also stain for basal lamina components after CNS injury [184] and may be the source of a thicker scar in implants that penetrate the meninges (as opposed to those that are fully implanted) [34;46]. The basal lamina is a sheet-like layer of ECM that can be found as a boundary layer in many tissues such as blood vessels and epithelium (Figure 3). It is primarily composed of four components: the ECM proteins collagen IV and laminin, and the proteoglycans perlecan and nidogen. The proteoglycans sequester and present cytokines and growth factors such as bFGF while the ECM proteins create a substrate for cells to attach [135;136;185]. Those same growth factors also cause ECM production by astrocytes [186]. It was the basal lamina formed after injury that blocked neurons from regrowing across a wound in one study and the removal of the basal lamina through anti-collagen antibodies rescued this ability [187]. Apart from the basal lamina layer, which thickens with more intense scarring, other chondroitin sulfate and heparin sulfate proteoglycans inhibitory to neuronal growth are deposited in the glial scar, creating a chemical barrier for neurons between the healthy brain parenchyma and the foreign body (or injury) surrounded by a glial scar [164;188].

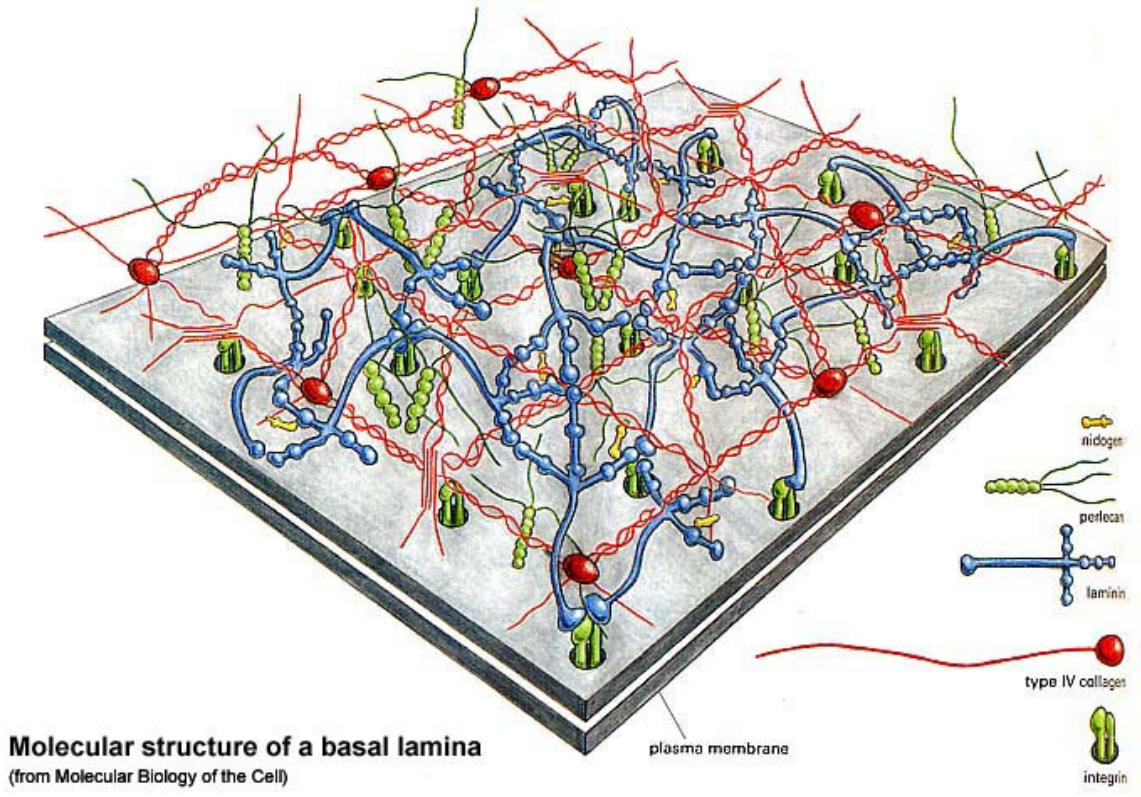


**Figure 3: Basal Lamina Structure. Basal Lamina is composed of ECM proteins (collagen and laminin) and proteoglycans (nidogen, perlecan). Growth factors are sequestered by the basal lamina and it functions as a boundary layer between cells. Originally from [189].**

### 2.2.7 Neuronal Response to Implant-Induced Injury

The density of neurons and their proximity to the electrode sites are the most accurate barometers of electrode performance in a chronic setting. Unfortunately, this response is not as well characterized as glial scar formation, as it seems to vary from implant to implant, and even between electrodes implanted at different sites in the same animal. One explanation of electrode signal degradation is the formation of a "kill zone" around the implant site resulting from the initial trauma or neuroinflammatory events [25;28] . This region is defined by a significantly

lower or nonexistent neuronal density up to some distance away from the electrode. One group found a kill zone of less than 10µm for electrode shafts that had not induced major trauma, with a larger kill zone of 20-60 µm for shafts that experienced minor lateral motion tangential to the brain surface during implantation [28]. The authors suggested a correlation between initial tissue damage and kill zone size, although this correlation has not been confirmed by others. Reported kill zone sizes have varied between 1 µm (no dead zone) and more than 100 µm [27;141;149].

An alternative explanation for a loss in signal strength is a slow regression of neurons away from the electrode. Proliferation of astrocytes and formation of the glial scar around the electrodes could be one mechanism by which gliosis displaces neurons near the implant site and pushes cell bodies away from electrode sites [28]. Liu et al. implanted iridium wire electrodes into feline cerebral cortex and tracked the stability of single units over time [22]. Histological examination upon explantation revealed that every electrode with stable unit recordings had at least one large neuron near the electrode tip, while every electrode that was not able to record resolvable action potentials was explanted from a site with no large neurons nearby. The study also observed that significant changes in recording capability occurred in the first 4-8 weeks post implantation, after which the signals stabilized (such stabilization also reported in [20]). The authors of the study speculated that electrode migration through tissue resulted in these changes since active restructuring of the adult mammalian brain is severely limited.

A recent study observed a significant loss of neurons around chronically implanted silicon arrays that was not seen in stab wound controls, indicating that the cell loss was associated with the foreign body response [25]. Immunostaining revealed significant reductions of neurofilament and NeuN at the electrode brain tissue interface that surrounded the implanted electrodes at two and

four weeks following implantation (Figure 4). In this study although the electrodes were non-functional they were tethered to the skull in a manner similar to working electrodes. In addition, the investigators observed a relationship between persistent ED-1 staining at the microelectrode brain tissue interface and loss of neuronal markers, leading them to speculate that persistent activation of microglia at the device surface leads to local neurotoxicity.

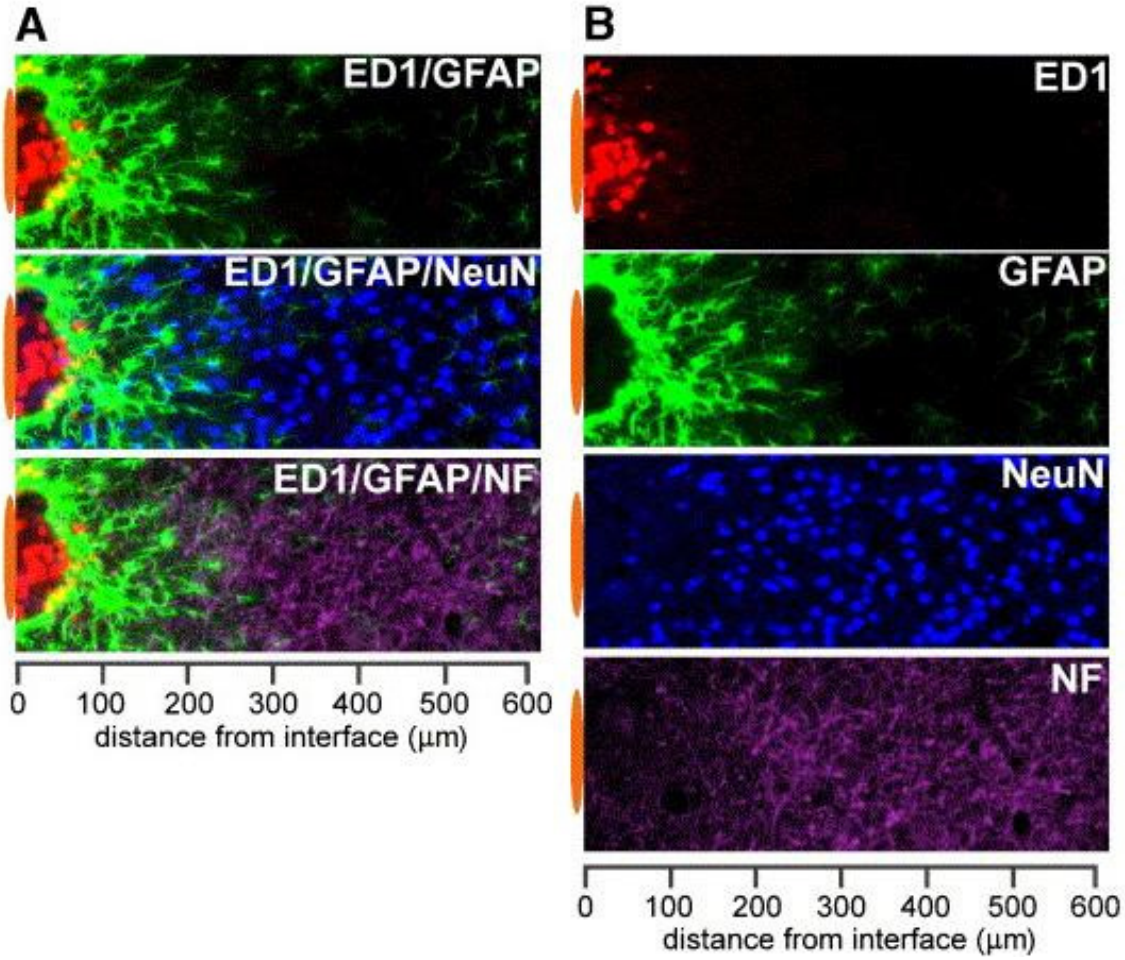


**Figure 4: Stratification of cellular immunoreactivity using cell-type-specific markers at the microelectrode–brain tissue interface. Representative images collected from two adjacent sections of an animal with a 4-week microelectrode implant illustrate the general appearance of the foreign body response characterized by minimally overlapping inflammatory (ED1) and astrocytic (GFAP) phenotypes adjacent to the implant interface. The area of inflammation and intense astrocyte reactivity contains a reduced number of $NeuN^+$ neuronal bodies and a loss of neurofilament (NF) density. The position of the microelectrode is illustrated by the orange oval (drawn to scale) at the left of each image. Images were captured in grayscale and pseudocolored for illustration. From [25].**

### 2.2.8 In Vivo Experimental Variability

The available evidence suggests there is significant variability in electrode performance within experimental groups, between different animal models, investigators, and even between different electrodes implanted in the same animal. There are no common handling, packaging, sterilization, implantation, fixation or analytical schemes employed. In addition, many of the experiments are improperly controlled, completely subjective and employ too few animals. While such variability is not uncommon for in vivo work of this kind, the different and often conflicting results obtained from these experiments leads to difficulty in drawing meaningful conclusions. For example, in the Edell et al. study on implanted electrode arrays, electrode shanks with seemingly identical characteristics and insertion techniques resulted in significantly different kill zones [28]. Another confounding example comes from Rousche and Normann (Figure 5), who show an H&E stained image of two adjacent electrode tracks from the same electrode array; one track has healthy neurons growing right up against it and no sign of an immune response, while the other very clearly shows the formation of a glial scar and a chronic inflammatory response [21]. In a study looking at insertion technique, the distribution of blood vessels in the tissue made a large impact on the amount of damage caused during the insertion and wide variability was observed for insertions made under the same conditions [137]. Perhaps the clearest example of this variability was observed in the in vivo response to plastic "mock electrodes" implanted in rabbit brain by Stensaas and Stensaas and explanted over the course of two years [141]. They separated the response into three types: Type 1 was characterized by little to no gliosis with neurons adjacent to the implant, Type 2 had a reactive astrocyte zone, and Type 3 exhibited a layer of connective tissue between the reactive astrocyte layer and the implant, with neurons pushed more than 100

µm away. All three responses are well documented in the literature; however this study found that the model electrodes produced all three types of reactions simultaneously, depending on where along the electrode one looked. Although these studies clearly suffer from the insensitivity of the chosen histopathological approach (non-specific tissue staining), it is clear that only a broader view of the evidence can yield meaningful conclusions in the face of such experimental variance.

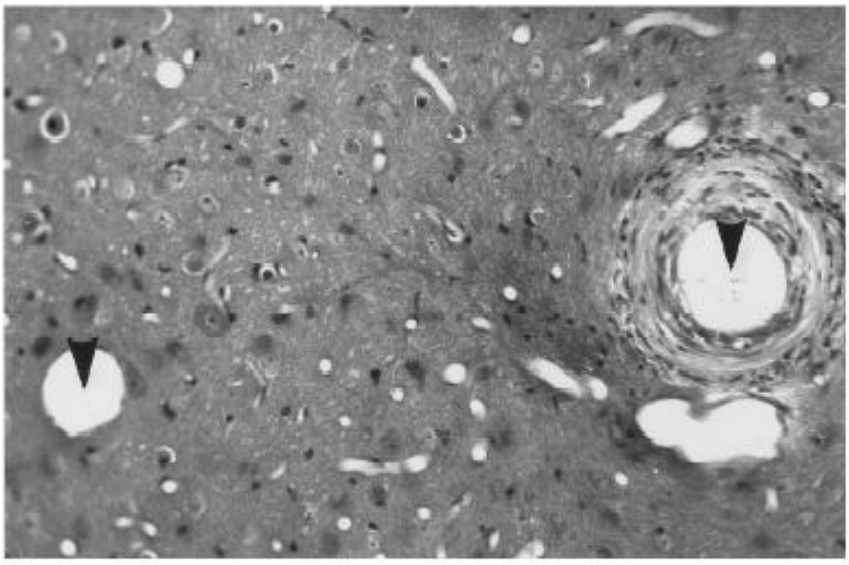

**Figure 5: An example of in vivo variability commonly encountered in implant literature. Arrows show adjacent tracks from two electrodes on the same array. The track on the right clearly shows heavy matrix deposition while that on the left seems to have no tissue reaction. From [21].**

## *2.3 Current Electrode Implant Systems*

The problems inherent in chronic recording electrode design have precluded the development of a "gold standard" electrode against which testing is performed. Historically, neurobiology research has used single wire or glass micropipette electrodes to record individual neuron waveforms in

acute experiments. However, the need to access populations of neurons and the desire of researchers to monitor neuron networks over time has added a new focus on arrays of wires, silicon shafts and other more complex micromachined silicon recording systems capable of high density sampling. Chronic implantation has also generated various surgical techniques aimed at reducing electrode failure and the foreign body response. This section details the most salient features of electrode array design and surgical techniques as they relate to biocompatibility.

### 2.3.1 Multiple Electrode Types

Of the two main types of electrode arrays currently being explored, microwire electrodes have the longest history and widest use in the field. Microwire electrodes are wires made of a conducting metal such as platinum, gold [32], tungsten [9], iridium [22], or stainless steel [20], that are coated with a non-cytotoxic insulator material. The tip of the wire is not insulated and can receive electronic signals from the surrounding neurons. In an effort to better separate single unit from multi-unit activity, experimenters often record from two (stereotrode configuration [190]) or four (tetrode configuration [191]) closely spaced microwires to allow relative signal strength to act as another parameter in single unit identification. Finally, microwires can be arranged in arrays to access the large numbers of neurons necessary for neuroprosthesis control. The number of wires used in a single implanted array has ranged from four [32] to over 100 [20]. A clear advantage of using microwire electrodes is the ease in array fabrication compared to more sophisticated silicon arrays, which are discussed later. Although microwire arrays are simpler, their performance in recording high numbers of single units often exceeds the quality of recordings obtained from silicon-based electrodes. Nicolelis and colleagues chronically implanted 10 microwire arrays into macaque monkey cortex for a total of 704 microwires, and were able to record 247 individual

cortical neurons in a single session from 384 of the microwires (Figure 6) [20]. While the number of units varied from day to day and between monkeys, the yield of units per recording site was much greater than that of the typical silicon array. Furthermore, microwire arrays can access deeper brain structures, but the precise location of the electrode tips and the interelectrode spacing cannot be controlled as the non-homogeneous nature of brain tissue will bend microwires during implantation [28].

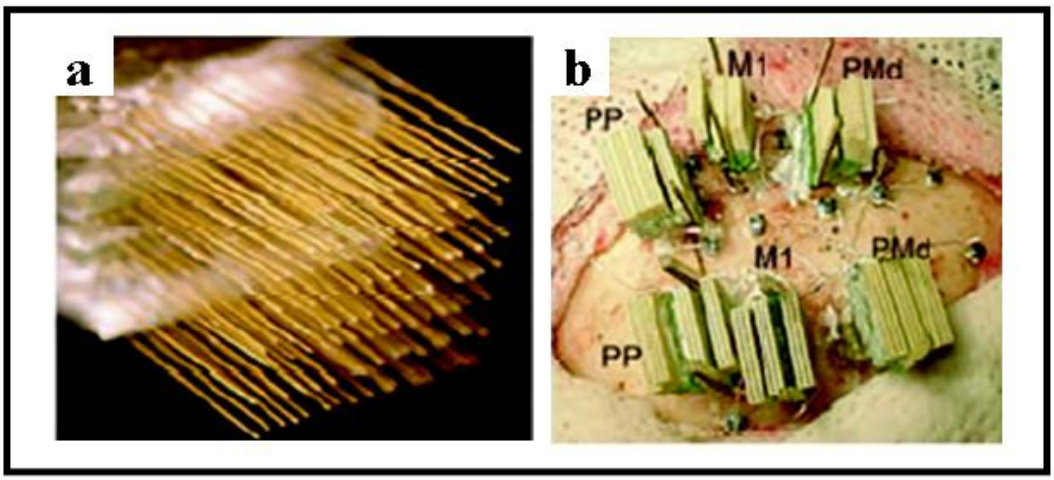


**Figure 6: a. Wire electrode arrays implanted in macaque monkey cortex. b. Layout of six such wire arrays in macaque monkey cortex. From [20].**

Although most neuroscience research continues to be conducted using these well-established microwire electrodes, the next generation of electrode arrays being developed is predominantly silicon based. Silicon micromachined electrodes allow for a more complex design and thus greater flexibility in strategies to minimize the foreign body response and greater control over electrode placement. The emergence of silicon micro-machining technology has yielded increasingly smaller and higher electrode count arrays capable of recording from greater volumes of neural tissue with improved spatial discrimination [15;142;192;193]. However, despite

substantial technological advances in their design, many such devices are unreliable for chronic recording applications in the CNS [22].

Silicon photolithographic processing allows for unsurpassed control over electrode size, shape, texture, and spacing, allowing multiple recording sites to be placed at variable heights on a single electrode shank. Such control provides the experimenter with absolute knowledge of the recording location, the ability to place the recording sites at different depths to suit the geometry of the neural system under study, and a larger overall number of recording sites on a smaller volume than is possible on wire arrays or bundles [194]. Circuits can be integrated directly on the probe for better signal acquisition, and on-chip microelectromechanical systems (MEMS) add additional possibilities such as heating elements and microfluidics [195;196]. Further decreases in electrode sizes and increases in recording site densities are currently limited by connectors and on-board systems that are unable to handle the hundreds of possible leads on a single array [11;16;193;195]

The designs of silicon based electrode arrays vary between investigators and research manufacturing centers (Figure 7) [26;27;27;28;142;195]. Nevertheless, two particular silicon electrode array designs have attained prominence in the field. The Utah Electrode Array (UEA) developed by Normann and colleagues has been in use for over 15 years [11;16;21]. The UEA is created from a single block of silicon which, through etching, doping, and heat treatment, results in a three dimensional array of needle-like electrodes with recording tips. It has been made in 25 and 100 shank versions of various shapes, with each shank 1.5 mm in length and ranging from 100 µm at its base to less than 1 µm at the tip (as compared to 25-50 µm diameter and up to 8 mm

in length for microwires [20]). The UEA was chosen by Cyberkinetics for its human clinical trial because of its long history of performance and supporting animal studies[12].

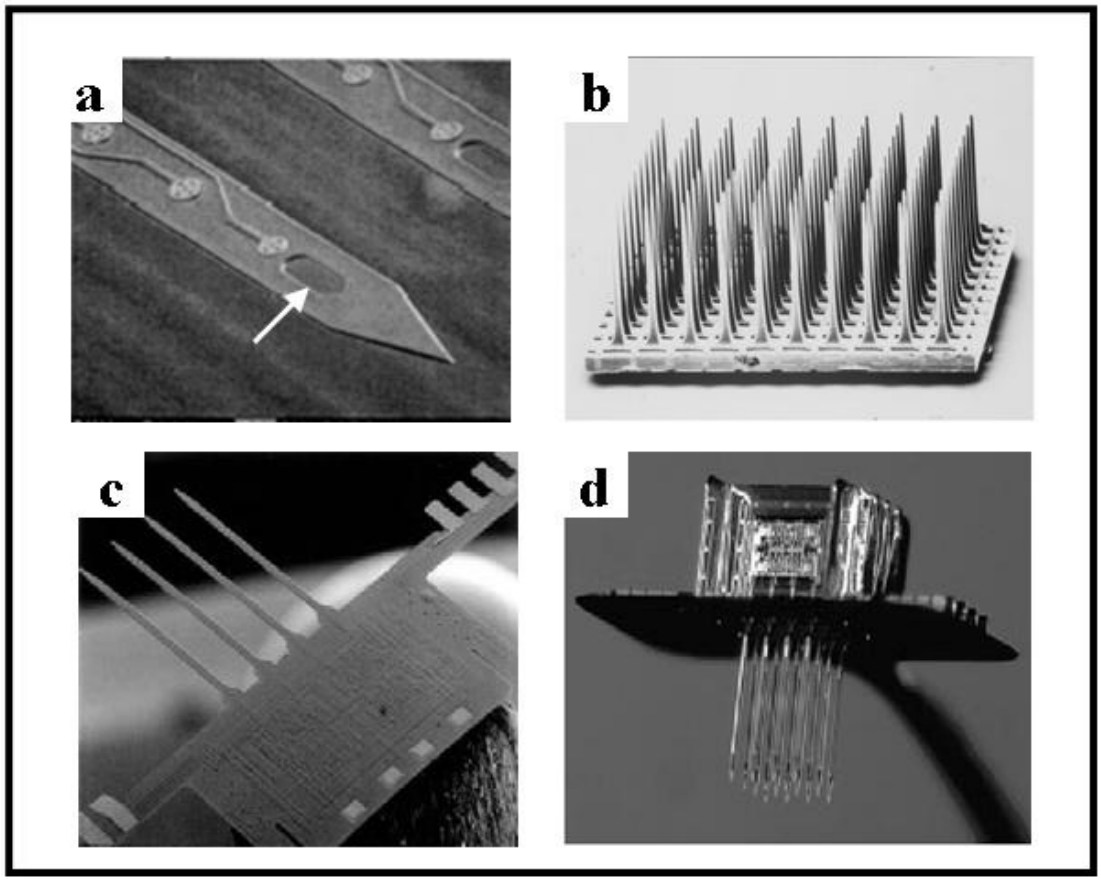


**Figure 7: Various designs of silicon micromachined electrode arrays. a. Arrow points to a "well" included in the electrode design for bioactive molecule incorporation. Multiple electrode sites are present on each electrode shank. From [193]. b. Utah Electrode Array formed from a single block of silicon. From [21]. c. and d. Multiple planar arrays of "Michigan" electrodes are stacked together to create a three dimensional array. From [195].**

The other prominent electrode design comes from the University of Michigan Center for Neural Communication Technology [26;31;193;197]. Unlike the UEA, the Michigan probes are planar arrays of electrode shanks made from a single thin sheet of silicon, but each 2 mm long, 100 μm x

15 μm shank has several recording sites placed at user-defined locations along the shank. The manufacturing process is similar to that used to create multilayer silicon microchips and requires 8 masks, but results in hundreds of user defined, reliable, and regular electrodes from a single block of silicon. A different group has developed a similar design with four recording sites per shank using ceramic rather than silicon for their electrodes, resulting in mechanically stronger electrodes with comparable recording capabilities [198;199]. Other micromachined electrodes have also recorded signals [200].

### 2.3.2 Materials Used for the Insulating Layer

Both microwire and silicon based electrode array systems require an insulation layer to shield the electrodes from unwanted electrical signals. The vast majority of tissue-electrode contact is with the insulating layer, so this material must be non-toxic and should act to reduce the foreign body response. Several different materials identified as minimally toxic have been used to coat electrodes. A simple coating of Teflon or S-isonel, a high temperature polyester enamel similar to Teflon, has been used with great success to coat wire electrodes [20;201]. Resins such as Epoxylite have also been used successfully [22]. Plasma-deposited diamond-like carbon (DLC) has recently been demonstrated in vitro as both a chemically inert insulator and as a good substrate for biological molecule attachment to control the foreign body response, although it has not been tested in vivo [202;203].

In addition to the normal silicon nitride or silicon dioxide insulation deposited during the fabrication of micromachined silicon electrodes [16;193], polyesterimide, or more commonly, polyimide is often used to coat silicon-based implants [9;16;32;195]. Only minimal degradation is

seen over time in polyimide coated microwires implanted in the brain [204]. Lee et al. reported that fibroblasts spread, adhered, and grew on polyimide electrode surfaces with no difference from tissue culture polystyrene controls [205]. The electrodes were also mounted on a thin (5-10 μm) silicon substrate to aid in electrode insertion through the pial membrane of the brain [205]. The flexibility of polyimide may improve the mechanical impedance mismatch between a rigid electrode and soft tissue that causes tissue damage if micromotion of the electrode occurs [10;34]. Rousche et al. eliminated silicon completely and created a flexible electrode out of polyimide and gold, where the gold recording sites and leads were sandwiched between two layers of polyimide [10]. A major drawback to this design was that the electrodes were not stiff enough to pierce brain tissue on their own, so implant sites had to be created with wire or a scalpel before insertion.

### 2.3.3 Electrode Insertion and Implantation Procedure

Many studies have attributed biologically induced electrode failure to the initial trauma of implantation, leading to a variety of strategies to minimize this early trauma in the hope of limiting the subsequent complications. Unfortunately, since each group of investigators works with a different electrode system, a different animal model, and a different set of hands, there is very little consensus regarding the optimal way to implant chronic recording electrodes and a shortage of well controlled quantitative studies. Approaches differ on the speed of electrode insertion, the method of insertion, the importance of limiting micromotion, and the depth of insertion.

Experimenters use a wide range of insertion speeds for electrode implantation. One theory holds that slow insertion allows for neuronal tissue to adjust to the implant, thus minimizing the damage caused by the electrode. In the experiments conducted by Nicolelis et al., a 100 µm per second microwire electrode insertion rate was cited as a major factor behind the unusually large number of single units recorded in the study [20]. However, other groups have reported problems with slow insertion, such as catching of the tissue, and dural dimpling [28]. A recent study directly observing insertion in a brain slice found greater vascular damage with slower insertion [137]. The other school of thought is that a rapid insertion minimizes trauma, since the force of the insertion cuts through the tissue in the array's path, but does not affect nearby tissue [16]. Groups using the UEA have found that a high velocity approach (8.3 m/s) prevents cortical surface dimpling and minimizes tissue damage [11;16;138]. Other groups use insertion speeds in between (i.e. 2 mm/s) these two extremes [26;27].

The method of insertion has also been a source of differing opinions. Some groups insert the electrodes by hand [9;22;26;32;141], while other utilize microdrives to make the delicate insertions and cite such custom built or commercially available devices as a major factor behind the success of their experiments [11;20;26;142]. Edell et al. suggested that maintaining an alignment between the electrode shaft and the axis of insertion was essential by calculating that a 1° misalignment in a 1 mm insertion can cause a 17 µm slash through the tissue at the insertion site, however, no experimental evidence was offered to substantiate this point [28]. Kewly et al. point to a misalignment of the probe shaft relative to the insertion axis as the major factor contributing to poor signal strengths of some implanted probes in their study [194].

Several strategies have been employed to minimize the foreign body response via adjustments to electrode implant attachments to limit micromotion. One recent study found that even normal breathing results in surface micromotion of the brain on the order of 10-30 μm [206]. One source of electrode micromotion can be the link between the electrode and its connector. A flexible polyimide connection between the rigid electrode and the connector cable was utilized in one set of experiments [205], while another group used a flexible printed circuit board to overcome the problem of micromotion [193]. Another set of experiments revealed that adhesions had formed between a UEA implant and the dural tissue above the brain, possibly due to a robust foreign body response mediated by micromotion of the implant relative to the dura [21]. Placing a Teflon sheet between the array and the dura, and a sheet of Gore-Tex® between the dura and the cranium in subsequent experiments significantly improved the performance of the electrode array over the course of nine months [11]. The Teflon sheet also affected implant migration within cortical tissue, a cause of signal degradation cited by another group that had observed longer microwires losing neuronal signals before their shorter counterparts within the same electrode array [22].

## *2.4 Strategies to Minimize the Immune Response to Implanted Electrodes*

With different electrode array technologies, machining options, biocompatible materials and implantation procedures available, various groups have altered the design of electrodes in an attempt to minimize or evade the immune response. Investigators better acquainted with the molecular biology of the neural environment have also added bioactive agents to the material science repertoire of electrode designers. This intersection of neural immunobiology and electrode design holds considerable promise for developing reliable and useful probes.

### 2.4.1 Material Science Strategies

The materials science and biocompatibility of packaging materials for sensors outside of the CNS has been reviewed previously [207-210]. The majority of previously attempted strategies for limiting the immune reaction to electrodes implanted within the CNS also revolve around material science and physical/mechanical approaches. Electrode size, shape and cross-sectional area have been modified to elicit the smallest possible tissue response. Some reports give significant weight to the texture of an implant [10]. Other studies stress the importance of electrode tip shape [20;28]. However, a study by Szarowski et al. downplayed the importance of electrode shape, size, texture, and tip geometry [26]. The study compared the immune response to silicon implants of different sizes, surface characteristics, and insertion techniques (Figure 8) through GFAP, vimentin, and ED1 immunostaining over the course of 12 weeks. Electrodes of three sizes (2,500$\mu m^2$, 10,000 $\mu m^2$, and 16,900 $\mu m^2$ cross sections), three cross sectional shapes (trapezoid, square, ellipse), two surface textures (smooth and rough), two tip geometries (sharp blade-like point, rounded tip), and two insertion methods (hand, precision drive) were tested in rats. Glial staining revealed that while there were minor temporal differences (on the order of 1-3 weeks) in the time course of the glial scarring, at 6 and 12 weeks post implantation the tissue response to all of these electrodes was essentially identical. The study concluded that while the various geometries may affect the initial wound healing response, glial scar formation was not affected, however, the lack of observable differences may have been due to the low animal number, a lack of controls and variability of response form animal to animal. Although different materials were not tested by Szarowski et al., other experiments have not shown any significant reduction in the immune response with various metals [203] or other materials such as DLC [202]. Such studies support the shift from a materials science strategy in evading the immune

response to strategies focusing on the molecular and cellular biology of the immune response. Only recently has a study shown that the mechanical design of the electrode can make a difference, with very thin electrode surfaces (4 µm square) producing less scarring within 25um of the probe as compared to the scarring found next to a 48 µm square surface [211].

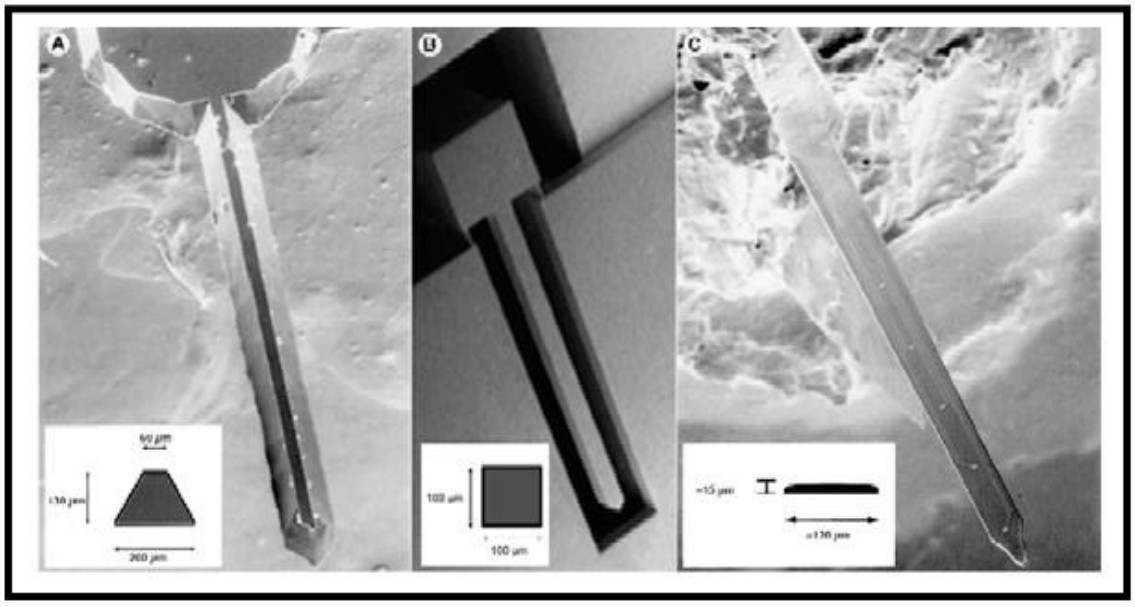


**Figure 8: Different sizes, shapes and cross sections of electrodes that produced the same foreign body response and glial scar, suggesting that strategies to improve biocompatibility through purely structural changes in the implant may be ineffective by themselves. From [26].**

## 2.4.2 Bioactive Molecule Strategies

With material science strategies failing to eliminate glial encapsulation, a failure that parallels sensor implants outside the CNS, a number of investigators are examining approaches that manipulate the biological response. Since the proximity of neurons correlates directly with signal strength, strategies that attract, attach, or preserve neurons near recording sites could minimize or

reduce the effect of the immune response on electrode performance. Such strategies have focused on coating electrodes with bioactive molecules such as cell adhesion promoting polypeptides or proteins. Neurons use environmental cues to grow, migrate, and stay viable. Some of these cues are in the form of polypeptide motifs on extracellular matrix proteins or on membrane bound molecules of neighboring cells. In addition to intact cell adhesion proteins such as collagen and fibronectin [203], several groups have employed cell adhesion peptides, such as RGD [212], found in many extracellular proteins, YIGSR [31;212] and IKVAV [212], found in laminin, and KHIFSDDSSE [212], found on NCAM (neural-cell adhesion molecule). Studies to establish neuronal reactions to these proteins and peptides have been conducted in-vitro. Ignatius et al. found that poly-D-lysine (a synthetic polypeptide that enhances neural cell adhesion) and laminin, when co-absorbed on various metals and glass, greatly improved cell attachment, spreading, and growth as compared to uncoated metals. Polyimide, the common insulating material discussed earlier, is also amenable to surface modification with bioactive molecules. Recent studies by Martin have focused on using conducting polymers of polypyrrole and poly(3,4-ethylenedioxythiophene) to provide better contact and a larger surface between the electrode and adjacent neuronal tissue [31;197;213]. These polymers can be "grown" in a controlled manner through an electrochemical process at the electrode recording sites and can easily incorporate bioactive molecules. Electron micrographs of the sites reveal finger-like fibers of polymer growing out of the gold electrodes, creating a "fuzzy" surface with a large surface area to maximize neuron-electrode interactions. The incorporation of the coatings resulted in lower impedance, slightly more active sites, and significantly more high quality units with SNR > 4 [214]. However, the effect of the coating decreased over time because of the glial scar[214]. Cui et al. incorporated the YIGSR peptide fragment from laminin into the polypyrrole coated recording sites [31;197]. The peptide-coated sites supported more neuron attachment in vitro

compared to peptide-free sites [197]. When the peptide-incorporated and peptide-free electrodes were chronically implanted in guinea pigs, 83% of peptide-incorporated vs. 10% of peptide-free electrode sites showed evidence of neuronal process proximity after 1 week, but the two types of implants produced similar recordings and exhibited similar glial scar reactions [31].

Bioactive molecule surface coatings have also been used to either attract or repel glial cells. Neurons in culture will grow on astrocyte monolayers and neuronal processes will extend along tracks provided by astrocytes, oftentimes regardless of the material beneath the astrocytes [215;216]. Attraction of astrocytes and other glial cells could potentially anchor the electrodes in the neural tissue and prevent micromotion, or even block negative components of the glial response [212]. Kam and colleagues found that astrocytes adhere preferentially to glass substrates covered with NCAM as compared to other adhesion molecules. A separate study found that astrocytes also prefer silk-like polymer fragments with fibronectin domains over laminin YIGSR domains, which are preferred by neurons [197]. Robust growth of glial cells on laminin, collagen and fibronectin coated surfaces was also observed [203]. Shain and colleagues have attempted to control and pattern astrocyte adhesion through the deposition of hydrophobic and hydrophilic self assembling monolayers of organosilanes using photolithography and microcontact printing [217-219]. Photolithography also allows the manufacture of silicon pillar arrays of varying dimensions [11;217;220], which are consistently preferred to smooth silicon by glial cells in vitro. Other studies have tried to prevent astrocyte adhesion in an effort to reduce or eliminate glial scar formation. Singh et al. found that a dextran coating of DLC-poly-lysine surfaces reduced glial cell adhesion more than 50 fold to 1.4 ± 1.2% of control surfaces [202]. The study however, was performed using cell lines in vitro, and did not address how such a coating would affect neurons and microglia. Whether such approaches work in vivo has not been determined.

Aside from helping neurons adhere to the electrode recording pads, a more active approach may be to release growth factors or chemoattractants to promote neuronal survival and growth towards the electrode. Numerous chemoattractants and trophic factors act during brain development to facilitate the creation of neural circuits, but growth factor based strategies have generally been disappointing in the adult CNS [221]. One promising result was obtained by Kennedy over 15 years ago when he seeded a standard glass pipette electrode with a piece of sciatic nerve and observed what happened upon chronic implantation of the so called "cone" electrode [201]. Neural processes from surrounding neurons grew into the electrode tip and this ingrowth could be tracked by the recorded signals. The recorded SNR was often 5-10 times that obtained with wire and silicon electrode arrays and continued for over 12 months, while control electrodes without the sciatic nerve insert showed no neurite ingrowth. Furthermore, the amount of this ingrowth and the resultant single versus multi-unit activity could be controlled by adjusting the size of the cone tip opening. Putatively, the sciatic nerve tissue released growth factors or chemoattractants that caused neurite ingrowth while the electrode design shielded the neurites from the foreign body response and from external electrical noise. Clearly this design cannot be scaled easily to electrode arrays for neural prosthetics, and explanting pieces of PNS tissue for such an array is prohibitive. As a proof of concept however, Kennedy showed the promise of soluble factors in attracting and retaining high quality neural signals.

Standard wound healing suppression and immunosuppression techniques are also options for minimizing the initial immune response and perhaps even the glial scar formation. Both local and systemic administration of corticosteroids and other drugs has been shown to reduce the wound healing response for implants outside of the CNS [222;223]. Upon implantation of the UEA into

cats by Maynard et al., two doses of Dexamethasone, a potent suppressant of the wound healing response, were administered 12 hours before surgery and again during surgery to control cortical edema, resulting in considerable improvements in implant performance [11]. While promising, the success was likely due to the implantation of the previously mentioned Teflon sheet. Shain et al. found that peripheral injections of Dexamethasone at the time of electrode insertion greatly attenuated glial scar formation at 1 and 6 weeks as shown by GFAP staining [148]. Some attenuation was seen with local release of Dexamethasone from implanted poly (ethyl-vinyl) acetate strips, but at 6 weeks post-implantation the effect was minor. A peripheral injection of Cyclosporin-A, another potent anti-inflammatory agent, in the same study seemed to increase the glial response. Recently, Dexamethasone released from a nitrocellulose coated implant significantly attenuated GFAP expression, neurofilament loss, and early microglial activation around the injury site [224]. Another group has incorporated NPC's into a coating for neural probes with mixed results [225].

With the surprising success of Kennedy's cone electrode came an equally surprising failure. When the same micropipette electrode was filled with a solution of neural growth factor (NGF) in various concentrations to mimic the effect of the sciatic nerve used in the successful trials, no ingrowth was observed [201]. Instead, a cystic cavity formed around the glass cone electrode, which the author attributed to hyperplastic growth of surrounding tissue that eventually outgrew its blood supply. This failure highlights the importance of developing appropriate drug delivery systems that can capitalize on the positive effects of growth factors or chemoattractants. The normal difficulties of delivering drugs to the CNS are compounded with the difficulties in delivering bioactive molecules over long implantation periods. Current delivery methods include polypyrrole grown on electrode pads and polypeptide-doped polyimide coatings [31;197]. Wells

etched into the polyimide electrode developed by Rousche et al. were filled with dextran as a proof of concept, but could potentially hold other diffusible compounds or hydrogels [10]. Chen et al. have attempted to address this drug delivery problem with the development of "puffer" probes that incorporate microfluidic channels inside of the electrode shank [196]. These bulk machined silicon probes have multiple 10 μm channels for chemical and drug delivery from orifices situated 2.5 μm from recording sites. There is currently no gating apparatus at the orifices to control of fluid release, but the authors suggest a shutter mechanism is being explored [196].

## *2.5 Barriers to developing a stable tissue-electrode interface*

### 2.5.1 Unanswered questions

In the 25 years since the idea of using neural signals to control an external prosthetic first surfaced[226], enormous strides have been made in understanding the neuronal circuitry of the relevant brain structures, developing the computer hardware and software algorithms capable of transforming the neuronal potentials into control signals, and in engineering high density recording arrays[17]. In contrast, there are a number of fundamental and unresolved questions as to the source of signal degradation in chronically implanted neuroelectrodes. Is it the result of insertion trauma, micromotion, mechanical mismatch, or simply the consequences of glial scar formation arising from a normal chronic foreign body response? What roles do electrode size, shape, surface chemistry, mechanical impedance, and insulating material play? What is the fate of neurons adjacent to the recording site as the signal degrades? Are they silenced, killed, or just pushed out of the way by the glial scar? Do these effects arise from inhibitory cues expressed in the glial scar, or by the inflammatory molecules released into the vicinity of the electrode? The

answers to these questions are largely unknown for two reasons. First, the current in vivo model of tissue compatibility assessment is simply too uncontrolled, not capable of real time specimen assessment, and not suited for iterative or combinatorial testing. Second, there are no reliable in vitro models that accurately mimic the brain tissue reaction to implanted electrodes and that allow for a controlled experimental environment to directly observe, in real time, the cellular and molecular mechanisms behind electrode failure.

### 2.5.2 Biocompatibility evaluation and models

The in vitro testing of material modifications for neuroelectrodes has been minimal, and is usually entirely forgone in favor of in vivo testing. The general experimental pattern involves creation of a new microelectrode design aimed at evading or overcoming the tissue response, implantation of the new design into an animal model (typically a rat model), sacrificing the animal at various time periods, and assessing the extent of the tissue reaction surrounding the implant. Any in vitro testing of the new microelectrode design, if performed at all, typically consists of recording impedance changes at the electrode sites while the electrode is in a saline solution, or basic cytotoxicity tests involving cell lines such as 3T3 fibroblasts grown on the electrodes. For a more in depth treatment of this topic, please refer to the appendix.

Some glial scarring models have been developed to study the biological reaction that occurs after CNS damage. Previously, the primary concern for researchers has been to stimulate the growth of axons across a scar (as in spinal cord injury), so most of these models have focused on the inhibitory proteoglycan extracellular matrix that is deposited within the glial scar. One such model involved implanting nitrocellulose filters which accumulated the deposited ECM,

explanting the nitrocellulose after the scarring response, and monitoring neurite growth in vitro across the filters [173;227]. Layered alginate hydrogels with grafted chondroitin sulfate proteoglycans [228] or proteoglycan gradients on nitrocellulose [229] have also been used as a model of the glial scar to study neuron process retraction in response to the scar. Some in vitro testing of biomaterials for neural implants has also been conducted, but primarily with cell lines or one cell type. For example, it was found that covalently attaching TGF-b to laminin coated on a biomaterial reduced proliferation of an astrocyte cell line [230]. In vitro "scrape" or "scratch" wounds (detailed in chapter 2) have also been conducted, but with just one cell type or cell line [116;231-233].

David Martin's group at Michigan developed a promising conducting polymer with the capability to display peptide sequences including the laminin YIGSR domain[197]. They showed preferential attachment to the recording sites by a rat glial cell line (C6) and a human neuroblastoma cell line (SH-SY5Y) after 3 days in vitro and implanted the polymer coated electrode into guinea pigs to assess biocompatibility. A drop in electrode performance was observed between 1 and 2 weeks and no functional data was recorded after 2 weeks. Stephen Massia's group at Arizona State University tested their microfabricated dextran coated probes with 3T3 fibroblasts before implantation[202]. Bill Shain's group at the Wadsworth Center in New York has conducted many in vivo studies to develop a time course for the development of a glial scar, but they have only conducted short term adhesion studies with an astroglial cell line or rat skin fibroblasts on different surface chemistries and electrode materials[212;217;218;220]. Daryl Kipke's group, also at Michigan, has conducted several excellent in vivo studies tracking the stability of the recordings obtained from different electrode designs, but they provide no in vitro testing beforehand [9;13;193]. The UEA developed by Richard Normann's group

consistently provides some of the most reliable recordings in vivo, but no in vitro studies have been presented to help explain the failures that inevitably occur [11;21;138;234;235]. In all of these studies, a new electrode design that promised to reduce the tissue response around the recording sites was tested in the uncontrolled environment of a living animal. The studies involve large expenditures of time, money, and animals, and provide little information regarding the reasons behind implant failure.

Certainly in vivo testing has provided a wealth of information regarding recording electrode stability and mechanisms of failure, yet the potential for a relatively cheap, quick, controllable and reproducible in vitro model has not been fully utilized. Unfortunately the problem of electrode stability in vivo still persists, and an in vitro model that accurately reproduces in vivo electrode-tissue interactions would be an invaluable addition to current in vivo biocompatibility studies.

# Chapter 3: Development and characterization of an in vitro model of glial scarring around neuroelectrodes chronically implanted in the CNS

## *3.1 Introduction*

This chapter presents the first in vitro model of glial scarring capable of recreating many of the hallmarks of the tissue reaction to chronically implanted neuroelectrodes observed in vivo. This cell culture system has been adapted from a primary neuron-glia culture used to study neuroinflammatory processes for the past 15 years and contains all of the brain cell types known to play a major role in this tissue reaction. The cellular responses of neurons, astrocytes, and microglia to injury were characterized using immunocytochemistry. Mechanical injury, in the form of a scrape to the confluent cellular layers, and chronically placed stainless steel microwire, mimicking the presence of a foreign body, resulted in cellular responses that were similar to those documented in vivo. This system is a first step in allowing experiments that mechanistically explore the biological phenomena behind glial scarring and the resulting implant failure.

## *3.2 Materials and Methods*

### 3.2.1 Reagents

Cell culture ingredients were obtained from Invitrogen (Carlsbad, CA, USA). Monoclonal antibodies against the CR3 complement receptor (OX-42) and against MAP-2 were obtained from

Chemicon (Temecula, CA, USA). Polyclonal antibody against IBA-1 was obtained from Wako Chemicals USA, Inc. (Richmond, VA, USA). Polyclonal antibody against glial fibrillary acidic protein (GFAP) was bought from DAKO Corporation (Carpinteria, CA, USA). Monoclonal antibody against vimentin was bought from Sigma-Aldrich (St. Louis, MO, USA). The Vectastain ABC kit and biotinylated secondary antibodies were purchased from Vector Laboratories (Burlingame, CA, USA). 50 µm diameter stainless steel microwire was bought from A-M Systems (Carlsborg, WA, USA). Secondary antibodies with fluorescent tags Alexa 594 and Alexa 488 were bought from Molecular Probes (Invitrogen Corporation, Carlsbad, CA, USA).

### 3.2.2 Animals

Timed-pregnant Fisher F344 rats were obtained from Charles River Laboratories (Raleigh, NC, USA). Housing and breeding of the animals were performed in strict accordance with the National Institutes of Health guidelines at the National Institutes of Environmental Health Sciences (Research Triangle Park, NC, USA).

### 3.2.3 Primary mesencephalic neuron-glia cultures

Neuron-glia cultures were prepared from the ventral mesencephalic tissues of embryonic day 14–15 rats, as described previously [236]. Briefly, dissociated cells were seeded at 5 x $10^5$/well into poly-D-lysine-coated 24-well plates. Cells were maintained at 37°C in a humidified atmosphere of 5% $CO_2$ and 95% air, in minimal essential medium (MEM) containing 10% fetal bovine serum (FBS), 10% horse serum (HS), 1 g/L glucose, 2 mM L-glutamine, 1 mM sodium pyruvate, 100 µM nonessential amino acids, 50 U/mL penicillin, and 50 µg/mL streptomycin. Seven-day-old

cultures were used for treatment after a media change to MEM containing 2% FBS, 2% HS, 2 mM L-glutamine, 1 mM sodium pyruvate, 50 U/mL penicillin, and 50 µg/mL streptomycin. Data shown are representative of at least 3 different culture preparations.

### 3.2.4 Scrape (Mechanical Injury) Model

At treatment time, a rectangular area in the middle of the culture well, approximately 2 mm on each side, was cleared of cells with a 2 mm long scrape of the tip of a cell scraper (#3010, Corning Inc., Corning, NY, USA). The injury was inflicted after the media change so that soluble factors released during the injury were present.

### 3.2.5 Wire (Foreign Body) Model

Wire (50µm diameter) was cut into 3-5 mm pieces and soaked in 70% ethanol for at least 30 minutes, after which it was allowed to dry in a laminar flow hood. At treatment time, 3-4 pieces of wire were placed into each treatment well at random locations using sterile forceps, so that the pieces would sink and rest atop the cultured cell layer.

### 3.2.6 Immunostaining

Microglia were detected with the OX-42 or anti-IBA-1 antibody, which recognizes the CR3 receptor as described [237], astrocytes were detected with an antibody against GFAP and neurons were imaged by staining with MAP-2 as described previously [238;239]. Immature glia were

detected with an antibody against vimentin. Briefly, formaldehyde (3.7%) -fixed cultures were treated with 1% hydrogen peroxide (10 min) followed by sequential incubation with blocking solution (20 min), primary antibody (overnight, 4°C), biotinylated secondary antibody (1 h), and ABC reagents (1 h). Color was developed with 3,3'-diaminobenzidine. Images were recorded with an inverted microscope (Nikon, Tokyo, Japan) connected to a charge-coupled device camera (DAGE-MTI, Michigan City, IN, USA) operated with the MetaMorph software (Universal Imaging Corporation, Downingtown, PA, USA). Fluorescently labelled cultures were stained in the same way, except a fluorescently labelled secondary antibody was used in place of ABC reagents. Fluorescent images were recorded with an inverted microscope (Nikon, Tokyo, Japan) connected to a charge-coupled device camera (Sensicam QE, Cooke Corporation, Romulus, MI, USA) operated with the IPLab software (Scanalytics, Rockville, MD, USA).

### 3.2.7 Patch Clamp Recordings

Patch-clamp was performed under IR-DIC visual control at room temperature, in the treatment medium. Whole-cell patch-clamp recordings were achieved using glass electrodes (4–10 MΩ) containing the following (in mM): 140 KmeSO4, 10 HEPES, 4 NaCl, 0.1 EGTA, 4 Mg-ATP, 0.3 Mg-GTP, and 14 phosphocreatine. Data were acquired in current-clamp mode using a Multiclamp 700B amplifier (Axon Instruments, Foster City, CA). Data were digitized using a custom software written using LabView 6.1 (National Instrument, Austin, TX), and data were acquired with a PCI16-E1 data acquisition board (National Instrument). The data acquisition rate was 10 kHz. Stimuli were designed on-line, or off-line as text files. All experiments were performed in accordance with animal protocols approved by the National Institutes of Health. Data shown are

representative of 5 cells recorded from two different culture preparations. Data were analyzed off-line using MATLAB (MathWorks, Natick, MA) and Excel (Microsoft Corp, Redmond, WA).

## *3.3 Results*

### 3.3.1 Scrape Model

To characterize the response of the neuron-glia culture to a mechanical injury of the sort experienced by neural tissue upon implant insertion, cultures were scraped with a cell scraper to create an area empty of cells and filled with cell debris. Using immunocytochemistry to stain for different cellular markers, the time course of the cellular response for astrocytes and microglia is shown in Figure 9. GFAP positive astrocytes (arrows) begin to extend short processes into the wound area at 6 hours post injury, extend their processes considerably through 24 hours and 48 hours, and by 7 days have completely repopulated the wound area, expressing an activated, enlarged phenotype. Microglia enter the wound site much quicker (in as early as 1 hour) and by 6 hours have already spread out within the wound. The microglial cell numbers increase throughout the 7 day time course as they are attracted by the open space, the chemoattractants released by other microglia, or to the cell remains within the Scrape. By 48 hours, there are more microglia inside of the scrape wound than in the surrounding tissue, as microglia migrate into the wound and line up along the striations of cell remains created by the cell scraper. Neurons, however, do not grow back into the wound area, even after it is repopulated by astrocytes, although some processes are extended beyond the initial boundary of the Scrape injury (data not shown). GFAP-/vimentin+ astrocyte precursor cells (arrowheads, Fig 1A) can be faintly seen (due to background staining) as spindle shaped cells migrating ahead of the astrocyte processes at 6 hours, spreading

inside the wound at 24 and 48 hours, and, after maturing and upregulating GFAP, eventually resulting in a carpet of activated GFAP+/Vim+ astrocytes at 7 days.

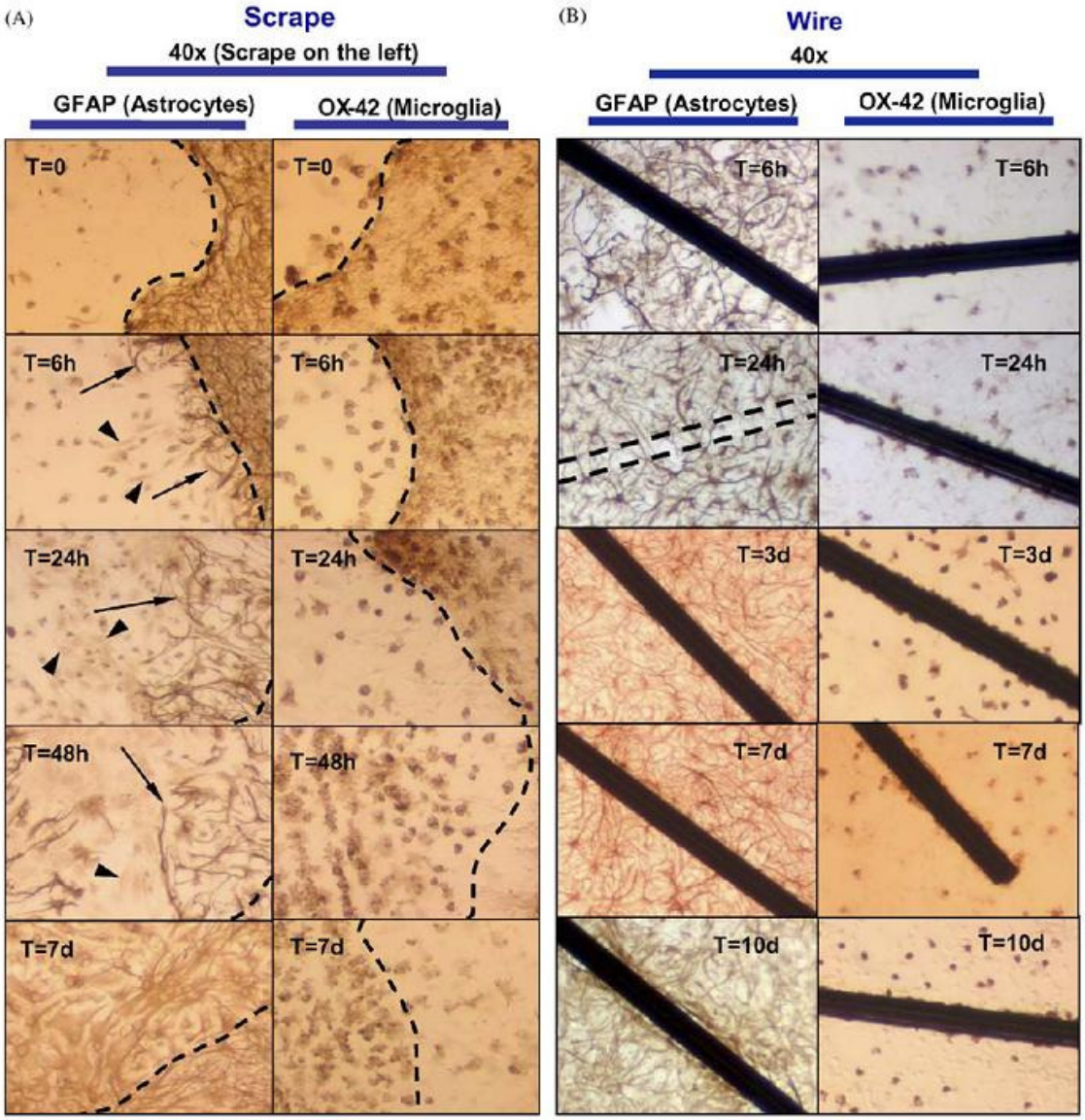


**Figure 9: A) Time course of cellular events in response to the Scrape wound. The area scraped free of cell is on the left of the dotted line. The left panel shows the time course of astrocytes as stained for GFAP and the right panel shows the microglial response over time as stained for MAC-1 (OX-24 antibody). Astrocytes are seen to send processes (arrows) into the wound beginning at 6 hours and continuing through 48 hours, and completely re-colonize the wound by 7 days. GFAP negative spindle-shaped precursor cells (arrowheads) that do not stain for microglial markers but stain for vimentin (not shown) migrate into and colonize the wound ahead of the GFAP positive processes.**

**Microglia migrate to and spread out within the wound by 24 hours and their numbers increase over time, until by 7 days there are more microglia inside the wound than in the surrounding culture. B) Time course of cellular events in response to the Wire placement. Microglia attach to the wire as early as 6 hours and increase in numbers until a layer of microglia 1-2 cells thick is formed covering the length of the wire. This layer remains through 10 days in culture. Astrocytes show now response to the microwire until 7 days after treatment, when the beginnings of a response may be seen. By 10 days after treatment, a layer of activated astrocytes with upregulated GFAP forms around the microwire, mimicking the glial scarring seen in vivo. The dotted lines at T=24h shows the location of a microwire that had floated away during the staining protocol.**

### 3.3.2 Wire Model

To characterize the response of the neuron-glia culture to a chronic foreign body placement, 3-4 pieces of 3-5 mm long, 50 μm diameter stainless steel microwire were placed into each treatment well with forceps and allowed to sink onto the cell layer. The wire is of the size and type commonly used by neurophysiologists to make in vivo recording arrays. Immunocytochemistry was again used to identify the cellular response to these model electrodes (Figure 9B). Microglia migrated to the microwire and sat atop the wire as early as 6 hours after wire placement. The number of microglia on the wire increased over time until the entire wire was coated with a layer of cells. This microglial layer remains for as long as the cultures have been maintained (14 days post treatment), although at later times the cells express a larger, rounded phenotype indicative of multinucleated giant cells. Astrocytes do not seem to respond to the microwire until around 7-10 days post treatment, at which time they begin to form a cellular sheath reminiscent of the glial scar around the microglia coated wire. A more detailed look the scar formation (Figure 10) shows that there is a wide variation in the intensity of scar formation around different wires, and in fact around different parts of the same wire. Furthermore, the in vivo layering of astrocytes surrounding a microglial core sitting atop an implant is maintained in this culture system as seen in Figure 11A and 11B. Previous in vivo studies have also shown upregulation of vimentin, a

structural protein expressed in immature cells, around glial scars. Staining for vimentin revealed it to be a useful marker for glial activation around the microwire, as vimentin was highly upregulated in the astrocyte processes forming the glial scar (Figure 11C).

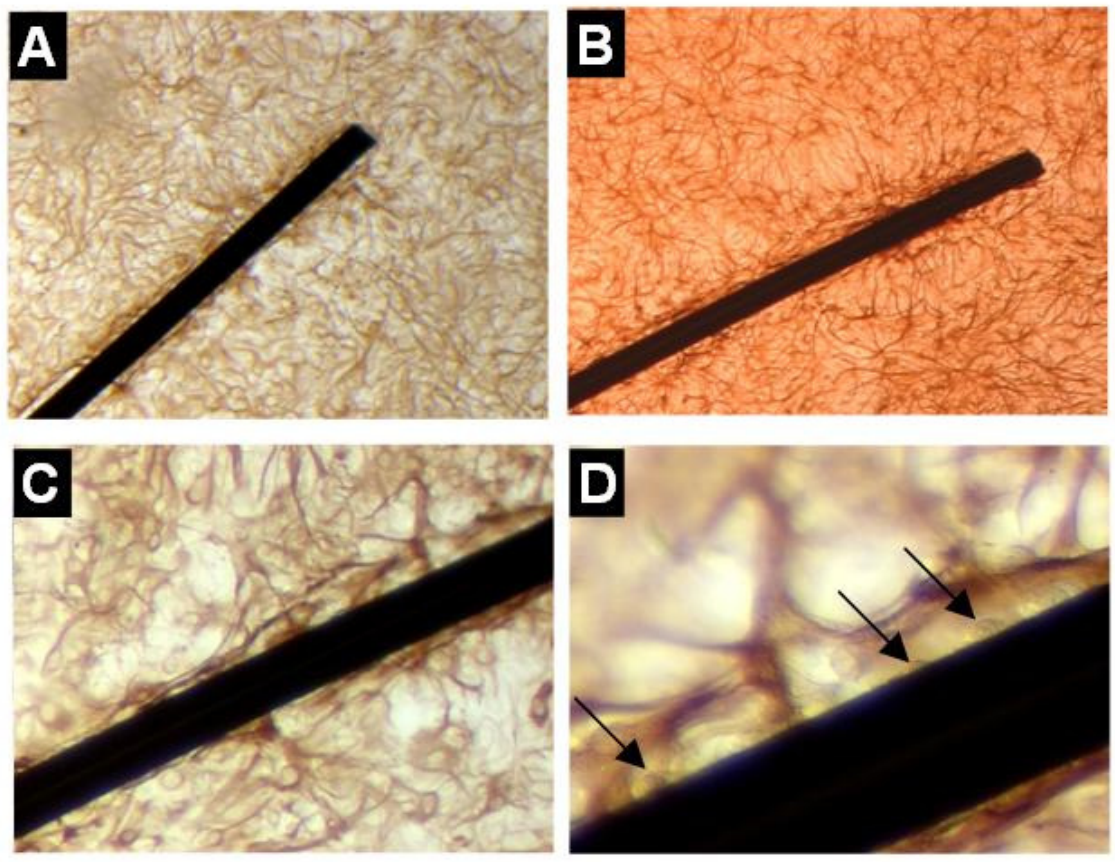


**Figure 10: Detail of the astrocyte glial scarring response to microwires placed in culture. All images are of cultures fixed 10 days after wire placement and stained for GFAP. For size reference, all wires are 50 µm in diameter. A-B) Astrocyte processes with upregulated GFAP surround a microwire along its entire length in a pattern similar to that seen in vivo around recording electrodes. C-D) Higher magnification images of glial scarring in A). Unstained cells (microglia) can be seen sitting directly on the wire inside of the GFAP positive processes (arrows).**

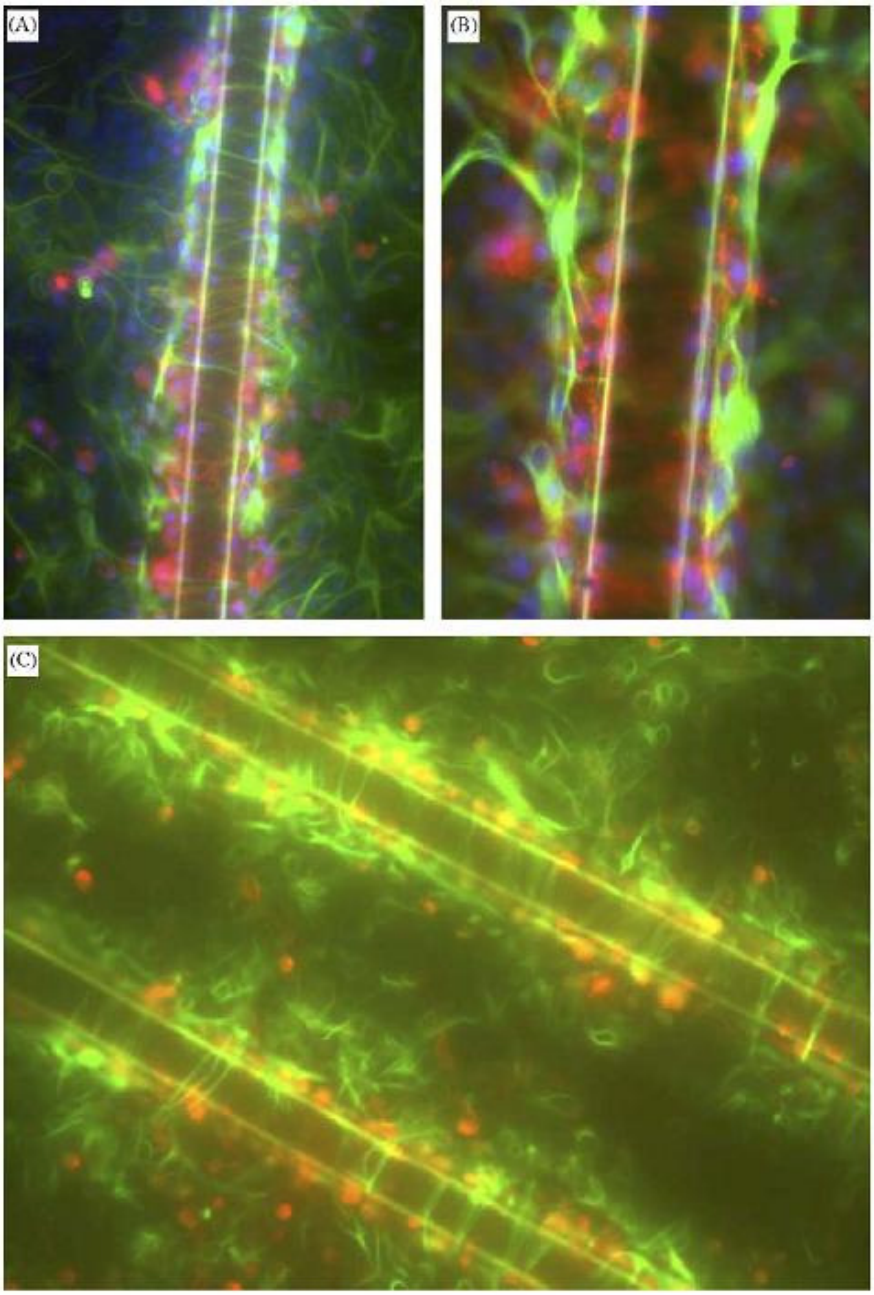


**Figure 11: A-B) Triple fluorescent labeling with DAPI staining nuclei blue, GFAP staining green, and OX-42 staining microglia red shows the relative positions of different cells near the wire after 10 days in culture. Just as observed in vivo, there is a layer of microglia (Red) adjacent to the microwire and astrocytes (Green) outside of the microglial layer showing upregulated GFAP. The image in B) shows the glial scarring at a higher magnification, clearly visualizing the prevalence of microglia around the microwire. For reference, the wire diameter is 50 µm in all images. C) Dual fluorescent labeling with Vimentin staining immature/activated astrocyte processes green and OX-42 staining microglia red. The layer of microglia sitting on the wire is surrounded by a bright halo of vimentin positive astrocyte processes forming the glial scar 10 days after wire placement.**

Staining for MAP-2 revealed that neurons are not affected by their proximity to the wire, as both neuronal soma and processes were maintained in the same density next to the wire as in areas of the culture away from the foreign body (Figure 12A). To verify whether the neurons in culture were healthy and electrically active, patch clamp recordings on individual neurons were performed. Neurons were identified by morphological markers and patch clamping was performed on neuron-glia culture preparations, at different post treatment time points, while the cells were in their treatment medium. Action potentials were clearly distinguishable (Figure 12C) and had a physiologically accurate shape profile (Figure 12D). Finally, it was confirmed that the neurons would respond to stimuli such as a depolarizing current by electrically activating the cells into producing action potentials (Figure 12E).

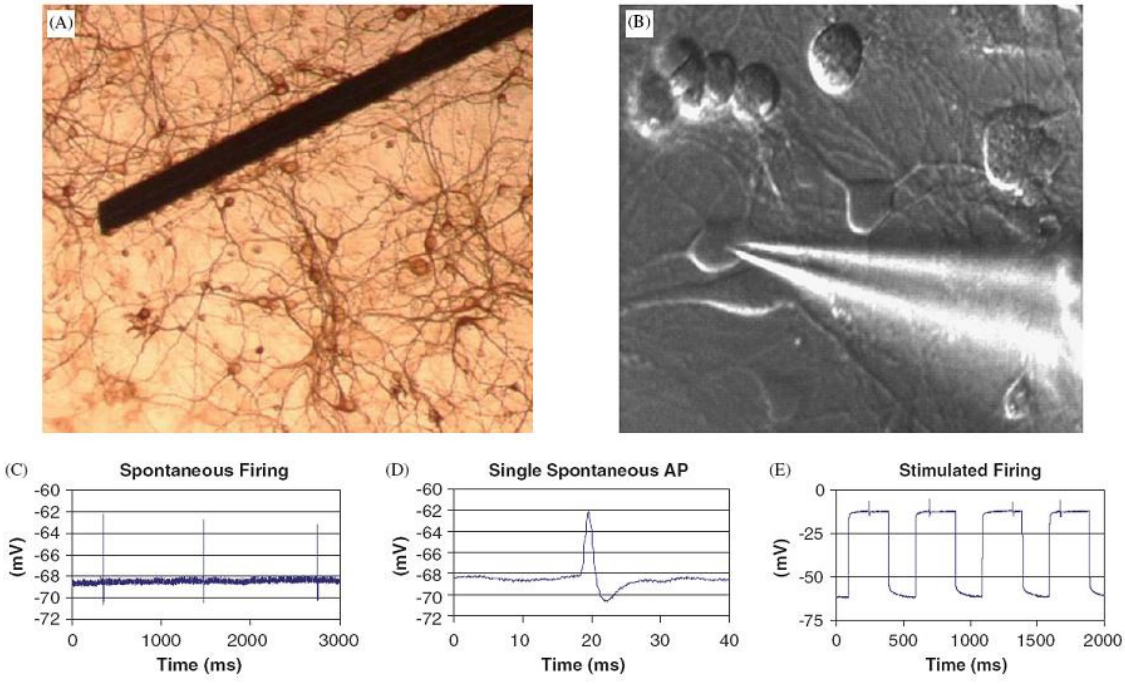


**Figure 12: Neuronal responses in the culture. A) MAP-2 staining shows a network of neuronal processes and soma that are not affected by the microwire 14 days after it was placed in culture. B).**

**Light microscope image of the microelectrode in a patch clamp on a neuron within the neuron-glia culture. C) Spontaneous firing of a neuron in a current clamp mode trace in which three action potentials are clearly seen D) A higher resolution picture of the first action potential in C, showing the physiologically accurate shape of the action potential. E) The clamped neurons could be activated with depolarizing current. Four action potentials can be seen in response to the four depolarizing steps.**

## *3.4 Discussion*

The development of implantable neuroelectrodes is following the well-worn path of all implantable biomedical sensors and electrodes; i.e. employing in vivo assessment for determining device suitability for chronic implantation. In vivo implantation studies are time consuming, expensive, and nearly impossible to control down to a level where the molecular mechanisms of implant failure can be understood[240]. The result is that innovations addressing implant-tissue compatibility invariably lag behind innovations in electrode design. This in vivo experimental paradigm has produced only incremental improvements in neuroelectrode tissue compatibility because it is used for what it does poorly, the primary screening of implant modifications, rather than for what it does well, the validation of implants that were pre-screened in vitro.

This chapter presents a novel in vitro model of the tissue response to chronically implanted neuroelectrodes. The model is an adaptation of the neuron-glia culture system developed over the past 15 years in the laboratory of Dr. J.S. Hong for examining the neuroinflammatory mechanisms behind neurodegenerative diseases. The strength of the system is the physiologically relevant mix of neurons, astrocytes, and microglia that cannot be replicated by traditional cell-line based in vitro systems. Furthermore, this culture system has been verified by numerous in vivo studies, lending credibility to the in vitro data [237;241;242]. As a result, the culture system is able to reproduce many of the hallmarks of the glial response to implanted neuroelectrodes.

The relative locations of the astrocytes and microglia and the time course of their responses in both the scrape and the microwire models correlate well with previously published in vivo data. Microglia are know to be the first responders to any injury in vivo as they constantly sample their local environment and migrate through neural tissue[23;139;243;244]. Therefore, it is not surprising that microglia were seen inside the scrape wound and atop the microwire in the first time points assayed, 1 hr and 6 hrs respectively. The commonly observed microglial accumulation at the site of injury was also seen in this culture system as microglia increased both within the mechanically damaged area and near the wire to levels that were visibly higher than in the surrounding culture. As observed in vivo, the response of the astrocytes followed that of the microglia. Astrocytes present at the borders of the scrape extended their processes into the empty area and continue to elongate those processes over several days. However, the majority of astrocytes populating the interior of the scrape after 7 days are morphologically distinct from the astrocytes in the rest of the culture. Typically, the astrocytes are thickened, have fewer processes, and arise from the Vim+/GFAP- precursor cells that migrate into the wound. Vim+/GFAP- cells have been shown to form a thin sheath around implanted electrodes in the region that is interior to the majority of the astrocytes forming the glial scar. The distribution of cells responding to the scrape correlates well to the concentric profiles of cells around the probe: an inner layer of microglia, an intermediate layer of Vim+/GFAP- cells, and an outer layer of astrocytes. The concentric profiles are also seen around the microwire, where microglia form the inner core of the glial scar and the astrocytes form the outer region. Although increased vimentin staining was seen around the microwire, a tight concentric ring was not observed. Every stainless steel microwire placed in culture thus far has developed an adherent layer of microglia, yet there is visible variation in the astrocyte response to the microglia coated microwire. Some microwires develop a

thick scar while others have only a few highly GFAP+ astrocyte processes around the foreign body. There is even variation on each microwire, with some sections of the microwire having thicker scarring than other sections. This variability may be a cause of concern in developing a reproducible in vitro model, however the in vivo response has been shown to be just as variable, if not more variable[21;28;141]. The variability of the in vivo tissue response has also been linked to the unreliable recording capabilities of implanted electrode arrays[13].

There is a clear difference between embryonic and adult mammalian CNS responses to injury[167-169]. Embryonic cells regenerate readily from mechanical insults and do not produce a typical glial scarring response[171;172]. One line of experiments has pointed to a critical period of development around postnatal week two or three after which a mature glial scar is capable of forming[171;174]. The embryonic day 14 cultures described in this paper are prepared before this critical period and may not fully represent the adult scarring environment. However, cultures preparations after the critical period are severely limited in their utility and relevance as the minimal regenerative potential of adult cells leaves only the most hardy, highly activated glia while all of the neurons and most of the glia die off. This culture system also does not contain vasculature, which has been shown to play an important role in the glial scarring process[245], although the presence of serum in both the growth medium and the treatment medium may help to alleviate this deficiency. Although there will always be differences between an in vitro culture and the in vivo environment, the similarities between the glial response in this culture to an in vivo mechanical injury or to a foreign body implantation suggest that these embryonic cultures are capable of providing useful insights into the scarring process.

The response of this in vitro system that contrasts most with some observed in vivo scarring

processes is the neuronal behavior. The neurons in this culture seem to be unaffected by the proximity of activated glial cells responding to both the scrape and the microwire. In vivo, neurons have been found to be depleted by an unknown mechanism around a recording electrode, presumably leading to signal degradation over time and eventual implant failure [25;28]. Such depletion was not observed around the microwire or on the boundaries of the scrape. Neurons extended processes around and under the microwire and there was no observable difference in neuronal cell body density around the microglia and astrocytes surrounding the microwire as compared to regions far away from the microwire. Although neurons did not re-colonize the scrape area, bordering neurons sent a few processes into the scrape atop of growing astrocyte processes. The lack of a clear neuronal response could be due to the same enhanced regeneration potential that allows neurons to survive the culture preparation. Alternatively, since the neurons do not survive in culture after 10 days post treatment (17 days post isolation), it may take longer than 10 days to see the neuronal depletion observed in vivo after 4-6 weeks. Also, if the depletion of neurons in vivo around the electrode occurs because the neurons are pushed away by glial cells forming the glial scar, this may not be reproduced in a two-dimensional in vitro culture where cells can grow atop one another and are not limited by three-dimensional space restrictions. However, most likely the lack of vasculature and the lack of micromotion to damage that vasculature and the nearby neurons resulted in healthy neurons adjacent to the glial scar around the microwires. The scrape injury showed that when neurons are killed in a region (i.e. around a microwire moving through micromotion), they do not grow back and the damaged region becomes repopulated with microglia, neural precursor cells, and eventually, scar astrocytes.

To test whether the neurons in this culture system display functional characteristics similar to cells in vivo, patch clamp recordings were performed to assess the activity of the neurons. The

neurons were confirmed to be spontaneously active, maintained a physiologically accurate action potential shape, and were responsive to depolarizing currents. This ability to record electrical signals from the culture bodes well for future work in creating a functional in vitro test bed capable of correlating the tissue reaction to neuroelectrode recording performance (see "Future Work").

## *3.5 Conclusions*

Due to the cost of in vivo experimentation in terms of resources, time, and animals, an in vitro cell culture system which recreates many of the characteristics of the in vivo reaction to chronically implanted neuroelectrodes can provide a significant benefit to the brain implant field as a test bed for novel neuroelectrode innovations and as a way to dissect the complicated mechanisms behind implant failure. Such an in vitro model was developed by adapting a culture system previously used for neuroinflammatory disease research. This culture system contains a physiologically relevant mix of astrocytes, microglia and neurons, resulting in cellular responses that closely mimic the tissue response seen in vivo. The response of the different cell types to a mechanical injury and to a foreign body contacting the cells was characterized in an effort to recreate the acute and chronic injury response seen in vivo. Microglia were observed responding to both types of injuries within a few hours, eventually coating a microwire placed in the culture. Astrocytes filled up the space left vacant by the mechanical injury and upregulated GFAP in a glial scar around a microwire in the culture. Both the time courses and relative positions of the glia in response to the different injury paradigms were similar to the response seen in vivo and the neurons were spontaneously active in culture, suggesting further work in the development of a functional in vitro test bed. However, there was a large degree of variability in the glial scarring

observed in the model. Although this mimics the variability seen in vivo, the protocol needs to be optimized to allow for a robust scar to develop with every culture preparation as a positive control for further mechanistic studies.

# Chapter 4: Optimization of an in vitro model of glial scarring through the rational variation of culture conditions to obtain a consistent, robust glial scar as a positive control for future model use.

## *4.1 Introduction*

The previous chapter described an in vitro, mixed cell culture based system that reproduced characteristic hallmarks of the in vivo glial scar; i.e. microglial activation and attachment to a mock stainless steel microwire electrode, and astrocyte activation beyond the microglial layer in the form of GFAP upregulation. The glial scarring model was unique in that it utilized a mixed primary culture containing neurons, astrocytes, microglia, and precursor cells, thus permitting the glia-glia and glia-neuron interactions normally present in vivo. While this model was able to re-create the glial scar, a phenomenon previously only fully observed in vivo, it was not able to do so reliably. This was in spite of tight control of all culture and dissection conditions. In order to make this in vitro glial scarring model experimentally meaningful, it was necessary to determine the culture conditions that would generate a glial scar positive control in every culture.

In this chapter, the "Original Protocol" developed in Chapter 3 was amended iteratively to increase the baseline level of scarring around microwire. After attempting a number of protocol variations, it was observed that culture conditions that mimicked protocols used for studying neural precursor cells [70;71;92;93;134;246-248] started to generate more consistent scars. The "Base Protocol" is derived from these protocols and served as the first "best guess" in the optimization process. The "Control Protocol" was achieved by systematically varying six critical

parameters of the culture conditions (growth media, seeding density, day of bFGF addition, serum concentration in the treatment media, treatment day, and duration of culture). This study resulted in both the desired positive control culture conditions, as well as a deeper understanding of the requirements for glial scarring, including the requirement of serum and of neural precursor cell growth factors.

## *4.2 Materials and Methods*

### 4.2.1 Reagents

Cell culture ingredients were obtained from Invitrogen (Carlsbad, CA, USA). Polyclonal antibody against glial fibrillary acidic protein (GFAP) was bought from DAKO Corporation (Carpinteria, CA, USA). The Vectastain ABC kit and biotinylated secondary antibodies were purchased from Vector Laboratories (Burlingame, CA, USA). 50 µm diameter stainless steel microwire was bought from A-M Systems (Carlsborg, WA, USA). Human plasma fibronectin was bought from Millipore (Billerica, MA, USA). Basic Fibroblast Growth Factor (bFGF) was obtained from R&D Systems (Minneapolis, MN, USA).

### 4.2.2 Animals

Timed-pregnant Fisher F344 rats were obtained from Charles River Laboratories (Raleigh, NC, USA). Housing and breeding of the animals were performed in strict accordance with the

National Institutes of Health guidelines at the National Institutes of Environmental Health Sciences (Research Triangle Park, NC, USA).

### 4.2.3 Primary mesencephalic neuron-glia cultures – Original Model Protocol

Neuron-glia cultures were prepared from the ventral mesencephalic tissues of embryonic day 14-15 rats, as described previously [236]. Briefly, dissociated cells were seeded at 5 x $10^5$cells/well into poly-D-lysine-coated 24-well plates. Cells were maintained at 37°C in a humidified atmosphere of 5% $CO_2$ and 95% air, in minimal essential medium (MEM) containing 10% fetal bovine serum (FBS), 10% horse serum (HS), 1 g/L glucose, 2 mM L-glutamine, 1 mM sodium pyruvate, 100 µM nonessential amino acids, 50 U/mL penicillin, and 50 µg/mL streptomycin. Seven-day-old cultures were used for treatment after a media change to MEM containing 2% FBS, 2% HS, 2 mM L-glutamine, 1 mM sodium pyruvate, 50 U/mL penicillin, and 50 µg/mL streptomycin.

### 4.2.4 Primary mesencephalic neuron-glia cultures – Base Protocol

Neuron-glia cultures were prepared from the ventral mesencephalic tissues of embryonic day 14-15 rats, as in the Original Model Protocol. 24-well plates were coated with poly-D-lysine for one hour, washed three times, and coated with 10ug/ml fibronectin in PBS overnight. Fibronectin-PBS was removed immediately before cell plating without further washing. Dissociated cells were seeded at 1 x $10^6$cells/well into the poly-D-lysine and fibronectin-coated 24-well plates. Cells were maintained at 37°C in a humidified atmosphere of 5% $CO_2$ and 95% air, in Neurobasal (NB) medium supplemented with B27 serum free supplement containing 2 mM L-glutamine, 50

U/mL penicillin, and 50 µg/mL streptomycin. 10 ng/ml of bFGF was added to the cultures three days after seeding (T=3d). Ten-day-old cultures were used for treatment. Treatment consisted of placement of four microwires in each well after a media change to NB with B27, 10% FBS, 2 mM L-glutamine, 50 U/mL penicillin, and 50 µg/mL streptomycin. Cultures were fixed with 3.7% formaldehyde 7 days after treatment (T=17d). Data shown are representative of at least 3 different culture preparations.

### 4.2.5 Microwire Placement

Stainless steel microwire (50 µm diameter) was cut into 3-5 mm pieces and soaked in 70% ethanol for at least 30 minutes, after which it was allowed to dry in a laminar flow hood. At treatment time, 4 pieces of wire were placed into each treatment well at random locations using sterile forceps, so that the pieces would sink and rest atop the cultured cell layer.

### 4.2.6 Immunostaining

Astrocytes were detected with an antibody against GFAP as described previously [4]. Briefly, formaldehyde (3.7%) -fixed cultures were sequentially incubated with blocking solution (20 min), primary antibody (overnight, 4°C), biotinylated secondary antibody (1 h), and ABC reagents (1 h). Color was developed with 3,3'-diaminobenzidine.

### 4.2.7 Scarring Index

Images were recorded with a Nikon Eclipse TE2000-U inverted microscope (Nikon; Tokyo, Japan) connected to a Nikon Digital Sight DS-2MV camera (Nikon; Tokyo Japan) operated with the Nikon NIS-Elements software (Nikon; Tokyo, Japan). A measure of glial scarring within each well was generated using a quantitative image analysis procedure by two observers blinded to the various culture treatments. Images of GFAP staining along the entire length of each wire segment were taken using the 10X objective such that each wire segment generated 4-6 images across its length. For each image, ImageJ software (National Institutes of Health; Bethesda, Maryland) was used to register the image so that the wire was on the horizontal, and a vertical intensity profile (Figure 13a, pink line) was generated across the length of the wire within the image (Figure 13a, yellow rectangle). This resulted in a line profile along the vertical direction averaged across the entire horizontal direction so that the many variations in scarring across the wire length were averaged out and one intensity profile was generated for each wire image. The resulting intensity plot (Figure 13b) displayed the extent of GFAP staining across each image of the wire segment. The intensity plot data was imported into Matlab where a custom-built image analysis script normalized the intensity plot and identified the dark region in each image generated from the wire, the background intensity far away from the wire, and the region of the intensity profile next to the wire where there was an increase in GFAP staining due to glial scarring. The "Scar Distance" was taken to be the distance from the wire where the GFAP intensity reached 90% of background intensity. The integrated intensity from the wire to the Scar Distance was termed the Image Scar Index (Figure 13C). Each image of each wire segment generated an Image Scar Index. The 4-6 Image Scar Index values for each wire segment were averaged together to generate a Wire Scar Index, and the four Wire Scar Index values for each well (there were four wires placed in each well) generated an overall Scar Index for the well. This overall Scar Index for each well was the average of all of the scarring along all the images of all four wires in the

well. There was often variation in scarring from one wire segment to another or from one end of a wire to the other end, as is always observed in vivo. This method averaged out this variation to provide one number for each experimental condition, which allows comparisons of one condition to another and highlights the power of this approach to answer scientific questions that an in vivo system cannot.

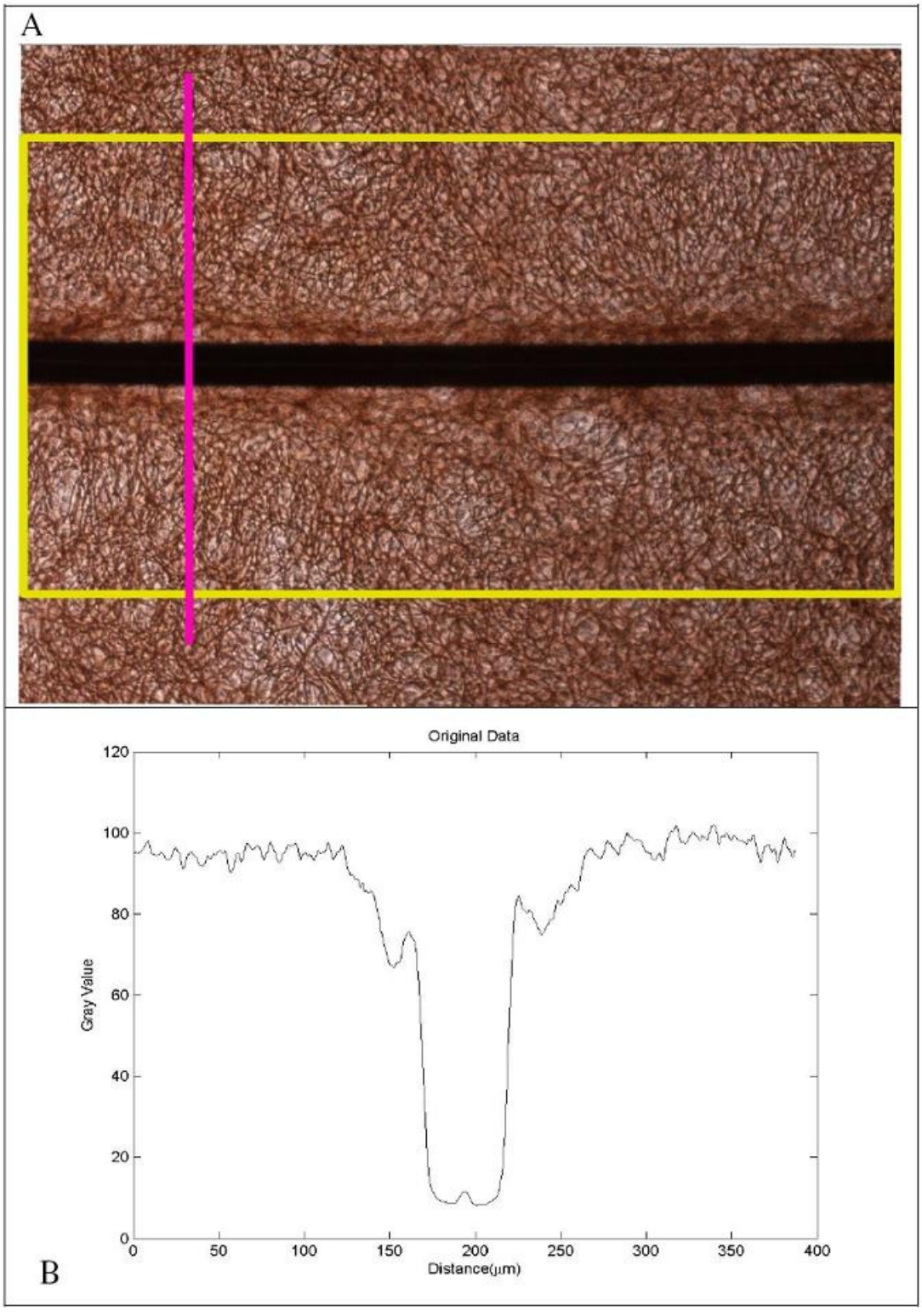
A
Original Data
120
100
80
60
40
20
0
Gray Value
0
50
100
150
200
250
300
350
400
Distance(μm)
B

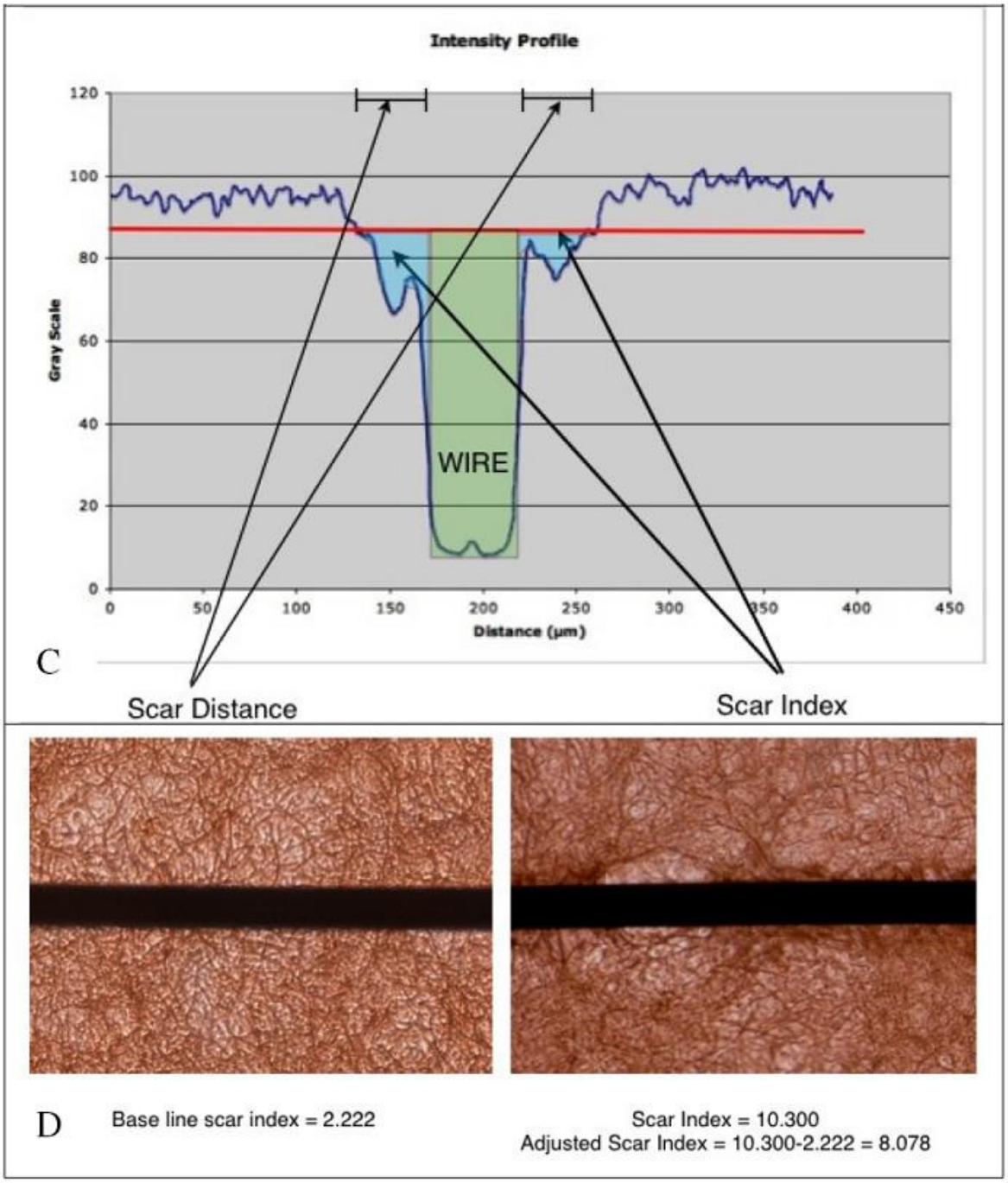


**Figure 13: A) A picture of GFAP stained culture around a microwire is rotated so the wire is on a horizontal and an intensity profile across the vertical is taken along the entire length of the wire, resulting in an intensity profile shown in B). C) The intensity profile is then imported into Matlab, where the profile is normalized, the background value is found (red marker), and the Scar Index and Scar Distance are calculated. D) To account for inaccuracies caused by shadows and the Matlab program, a baseline scar index was subtracted from calculated scar indices.**

Scar Indexes from wells from at least three different dissections (on different days) generated the Scar Indexes reported in the figures. A fifth segment of microwire was added to each culture after the culture was fixed and stained (no cell interaction with microwire) to generate a baseline Scar Index value to account for shadow from the microwire and any inaccuracies introduced by the automatic detection Matlab code (Figure 13D). The Scar Index reported in Figures 14-19 has the baseline Scar Index already subtracted out.

### 4.2.8 Statistical Analysis

Statistical significance was determined by repeated measures analysis of variance (ANOVA) with a $p<0.05$ significance level and Dunnett's or Tukey's post-hoc tests. Analysis was performed on log-transformed data because of heterogeneous variance. The true variability between the different treatments is actually smaller than the error bars shown in the figures would suggest because of plate-to-plate and dissection-to-dissection variation, but this is accounted for by using repeated measures ANOVA. Statistical tests were conducted using the GraphPad Prism software (GraphPad Software, Inc. La Jolla, CA, USA).

## *4.3 Results*

Table 1 compares the new Base Protocol to the Original Protocol. In the Base Protocol cells were seeded in 1ml of serum-free Neurobasal (NB) media supplemented with the B27 supplement and grown (without feeding) to confluency over 10 days. On the third day, 10ng/ml bFGF was added to the culture. Media was replaced with NB+B27 medium containing 10% fetal bovine serum

(FBS) and microwires are placed on top of the culture. The Base Protocol differs from the Original Protocol, which seeded cells in high serum at lower density, did not use bFGF, and maintained cells in an MEM-based media. The Base Protocol resulted in scar formation (arbitrarily defined as a scar index greater than 4, which is visually equivalent to "weak" or "minor" scarring) in 100% of the cultures tested (18/18) with a mean scar index of 7.6 +/- 0.66. Scar index measurements were not made with cultures generated through the Original Protocol (the Original Protocol was only employed before the Scar Index analysis was performed), but approximately less than 30% of cultures generated scars according to this metric. The level of consistency that had been desired (>95%) is possible through the Base Protocol, which was a "best guess" based on over 2 years of iterative changes to the Original Protocol.

**Table 1: Base Protocol Compared to Original Protocol**

| Procedure | | Original Protocol | Base Protocol |
|---|---|---|---|
| **Seeding Media** | Base | MEM | Neurobasal |
| | Serum | 10% FBS, | - |
| | | 10% Horse Serum | - |
| | Supplements | 1 g/L glucose, | - |
| | | 2 mM L-glutamine | 2 mM L-glutamine |
| | | 1 mM sodium pyruvate | - |
| | | 100 µM nonessential amino acids | - |
| | | 50 U/mL penicillin | 50 U/mL penicillin |
| | | 50 µg/mL streptomycin | 50 µg/mL streptomycin |
| | | - | B27 |
| **Plate Coating** | | Poly-D-lysine | Poly-D-lysine |
| | | - | 10ug/ml Fibronectin |
| **Seeding Density** | | 1 x $10^6$ cells/ml in 0.5 ml/well | 1 x $10^6$ cells/ml in 1 ml/well |
| **Cell Feeding** | | Add 0.5 ml media at day 3 | - |
| | | - | Add 10 ng/ml bFGF at day 3 |
| **Treatment Day** | | Day 7 | Day 10 |
| **Treatment Media** | Base | MEM | Neurobasal |
| | Serum | 2% FBS, | 10% FBS |
| | | 2% Horse Serum | - |
| | Supplements | 2 mM L-glutamine | 2 mM L-glutamine |
| | | 1 mM sodium pyruvate | - |
| | | 50 U/mL penicillin | 50 U/mL penicillin |
| | | 50 µg/mL streptomycin | 50 µg/mL streptomycin |
| | | - | B27 |
| **Treatment Protocol** | | Change media and place microwire | Change media and place microwire |
| **Culture stop day** | | Day 17 (10 days after treat) | Day 17 (7 days after treat) |
| **Frequency of scar formation** | | <30% | ~100% |
| **Typical Scar Index** | | 0-2 | 7-8 |

Once this "best guess" Base protocol was established, six different culture conditions were varied independently to identify features of the culture important to scarring. The six dimensions varied were: A) growth media, B) seeding density, C) bFGF addition day, D) serum concentration in

treatment media, E) treatment day, and F) duration of culture. At least three different dissections were performed for each variation in a single dimension while all other dimensions were held at Base Protocol values. In each of the following figures, the culture conditions that correspond to Base Protocol conditions are represented by solid bars.

### 4.3.1 Growth Media

Four different kinds of growth media were investigated, made up of three types of basal media (Neurobasal, 1:1 DMEM/F12, and Minimum Essential Media (MEM)), and three types of serum free supplements (N1, N2, and B27). The four different growth media preparations were: Neurobasal + B27 (Base), DMEM/F12 + N2, DMEM/F12 + B27, and MEM+N1. Cultures were treated in the same media formulation as they were seeded, except 10% FBS was added. The Base Protocol growth media (Neurobasal+B27) generated a significantly higher scarring index ($p<0.05$ ANOVA, $P<0.05$ compared to DMEM/F12 + B27, and MEM+N1 according to Dunnett's post-hoc test) among these four options (Figure 14).

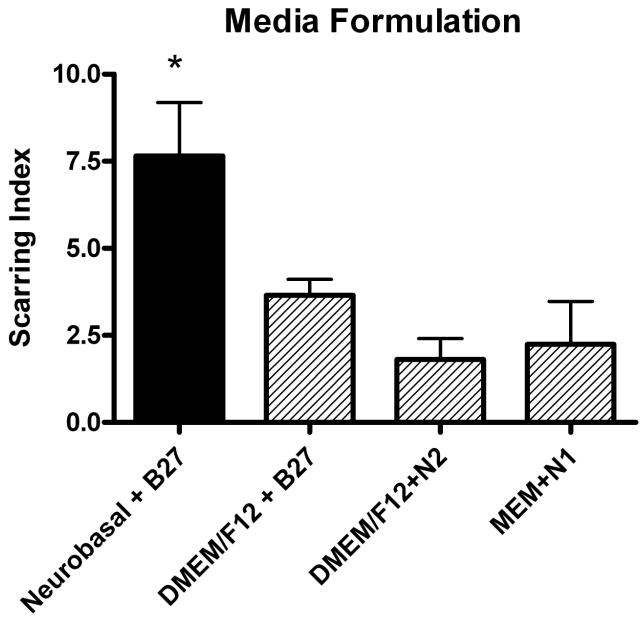


**Figure 14: Four different growth media were investigated to see which one caused more consistent scarring. Neurobasal combined with B27 supplement generated significantly larger scars ($p<0.05$) than DMEM12 + B27 and MEM+N1. Black bar indicates "Base Protocol" conditions.**

### 4.3.2 Seeding Density

Six different seeding densities were investigated, ranging from 500,000 cells/well in 1 ml of media to 2 million cells per well in 1 ml. There was no significant difference among the various seeding densities, suggesting that a lower seeding density (and thus more experiments/dissection) could be utilized without a loss in scarring potential (Figure 15). Therefore, although the lowest seeding density did not result in greater scarring, it was selected for its beneficence: i.e. uses the least number of cells and therefore the smallest number of animals. Even though serum is not present during the growth phase of these cultures, bFGF acts as a strong mitogen for the cells, thus allowing smaller numbers of cells to grow to confluence over the course of the 10 day growth phase.

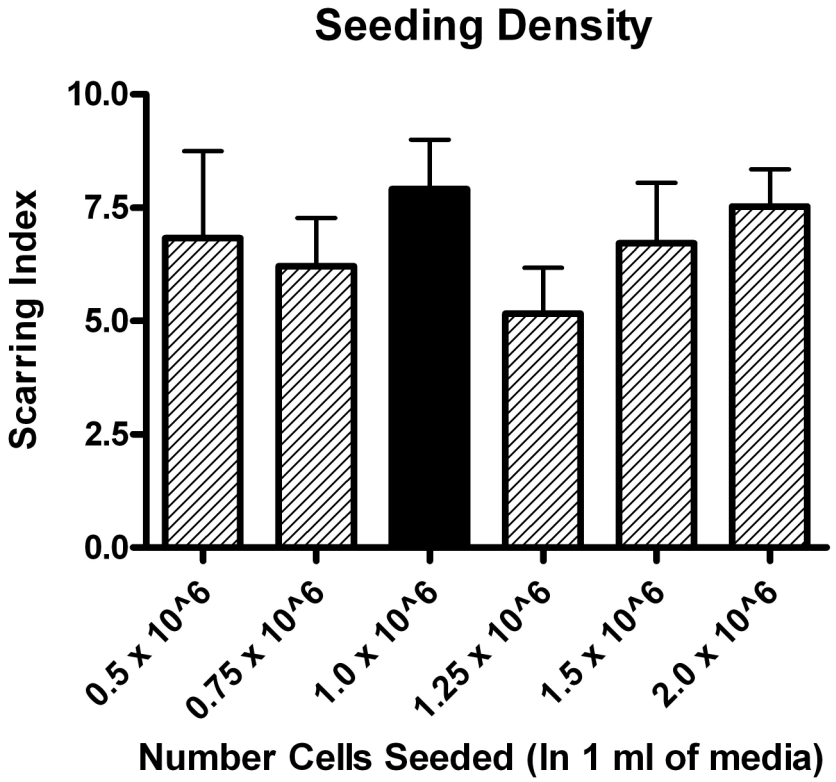


**Figure 15: Six different seeding densities were investigated with all other factors being held constant. There was no significant difference between the Base Protocol (1 million cells/well) and the lowest seeding density investigated (500,000 cells/well). Black bar indicates "Base Protocol" conditions.**

### 4.3.3 Day of bFGF addition

The Base Protocol involved adding 10ng/ml of bFGF, a growth factor for precursor cells, to the cultures at T=3 days. The day at which bFGF was added, as well as whether bFGF was necessary for scar formation was investigated. Figure 16 shows that not only was bFGF essential for significant scar formation, but there was a statistically significant linear correlation between the length of time bFGF was in culture and the extent of scar formation (r = .51). Since media is

replaced with treatment media without bFGF at T=10 days, cultures treated with bFGF at T=9 days only experienced a benefit from bFGF for 1 day before bFGF was removed. The largest effect was when bFGF was administered at seeding time (T=0 days) or at treatment time (T=10 days). Adding bFGF at treatment time (T=10d) generated a significantly larger scar than adding bFGF before treatment (ANOVA $p<0.05$, Dunnett's Post Hoc test $p<0.05$). This data suggests that bFGF should be administered either at seeding time or at treatment time, or perhaps at both times.

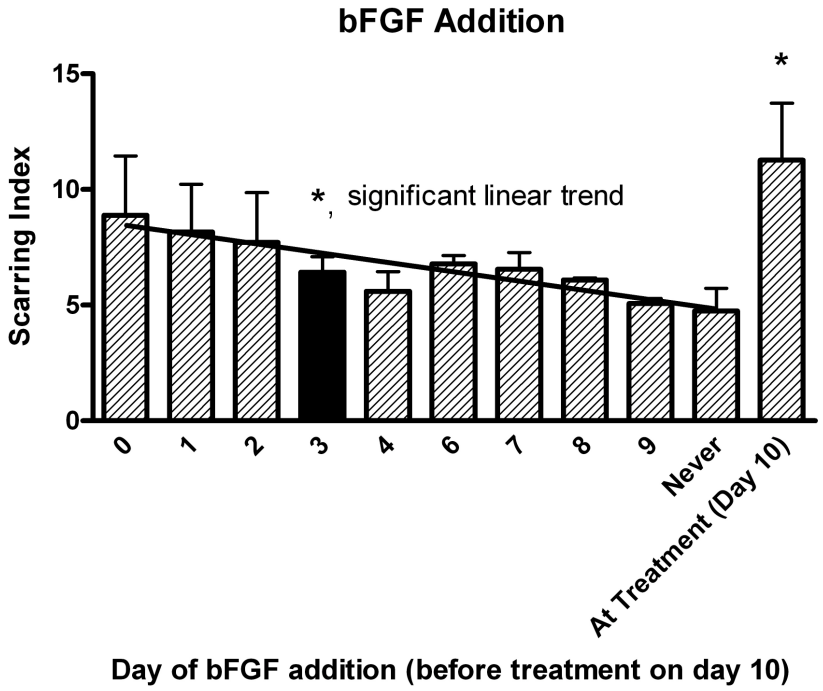


**Figure 16: bFGF was administered to the culture at different days. bFGF was necessary for optimal scar formation and the longer bFGF was present in the culture, the larger the scar ($p<0.05$ significant linear trend, $r=0.51$). bFGF administration in the treatment media resulted in significantly larger scars ($p<0.05$) compared to bFGF addition during the growth phase before treatment at T=10d. Black bar indicates "Base Protocol" conditions.**

### 4.3.4 Serum concentration at treatment

A consistent observation from the beginning of the development of this in vitro model has been that the presence of serum is necessary for scar formation. The Base Protocol involves adding 10% FBS to the culture at treatment time. This study varied serum concentration in the treatment media from 0% to 20%. Figure 17 reports that serum is indeed necessary for significant scar formation, although even small amounts of serum (0.1%) are adequate for scar formation and a plateau is reached at 5% FBS. The effect of serum on scar formation is statistically significant (ANOVA $p<0.05$) with scars in cultures with any amount of serum significantly higher than scars in cultures with no serum ($p<0.05$ Tukey's multiple comparisons post-hoc test). Surprisingly, there is no statistically significant difference between scars formed in 0.1% serum and those in 20% serum according to the post-hoc test.

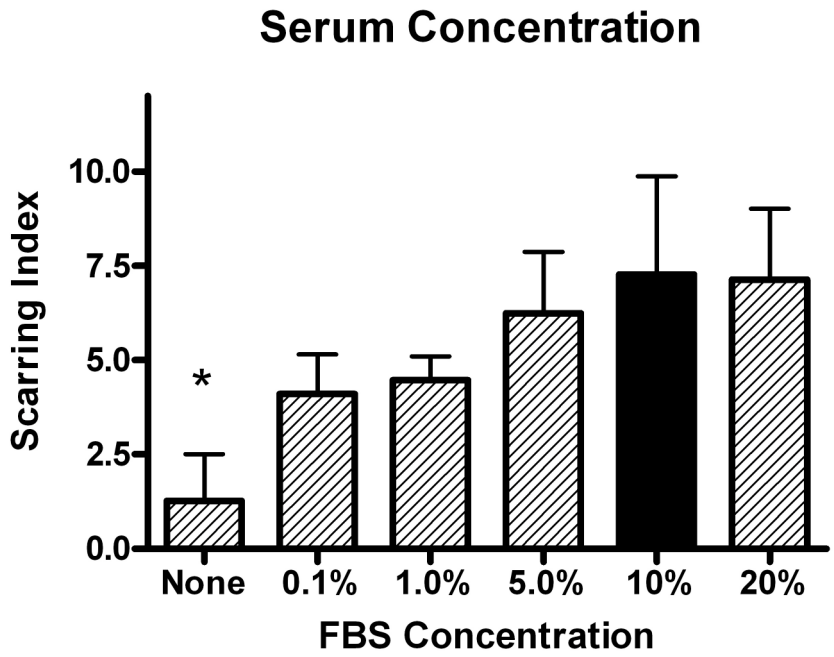


**Figure 17: The requirement and optimal concentration of serum was tested in the culture. Serum was shown to be a necessary factor driving glial scar formation ($p<0.05$ no serum condition vs. any condition with serum) but even very low amounts of serum could induce some scar formation. While there was a qualitative correlation between higher serum and greater scarring, there was no significant difference between conditions as long as some serum was present. Black bar indicates "Base Protocol" conditions.**

### 4.3.5 Treatment day

The Base Protocol involved changing of the growth media to treatment media and wire placement at T=10 days. This study aimed to find the optimal treatment day. Figure 18 shows that any day between 6 and 12 days after seeding will yield significant scarring. There was statistically higher scarring when treatment occurred after 4 days as compared to treatment at 0-2 days (ANOVA $p<0.05$, $p<0.05$ Tukey's multiple comparisons post-hoc test). Cultures treated at days 4, 13, and 14 developed smaller scars, but not to a significance level of $p<0.05$.

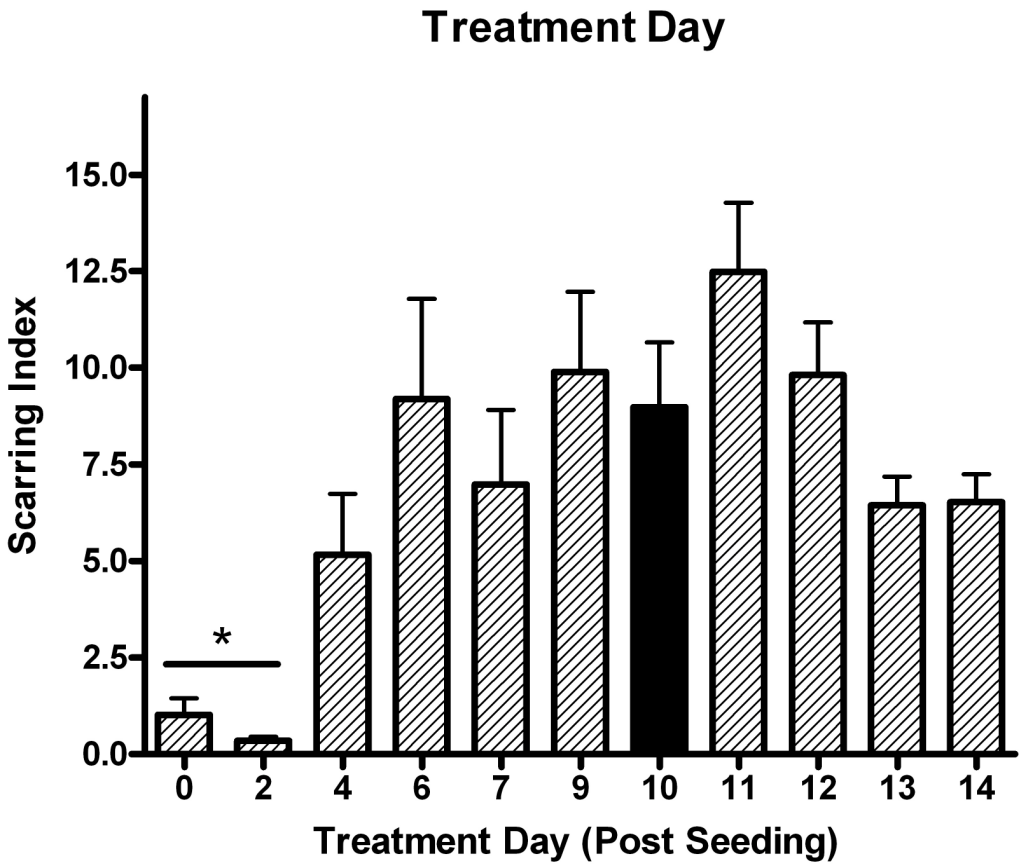


**Figure 18: The day at which growth media was replaced with treatment media and wires were placed in the culture was varied. Optimal times for treatment ranged from T=6 days to T=12 days. Treatment after at least 4 days of culture growth resulted in significantly larger scars ($p<0.05$, T=0-2d vs. treatment any later day). Black bar indicates "Base Protocol" conditions.**

### 4.3.6 Culture stop day

The Base Protocol involved stopping the culture at T=17 days after seeding (7 days after treatment). This study aimed to find the optimal day to stop the culture to see if taking the culture

out longer would result in larger scars. Figure 19 suggests that while it takes the scar 4-5 days to mature to its optimal level, it does not grow larger once that level is reached at T=15. The scars were smaller in cultures stopped at T=11 to T = 14, where only 1-4 days were available for scar formation. These two growth phases were analyzed separately. There was a statistically significant ($p<0.05$) increase in scarring with longer times in culture up to stop day 15 (ANOVA $p<0.05$, $r=0.72$) and no significant change in scarring after day 15.

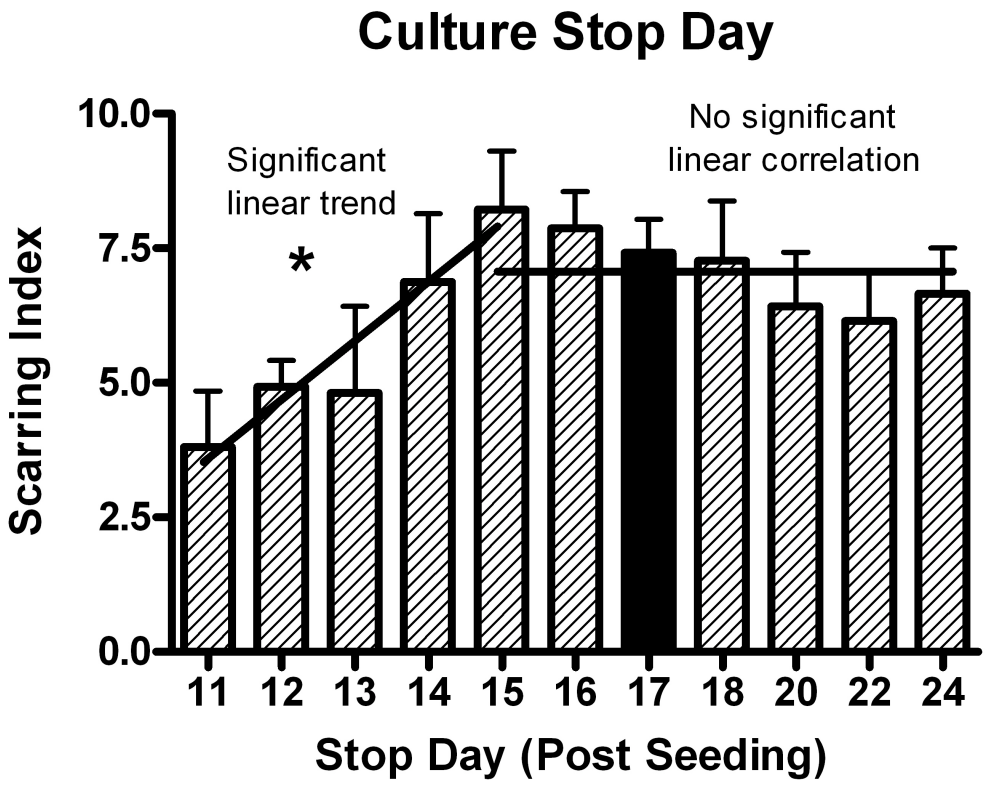


**Figure 19: The number of days the scar was allowed to grow (after treatment at T=10d) was varied by stopping the culture at different times. Between 1 and 5 days of scar growth (Stop day 11-15), scarring increased with time (r=0.72), but once an optimal scar formed at T=15 days (5 days after treatment), it did not get larger with longer time available for scar formation (no significant linear trend). Black bar indicates "Base Protocol" conditions.**

## *4.4 Discussion*

In Chapter 3 it was shown that a well-documented embryonic neuron-glia culture system developed for studying adult Parkinson's disease can reproduce many of the hallmarks of the glial scarring around neuroelectrode materials [168;238;239;249-251]. This neuron-glia model was adopted after testing and rejecting many different culture systems – from cell-lines to adult primary mixed-glia cultures, to brain slices – none of which were successful in recreating the glial scar around the electrode specimen. Presumably it was the presence and interaction of all the cell types necessary for scar formation – astrocytes, microglia, neurons, and precursor cells – that finally resulted in the glial scar. The optimized model presented in this chapter is open to the same two commonly expressed criticisms as the original model: the use of embryonic cells and the presence of serum in the medium – both of which are absolutely essential.

To reiterate, although glial scarring in vivo is a phenomenon observed in adult animals, adult neurons do not survive the cell isolation process and therefore nearly all primary cultures that aim to study high density neuron-neuron and neuron-glia interactions utilize embryonic cells. The primary mesencephalic neuron-glia embryonic cell cultures described here have successfully been used to study the mechanisms involved in Parkinson's disease, an adult disease that does not exist in embryonic animals. Also, the embryonic cells in the model are "aged" for 10 days before treatment and, regardless of their embryonic origin, they ***do*** form glial scars, which was the objective. There are always major deficiencies with using an in vitro model to study a process like glial scarring (embryonic cells, 2-d environment, lack of vasculature, etc), but there are also potentially large benefits over in vivo studies (strict control over environmental factors, quantifiable results, reproducibility, high throughput, mechanistic insight, etc.).

The presence of serum in the culture medium is criticized because neurons exist beyond the BBB. While healthy intact brain tissue lacks serum, trauma causes blood to seep into brain tissue. There are no known conditions were glial scarring forms without a breach of the BBB. As demonstrated below, serum appears to be a necessary stimulant for gliosis both in vivo and in vitro.

The objective of this study was to modify the previously described Original Protocol that yielded a robust glial scar in less than half of all culture preparations, even under rigidly controlled conditions. This partly reflects the in vivo observation that the brain's tissue response to implanted materials is highly variable, a fact that has frustrated development of a chronically implantable recording array. Such variability, however, is poorly suited for the development of an in vitro model positive control that could be used to understand the mechanisms behind scarring around neuroelectrode materials. The Base Protocol presented here results in significant glial scarring in every culture preparation, thus allowing its use as a positive control for further investigation.

Using the Base Protocol as a starting point, the protocol was varied on six dimensions to further increase the extent of scarring, and thus possibly glean insights into glial scar formation. The Control Protocol is compared to the original "best guess" Base Protocol in Table 2 with changes highlighted.

**Table 2: Changes to the Base Protocol to generate the Control Protocol**

| Procedure | | Base Protocol | Control Protocol |
|---|---|---|---|
| **Seeding Media** | Base | Neurobasal | Neurobasal |
| | Serum | - | - |
| | Supplements | 2 mM L-glutamine | 2 mM L-glutamine |
| | | 50 U/mL penicillin | 50 U/mL penicillin |
| | | 50 µg/mL streptomycin | 50 µg/mL streptomycin |
| | | B27 | B27 |
| **Plate Coating** | | Poly-D-lysine | Poly-D-lysine |
| | | 10ug/ml Fibronectin | 10ug/ml Fibronectin |
| **Seeding Density** | | 1 x $10^6$ cells/ml in 1 ml/well | **0.5 x $10^6$ cells/ml in 1 ml/well** |
| **Cell Feeding** | | Add 10 ng/ml bFGF at day 3 | **Add 10 ng/ml bFGF at day 0** |
| **Treatment Day** | | Day 10 | **Any day 6-12 days after seed** |
| **Treatment Media** | Base | Neurobasal | Neurobasal |
| | Serum | 10% FBS | 10% FBS |
| | Supplements | 2 mM L-glutamine | 2 mM L-glutamine |
| | | 50 U/mL penicillin | 50 U/mL penicillin |
| | | 50 µg/mL streptomycin | 50 µg/mL streptomycin |
| | | B27 | B27 |
| **Treatment Protocol** | | Change media and place microwire | **Change media and place microwire. Add 10ng/ml bFGF.** |
| **Culture stop day** | | Day 17 (7 days after treat) | **Any day 15-17 (at least 5 days after treat)** |

In the process of varying culture conditions to arrive at the final Control Protocol, four important trends became apparent. First, it was clear that bFGF was a key driver of glial scar formation in this model, and the longer bFGF-containing media was available to the cells, the greater the scarring. Dozens of other factors linked to glial scar formation (i.e. TNF-α, IL-1β, IL-6) were added to the cultures in the search for a more robust and reproducible scar over the course of 2 years of culture development, but all had little to no effect, except bFGF.

Cultures that received no bFGF or were only exposed to bFGF for one day (as opposed to the optimal 10 days) generated significantly smaller glial scars. For example, treatment at T=0 and T=2 days rather than at T=10 days (Figure 18) produced almost no scarring, likely because treatment occurred before bFGF administration (in the Base Protocol, bFGF is administered at T=3 days in growth media, so wells treated at T=0 and T=2 days do not have bFGF added at any time). A lower Scar Index at T=4 days was also observed, possibly since bFGF was only available in the media for one day before the media was replaced during treatment. It is also possible that treatment at T=0, T=2, and T=4 days produced less scarring because cultures were not given opportunity to grow to confluence, or because scarring is not observed in embryonic animals in vivo and the "immature" cells at the earlier treatment time points were unable to form scars. Still, it was clear that bFGF significantly enhanced glial scarring, which was at its highest level when bFGF was administered in the treatment medium (T=10 days), thus affecting cells as they were forming the scar.

The second trend observed was that the glial scar in our model takes five days to fully form. Lower scarring when the culture was treated at T=13 and T=14 days (Figure 18) can be explained by this fact as the scar may not have fully matured by the time the culture were stopped at T=17 days. The requirement of 4-5 days for scar maturity was corroborated by Figure 19, which shows the culture maturing at T=14-15 days, or 4-5 days after treatment at T=10 days. This timing is well supported by in vivo studies that have aimed at identifying the timeline of glial scar formation [26;27].

Third, a picture of glial scarring emerged that implicates glial precursor cells as key mediators of glial scarring, a conclusion that reinforces much of what has been presented recently in the in

vivo literature. It is clear that Neurobasal medium, combined with B27 media supplement and bFGF strongly amplifies glial scar formation within the culture. A protocol that utilizes Neurobasal + B27 media with 10ng/ml bFGF added is found in one other area in neural cell culture literature: optimized conditions for the growth and maintenance of neural stem and precursor cells [134;246;248]. In fact, bFGF is a necessary growth factor for the proliferation and maintenance of neural precursor cells. The data supports a conclusion that increasing neural stem/precursor cell growth results in a larger, more robust glial scar. Such a conclusion is well supported by recent reports of NG2+ oligodendrocyte precursors and other undifferentiated, multipotent cells migrating to injury sites and differentiating into scar astrocytes [73;76;78], a notion that is at odds with the previously established view that it is the nearby mature astrocytes that proliferate, become reactive, and form the glial scar.

Fourth, the data suggested a clear requirement for serum in glial scar formation. This requirement is corroborated by a vast array of literature that suggests gliosis is a natural brain response to any breakdown of the BBB that releases serum components into the normally serum-free brain parenchyma, whereas injuries that do not result in serum release do not induce significant glial scarring [170;252-255]. These data suggest that even a small amount of BBB breakdown will initiate a glial reaction, with 0.1% serum still capable of increasing glial scarring within this culture model. Serum may also be important in stimulating the migration to, and proliferation and differentiation at the site of injury. Without serum, glial precursors do not migrate to an injury site in vitro when a portion of the culture is scraped free of cells ([4] and unpublished observations). Furthermore, serum is often used as a differentiating factor within culture models studying neural and glial precursor cells, with serum driving the differentiation into an astrocytic cell type at the expense of other neural cell fates like oligodendrocytes or even neurons [71;256-258]. The

requirement of serum in glial scarring suggests neuroscientists should concentrate on leaving as much vasculature intact as possible during electrode implantation for chronic applications.

All three conditions described above: serum, appropriate stem/precursor cell media (NB+B27), and bFGF, are necessary for robust scar formation. When all three are present, the scar index is 7.6 +/- 0.66, well above 4, the index which was arbitrarily chosen to signify the presence of "scarring." When serum is taken away (Figure 17), the scar index drops to 1.3 +/- 1.2 and scarring is almost never observed. If serum and bFGF are present but NB+B27 media is replaced with another commonly used medium for neuron cell culture (DMEM/F12 + N2), the scar index drops from 7.6 to 1.8 +/- 0.6 and scarring is not observed (Figure 14). Finally, without bFGF, the scarring index drops to 4.7 +/- 1.0, and minor scarring is observed (Figure 16), but scarring is at such a low level as to be insufficient for the culture to be used as a positive control for future studies. This study points to the need for all three conditions to be present for robust scarring to occur in vitro.

## *4.5 Conclusions*

Chapter 3 described an in vitro model of glial scarring that allowed direct observation of the progression of gliosis around neuroelectrode materials. The original intent was to develop a new test for studying new electrode designs that would reduce glial scarring [4]. However, scarring in this in vitro model was highly variable (similar to what occurs in vivo). This chapter described the results of a search for culture conditions that can create a strong positive control: a reproducible, predictable robust scarring around electrode materials. This study yielded two main findings. First, from a materials testing perspective, the Control Culture conditions were

identified (i.e. necessity of serum release after BBB breakdown, bFGF as a growth factor, neural precursor cell survival and growth essential to glial scar formation). Second, and perhaps more significantly, this was the first controlled, systematic study of the critical factors that lead to glial scarring around materials. All of the insights gained by this in vitro study are corroborated in the in vivo literature. Combined, these findings suggest that the model is not only a useful model for in vitro testing of anti-gliosis strategies, but also a useful vitro model for dissecting complicated biological phenomena involved in glial scarring.

# Chapter 5: Utilizing an in vitro model of glial scarring to gain mechanistic insights into the factors affecting glial scar formation

## *5.1 Introduction*

The two previous chapters dealt with the development and optimization of an in vitro, mixed cell culture based system that reproduces characteristic hallmarks of the in vivo glial scar that forms around microwire electrodes [4;5]. This model has recapitulated in vivo behavior such as microglial activation and attachment to stainless steel microwires, astrocyte activation beyond the microglial layer in the form of GFAP upregulation, neural precursor cell migration to a site of injury and differentiation into GFAP-expressing astrocytes, and the presence of healthy, electrically active neurons. Furthermore, this in vitro model, with the presence of serum and of conditions that allow for the maintenance and growth of neural precursor cells (Neurobasal media, B27 supplement, bFGF), results in consistent, robust glial scar formation around a mock microwire electrode in every culture preparation. These conditions allow for a stable positive control, and removal of one of these conditions (bFGF in this study) results in minimal scarring and therefore acts as a negative control.

Although the glial scar is primarily a cellular scar of microglia, astrocytes, NPC's, and cellular processes, the extracellular matrix (ECM) laid down at the injury site plays an important role in organizing the scar and creating a chemical barrier to neurons [177]. A basal lamina is often seen (and may be present each time but just not stained for) in the glial scar, typically between the microglia coating the implant and the cellular layers of NPC's and GFAP+ astrocytes in the scar,

or between the astrocyte and meningeal layers after the glia limitans is reformed after injury [46;164;169;179;180]. The basal lamina is a sheet-like layer of ECM that can be found as a boundary layer in many tissues such as blood vessels and epithelium. It is primarily composed of four components: the ECM proteins collagen IV and laminin, and the proteoglycans perlecan and nidogen [189]. The proteoglycans sequester and present cytokines and growth factors such as bFGF to nearby cells while the ECM proteins create a substrate for cells to attach [135;185]. Commercially available basal lamina preparations such as Matrigel® are commonly used in cell culture to grow and differentiate different types of cells [259;260].

Rather than treating the in vitro culture directly with stainless steel microwires as described previously [4;5], this study employed microwires sheathed with a Matrigel/Alginate hydrogel to simulate the basal lamina. This scheme allowed us to directly deliver a basal lamina into the culture rather than waiting for ECM deposition and organization by glial cells (a process which occurs over time but has not been specifically tested in our model). Since the culture has a limited testing window, the gel-coated microwires allowed us to concentrate on a specific portion of the multifaceted glial scarring process, namely the chronic NPC and astrocytic response as opposed to the acute microglial response. The coating also allowed us to remove the responding cells for further analysis, which is not possible with uncoated microwires.

With the positive control providing a robust glial response, the ECM-coated microwires were used to probe the role of NPC's and astrocytes migrating to and proliferating at the site of injury. Cells responded to the coated microwires by migrating to the hydrogel and accumulating on the surface. By removing the coated microwire from the culture after the experimental period, it was possible to quantify the number of cells responding to the microwire under different conditions.

Conditions tested included different concentrations of serum and bFGF in the media, as well as the presence of various soluble factors presumed to affect glial scar formation in vivo.

The extent of cell accumulation on the coated microwires was significantly increased by titration of the culture with serum, the pleotropic growth factor bFGF, the inflammatory cytokines IL-1β and IL-1α, and the growth factors PDGF and BMP-2. Although administered at concentrations that were often above typical concentrations used in neural cell culture, or sometimes at just below cytotoxic concentrations (several concentrations were attempted for each factor), the other fourteen soluble factors tested had little to no effect on the number of cells that attached to the coated microwires. Only a specific blocker of the bFGF receptor was able to abrogate the effect of bFGF. This study suggests essential roles in glial scarring of serum, which infiltrates brain tissue upon disruption of the blood-brain barrier, and bFGF, which is a necessary growth and survival factor for the neural precursor cells that respond to injury [124;128;135].

## *5.2 Materials and Methods*

### 5.2.1 Reagents

Cell culture ingredients were obtained from Invitrogen (Carlsbad, CA, USA). Certified serum (Invitrogen Cat# 16000) contained less than 0.06 units/ml endotoxin and less than 2 mg/dl hemoglobin. Polyclonal antibody against glial fibrillary acidic protein (GFAP) was bought from DAKO Corporation (Carpinteria, CA, USA). The Vectastain ABC kit and biotinylated secondary antibodies were purchased from Vector Laboratories (Burlingame, CA, USA). 50 µm diameter stainless steel microwire was bought from A-M Systems (Carlsborg, WA, USA). Basic Fibroblast

Growth Factor (bFGF) was obtained from R&D Systems (Minneapolis, MN, USA). The various soluble factors and the concentrations used are presented in Table 3. Several different concentrations of each factor were used with concentrations often reported in the literature taken as a lower bound. The concentration reported is the highest concentration attempted that (a) did not result in large-scale cell death or (b) was double the highest literature-reported concentration found. RGD-coupled ultrapure sodium alginate (>1.5 ratio of guluronate content to mannuronate content) was purchased from Novamatrix (Sandvika, Norway) because of its low endotoxin levels (<100 EU/g) and its excellent safety and toxicity profile because of its frequent use in clinical trials.

**Table 3: Soluble Factors Added into the Media**

| Soluble Factor | Company/ Catalog # | Concentration | Description |
|---|---|---|---|
| **Pro- Inflammatory agents** | | | |
| IL-1β | R&D Systems: 501-RL-010 | 20 ng/ml | Cytokine released by microglia at the site of injury [55]. |
| IL-1α | R&D Systems: 500-RL-005 | 10 ng/ml | Cytokine released by microglia at the site of injury [261;262]. |
| IFN-γ | 585-IF-100 | 50 ng/ml | Cytokine that acts as a strong activator of immune cells in the body [263]. |
| **Anti-inflammatory agents** | | | |
| Dexamethasone | Sigma: D4902 | 50 μM | Steroid shown to reduce glial scarring in vivo [224]. |
| IL-10 | R&D Systems: 522-RL-005 | 100 ng/ml | Cytokine shown to reduce glial scarring in vivo [261;264]. |
| **Growth factors:** | | | |
| PDGF | R&D Systems: 520-BB-050 | 50 ng/ml | Shown to affect NPC's, astrocytes, and fibroblasts [265;266]. |
| BMP-2 | R&D Systems: 355-BM-010 | 50 ng/ml | Known to be produced within the glial scar and to differentiate NPC's into astrocytes [79-84;87;91]. |
| BMP-4 | R&D Systems: 314-BP-010 | 50 ng/ml | Known to be produced within the glial scar and to differentiate NPC's into astrocytes [79-84;87;91]. |
| bFGF | R&D Systems: 3339-FB-025 | 10 ng/ml | Known to be produced in the glial scar and essential for the maintenance, migration, and proliferation of NPC's [97;98;124-130;135]. |
| GDNF | Millipore: GF030 | 50 ng/ml | Neurotrophin that helps keep neurons alive [267]. |
| **Growth factor inhibitors:** | | | |
| Noggin | R&D Systems: 1967-NG-025 | 250 ng/ml | Regulator of BMP's at wound sites [122;123]. |
| Su5402 | EMD Chemicals: 572631 | 10 μM | Blocks the bFGF receptor [99]. |

| Table 3, continued: | | | |
|---|---|---|---|
| DAPT | Sigma: D5942 | 100 µm | γ-secretase inhibitor used to block the Notch pathway, which has been implicated in the differentiation of NPC's into astrocytes [99]. |
| **GP130/IL-6 family of cytokines upregulated in glial scar** | | | |
| LIF | Millipore: ESG2206 | 20 ng/ml | Turns on the genes that convert astrocytes and NPC's into reactive, GFAP expressing astrocytes [81;83;85;89;93;94;112]. |
| IL-6 | R&D Systems: 506-RL-010 | 133 ng/ml | Turns on the genes that convert astrocytes and NPC's into reactive, GFAP expressing astrocytes [81;83;85;89;93;94;112]. |
| CNTF | R&D Systems: 557-NT-010 | 50 ng/ml | Turns on the genes that convert astrocytes and NPC's into reactive, GFAP expressing astrocytes [81;83;85;89;93;94;112]. |
| **GP130/IL-6 family Inhibitor** | | | |
| Tyrphostin AG 490 | Sigma: T3434 | 10 µM | Blocks certain key elements of the IL-6 cytokine family signal transduction pathway [268]. |
| **Astrocyte Activator:** | | | |
| N6,2'-0-dibutyryladenosine 3'5'-cyclic monophosphate sodium (dB-cAMP) | Sigma: D0627 | 1 µM | Constitutively active analog of the signaling molecule cAMP. Shown to induce GFAP [47] and IL-6 expression in astrocytes [269]. |

### 5.2.2 Animals

Timed-pregnant Fisher F344 rats were obtained from Charles River Laboratories (Raleigh, NC, USA). Housing and breeding of the animals were performed in strict accordance with the National Institutes of Health guidelines at the National Institutes of Environmental Health Sciences (Research Triangle Park, NC, USA).

### 5.2.3 Primary mesencephalic neuron-glia cultures

Neuron-glia cultures were prepared from the ventral mesencephalic tissues of embryonic day 14-15 rats, as described in the "Control Protocol" in [5] with minor modifications. 24-well plates were coated with poly-D-lysine for one hour, and washed three times with PBS. Dissociated cells were seeded at 1 x $10^6$cells/well. Cells were maintained at 37°C in a humidified atmosphere of 5% $CO_2$ and 95% air, in Neurobasal (NB) medium supplemented with B27 serum free supplement containing 1% Fetal Bovine Serum (FBS), 10 ng/ml of bFGF, 2 mM L-glutamine, 50 U/mL penicillin, and 50 µg/mL streptomycin. Ten-day-old cultures were used for treatment. Treatment consisted of placement of four microwires coated with Matrigel/Alginate hydrogel in each well after a media change to NB with B27, 2 mM L-glutamine, 50 U/mL penicillin, and 50 µg/mL streptomycin. FBS (1%) and 10 ng/ml of bFGF were also added at treatment for "With bFGF" soluble factor studies, while only FBS (1%) was added for soluble factor studies "without bFGF." Cultures were fixed with 3.7% formaldehyde 7 days after treatment (T=17d). Data shown are of at least 3 different culture preparations.

### 5.2.4 Hydrogel Coating

Hydrogel coating was made of basal lamina ECM and sodium alginate. The sodium alginate was used exclusively to shape the ECM around the microwires, not to affect cellular behavior, as ECM-only preparations did not result in a hydrogel that could be inserted into the culture while alginate-only preparations did not influence cell behavior (cells did not attach, results not shown). A 50-50% mixture of Growth Factor Reduced Matrigel Matrix Basement Membrane (Matrigel)

(BD Biosciences, San Jose, CA, USA) and 2% Novatech RGD-coupled ultrapure sodium alginate (1% final sodium alginate concentration) was pipetted into a 15 mm length of Teflon tubing (0.81–0.97 mm inner diameter). Microwire was cut into ~10 cm lengths and soaked in 70% ethanol for at least 30 minutes, after which it was washed with water 3 times. A length of microwire was inserted into the tubing so that a small piece was sticking out of one end and the rest of the microwire was sticking out of the other end (Figure 20). The small piece and half of the hydrogel-filled tube was dipped into a 1.5% solution of calcium chloride. The small piece of microwire was gripped by forceps and withdrawn from the tube so that as the microwire was withdrawn into the calcium chloride solution, the Matrigel/Alginate solution wicked onto the microwire and solidified into a hydrogel as it hit the calcium chloride. The coated length of microwire was then cut into smaller 3-5 mm pieces to be placed into the culture during treatment. At treatment time, 4 pieces of coated microwire were placed into each treatment well at random locations using sterile forceps, so that the pieces would sink and rest atop the cultured cell layer.

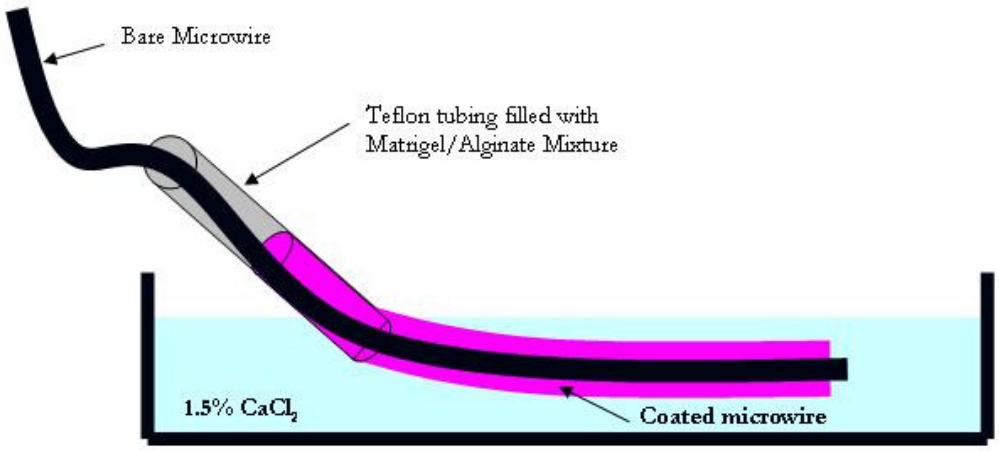


**Figure 20: Extrusion process for coating microwire with hydrogel**

### 5.2.5 Immunostaining

Microglia were detected with the OX-42 antibody, which recognizes the CR3 receptor as described [24], or anti-IBA-1 antibody, which recognized a calcium binding protein specific to microglia. Astrocytes were detected with an antibody against GFAP, and neurons were imaged by staining with MAP-2 as described previously [4]. Immature glia were detected with an antibody against vimentin. Briefly, formaldehyde (3.7%) -fixed cultures were sequentially incubated with blocking solution (20 min), primary antibody (overnight, 4°C), biotinylated secondary antibody (1 h), and ABC reagents (1 h). Color was developed with 3,3'-diaminobenzidine. Nuclear staining was with 4',6-diamidino-2-phenylindole dihydrochloride (DAPI) from Sigma (St. Louis, MO, USA). Secondary fluorescent antibodies Alexa-fluor 546 goat anti-mouse and Alexa-fluor 488 goat anti-rabbit were obtained from Invitrogen (Carlsbad, CA, USA).

### 5.2.6 Normalized Cell Counts

To develop a quantitative measure of the effect of various factors on the cellular response to the hydrogel coated microwires, the relative number of cells present on or within the hydrogel (almost entirely on the outside surface) was quantified. After immunostaining, each microwire in the well was removed from the well using forceps under a dissecting microscope and placed on a blank microscope slide. The stainless steel microwire was separated from the cell-coated hydrogel and placed on one end of the microscope slide under its own coverslip. The cell-coated hydrogel was placed under another coverslip and the coverslip was pressed down firmly to break apart the hydrogel into one 2-d plane for further analysis. Images of the DAPI labeled cells were recorded with a Nikon Eclipse TE2000-U inverted microscope (Nikon; Tokyo, Japan) connected

to a Nikon Digital Sight DS-2MV camera (Nikon; Tokyo Japan) operated with the Nikon NIS-Elements software (Nikon; Tokyo, Japan). Each hydrogel image of DAPI stained nuclei was thresholded and the total DAPI-stained area was recorded. Cell nuclei area, rather than nuclei counts, was used because the software did not accurately count cells when several nuclei were clustered together and manual counting was not feasible since a typical hydrogel might contain 5,000-10,000 cells. Several manual counts were performed to validate this method and it was found that measuring cell nucleus area was a good proxy for cell counts. No significant variation in nuclei sizes was visible to the authors, although this was not specifically measured. The total cell nucleus area for each microwire segment was divided by the length of the microwire segment since microwire lengths varied from 3-5 mm on average. The normalized cell counts presented in the figures are calculated as (sum of cell nucleus area within hydrogel in $\mu m^2$)/(microwire length in μm). At least three wells, each from a different dissection were used to generate the data, with 1-4 microwires in each well. The minimum number of wire segments used to generate a data point was 4, the maximum was 12, and the average n was 9.6.

### 5.2.7 Statistical Analysis

Statistical significance was determined by analysis of variance (ANOVA) with a $p<0.05$ significance level and Dunnett's Multiple Comparisons post-hoc tests. Statistical tests were conducted using the GraphPad Prism software (GraphPad Software, Inc. La Jolla, CA, USA).

## *5.3 Results*

In our previous studies developing and optimizing the in vitro model utilized in this paper, uncoated stainless steel microwires were used as a model foreign body to view the cellular

response. In this study, a hydrogel component to the microwires was added. This addition allows us to measure the glial scarring reaction after the implanted foreign body is covered with microglia, provisional matrix is formed through platelet and serum release, and the basal lamina is formed. Additionally, it allows the removal of the microwire and hydrogel from the culture, along with the cells that have responded, for more in depth and more accurate data analysis. Finally, it allows the incorporation of various extracellular molecules and soluble factors into the hydrogel in future studies. Under the appropriate conditions (detailed in [5]), the hydrogel is covered by a layer of responding cells. Although the quantification of relative quantities of different cell types and expressed proteins is left for future studies, it was observed that the majority of cells covering the hydrogel-coated microwire were GFAP-expressing astrocytes with enlarged, activated, scar-like phenotypes. A large number of the cells present were not labeled with astrocyte, microglial, or neuronal markers although some labeled with Vimentin, and are likely to be neural precursor cells that have not yet differentiated into scar astrocytes. Very few microglia were present on the surface of the hydrogel, although a small number could be found on the surface of the microwire between the stainless steel of the microwire and the hydrogel coating. No neurons were found on the coated microwires, although they were present next to the hydrogel in the neuron-glia layer. A 3-dimensional fluorescent image of the end of one such hydrogel coated microwire still in culture, along with the cells that have grown on top of it, is shown in Figure 21a. Rotated variations of the same image with GFAP (green) Vimentin (red) and DAPI (blue) separated out are shown in Figure 21b. The high levels of GFAP and Vimentin in “scar” layer coating the hydrogel relative to the cells in the 2-D layer of neuron-glia culture are clearly visible, although the density of nuclei is nearly the same.

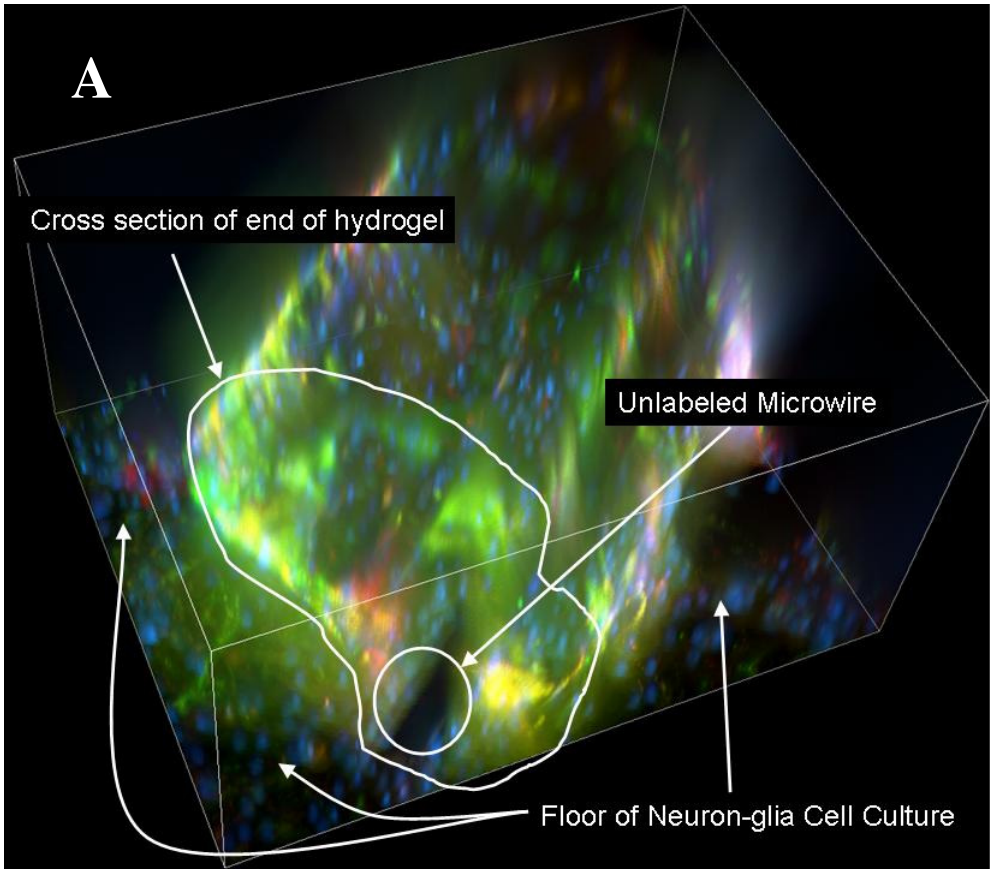
A
Cross section of end of hydrogel
Unlabeled Microwire
Floor of Neuron-glia Cell Culture

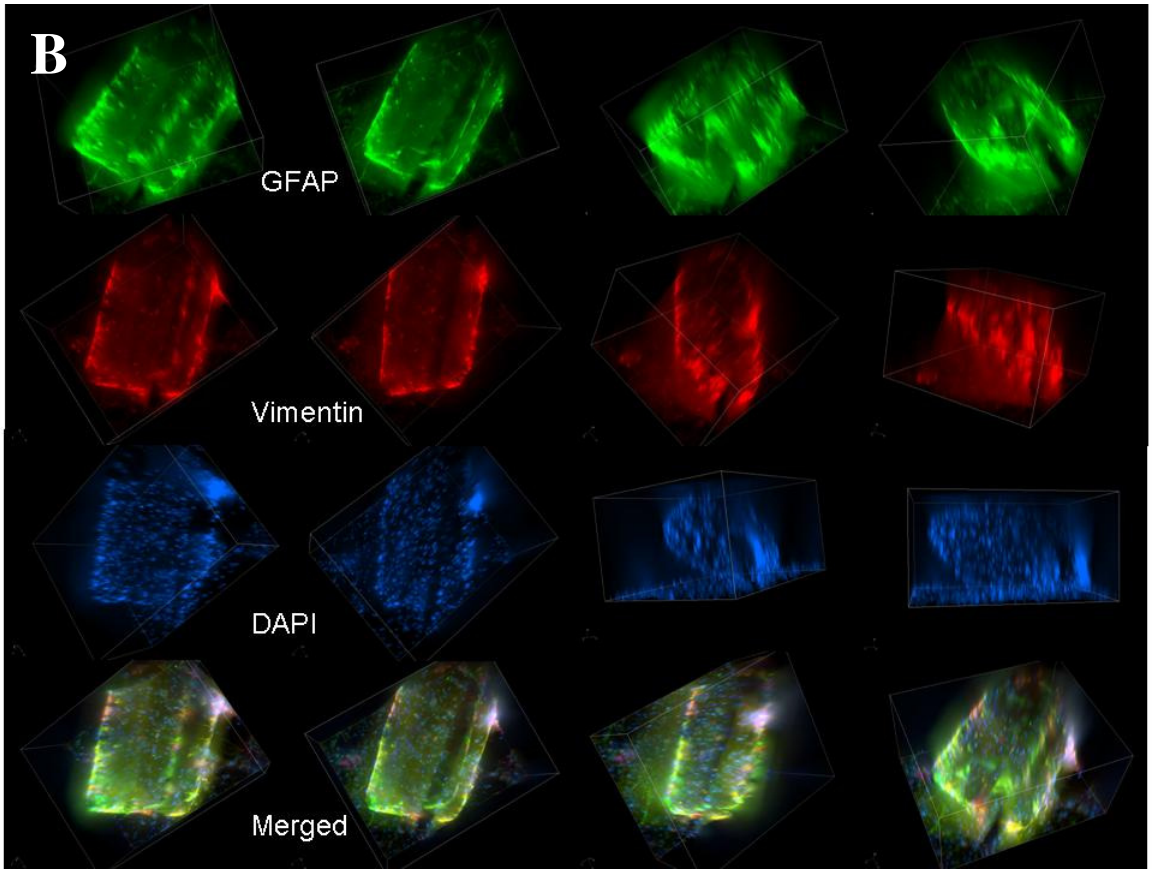


**Figure 21: (A) 3-D image of the end of a microwire coated with hydrogel and covered with cells. The layer of cells in the neuron-glial cell culture is on the the plane at the back side of the cube with the hydrogel sticking up above it. The metal of the microwire does not fluoresce so a dark area where the microwire is present can also be seen. The full length of the coated microwire extends up and to the right beyond the picture. (B) Rotated renderings of the image in A with different stains shown. The DAPI images show the entire surface covered by cells, many of which express GFAP and Vimentin. The levels of GFAP and Vimentin are much higher on the "scar" covering the hydrogel than in the neuron-glia culture below. The empty non-fluorescing space formed by the metal microwire can be seen in many of the images. As reference, the unstained microwire is 50uM in diameter.**

With the ability to remove these coated microwires from the culture and to perform analysis on the cells within the "scar" coating the hydrogel, the study examined the effect of two factors previously found to be important in scar formation in vitro: serum and bFGF. A cell count measure was found by summing up the nuclear area (DAPI fluorescent area) and normalizing it to the length of the hydrogel so that a normalized cell count was obtained for each microwire

segment. Cultures were exposed to varying levels of serum (0%, 0.1%, 1.0%, 5.0%, 10%, and 20%) and of bFGF (0 ng/ml, 1ng/ml, 10 ng/ml, 50 ng/ml) in the media at treatment time, when the coated microwires were placed on top of the neuron-glia cell layer. The number of cells coating the hydrogel increased with increasing levels of both bFGF and serum with maximum values at 10% FBS and 50ng/ml bFGF, with a slight decrease from the maximum levels with 20% FBS and 50ng/ml bFGF (Figure 22). The effect of both serum and of bFGF were statistically significant to $p<0.0001$ in a 2-factor ANOVA although there was no significant interaction between serum and bFGF.

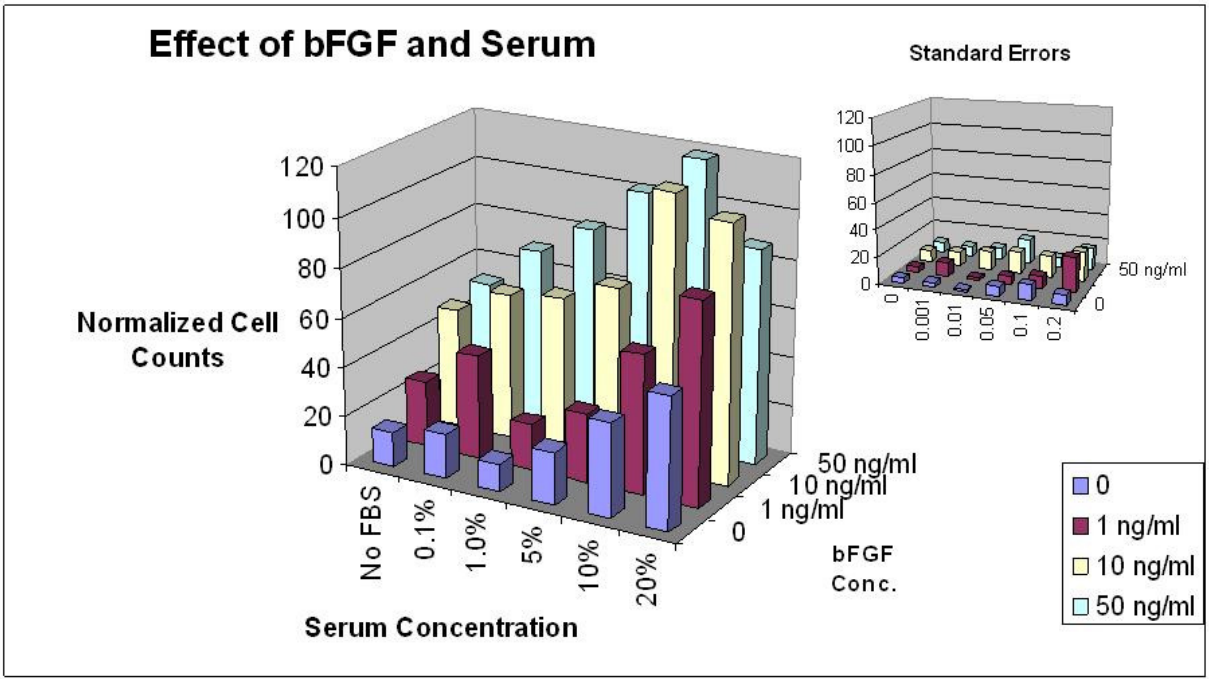


**Figure 22: Cultures were exposed to varying levels of serum and of bFGF in the media at treatment time. The number of cells coating the hydrogel increased with increasing levels of both bFGF and serum. The effect of both serum and of bFGF were statistically significant to $p<0.0001$ in a 2-factor ANOVA although there was no significant interaction between serum and bFGF. Cell numbers were obtained by comparing nuclear area and normalizing to microwire length.**

To further understand the biological mechanisms at play in this component of the scarring process, the study tested the effect of various soluble factors (and some of their inhibitors) on the amount of scarring. To see which factors increased scarring, cultures were treated with 1% serum but no bFGF (negative control, non-scarring conditions) and the soluble factor was added into the media (Figure 23). Inflammatory cytokines IL-1β and IL-1α significantly increased the level of scarring as measured by the number of cells on the hydrogels ($p<0.01$) although IFN-γ had no discernable effect. None of the anti-inflammatory, neurotrophin, inhibitors, or IL-6 family cytokines significantly increased the level of scarring. Glial growth factors PDGF ($p<0.01$) and BMP-2 ($p<0.05$) increased the level of scarring, as did bFGF (as expected).

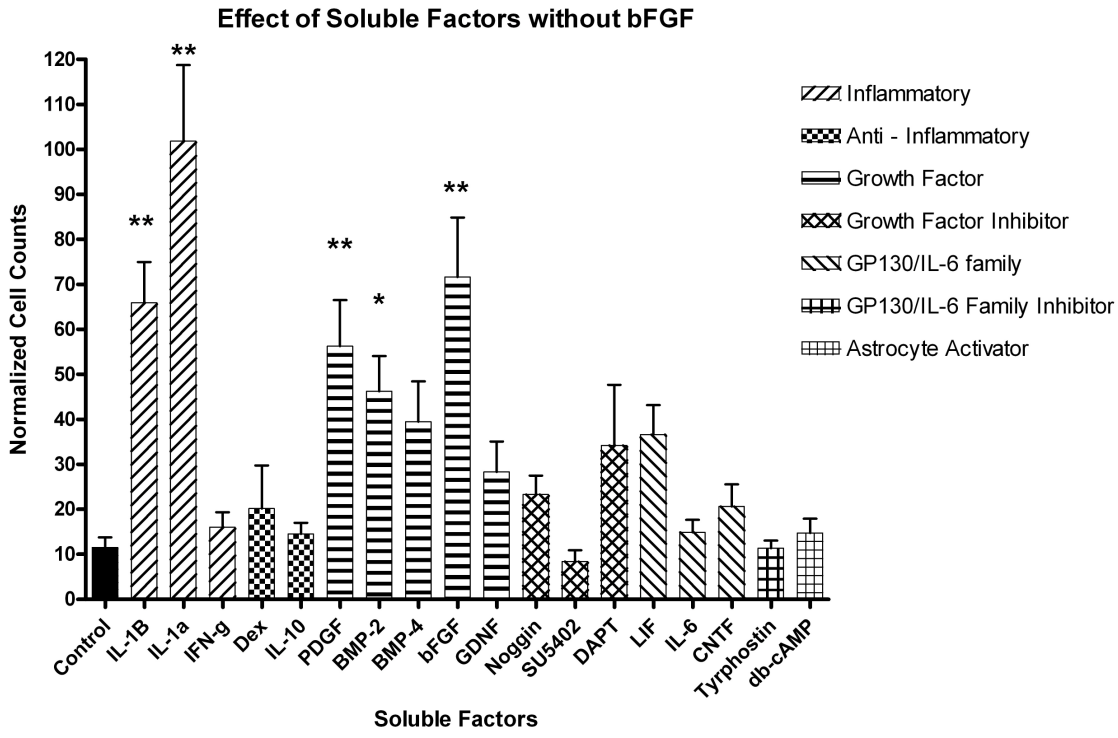


**Figure 23: Hydrogel coated microwires were placed in the culture (1%FBS, no bFGF) along with various soluble factors. The normalized cell count was determined for each added factor to see the effect on scarring. (ANOVA $p<0.0001$, ** signifies $p<0.01$ and * signifies $p<0.05$ relative to control via Dunnett's Multiple Comparisons post-hoc test).**

To see which of these factors can decrease the high level of scarring obtained with bFGF in the culture, or which can raise scarring to an even higher level, the experiment was also run with 10 ng/ml of bFGF in the media (positive control, high scarring conditions) as the soluble factors were added in (Figure 24). IL-1β and IL-1α both significantly increased the level of scarring beyond what was seen in the control cultures containing bFGF. The bFGF inhibitor SU5402 completely blocked the effect of the bFGF in the culture and scarring dropped to levels observed without bFGF in Figure 23. While some decrease was observed with anti-inflammatory compounds, and an IL-6 family inhibitor, these decreases did not reach significance.

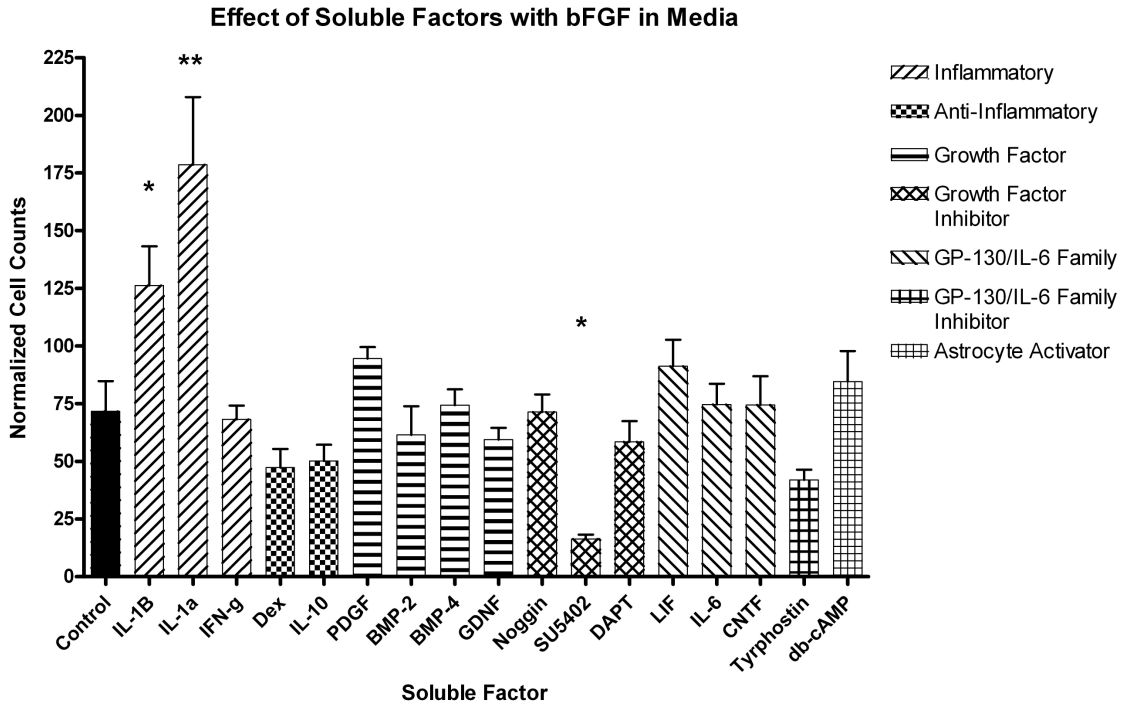


**Figure 24: Hydrogel coated microwires were placed in the culture (1%FBS, 10ng/ml bFGF) along with various soluble factors. The normalized cell count was determined for each added factor to see the effect on scarring. (ANOVA $p<0.0001$, ** signifies $p<0.01$ and * signifies $p<0.05$ relative to control via Dunnett's Multiple Comparisons post-hoc test).**

## *5.4 Discussion*

Previously we showed that a well-documented embryonic neuron-glia culture system developed for studying adult Parkinson's disease can reproduce many of the hallmarks of the glial scarring around neuroelectrode materials [4;168;238;239;249-251]. We optimized the model such that a glial scar formed every time the culture was run [5]. The optimization process also allowed us to observe the importance of serum, bFGF, and media conditions favorable to neural precursor cell growth and survival in forming the scar around a model electrode. This study goes further in exploring the effect of serum and bFGF on glial scarring and explores the role of several commonly cited cytokines and growth factors on glial scarring within the model.

Recording electrodes chronically implanted in the brain often fail after several weeks to months as they are surrounded by a glial scar formed of microglia, astrocytes, NPC's, and extracellular matrix. The development of the glial scar is a process that occurs over multiple time scales (seconds to months) and distance scales (nm to mm)[3]. One of the first events that occurs as the electrode is inserted is that vasculature (and the blood-brain barrier) is broken, serum is released, and mechanical damage kills nearby cells. Within minutes, microglia localize and migrate to the damaged area. Serum proteins adsorb to the electrode within seconds providing attachment points for the microglia, which attach to the foreign body (in this model a stainless steel microwire) and release enzymes in an attempt to degrade it [266;270]. Other microglia clean up cellular debris and release inflammatory cytokines to call in other microglia and wound healing cells. Over minutes to hours, the blood clot hardens into a provisional wound healing matrix and eventually the matrix is re-formed into a basal lamina composed of collagen, laminin, and proteoglycans that concentrate and present growth factors such as bFGF to the nearby cells. This basal lamina is

usually found between the layer of microglia attached to the foreign body and the layer of undifferentiated neural precursor cells or immature astrocytes beyond it [178-181]. A thicker layer of already differentiated thickened scar astrocytes expressing GFAP lies beyond this first layer of precursors [26].

In the previous version of the model, uncoated stainless steel microwire was placed in the culture and the microwire was quickly covered with a layer of microglia sitting atop the foreign body and a layer of GFAP expressing astrocytes beyond the microglia [4;5]. While an uncoated wire allows the visualization of the microglial response, it makes it difficult to study the astrocytic response. In those previous studies, microwires removed from the culture after the culture was stained only had microglia attached (also commonly seen in vivo when a probe is removed from the brain for tissue processing) while the GFAP expressing scar astrocytes were left on the culture plate intermingled with non-scar astrocytes. By adding the hydrogel layer of Matrigel, a commonly used basal lamina formulation, we were able to study the process that occurs *after* microglial attachment and basal lamina formation. The early microglial response is rapid, common to all tissues in the body with vascular breakdown after foreign body insertion, and is likely necessary for wound healing and therefore a less attractive target for intervention. However, the astrocytic response is unique to the CNS, occurs over days to weeks, and may be easier to modulate than the microglial response. The astrocyte response and the role of precursor cells in migrating to the injury site, proliferating, and differentiating into scar astrocytes is still largely unknown, and was the focus of this study.

This study highlighted the role of serum, which is released during electrode insertion, *and more importantly if further micromotion of the implant damages vasculature*, to increase the level of

scarring at the surface of the basal lamina lying beyond the microglial layer. A vast array of literature suggests gliosis is a natural brain response to any breakdown of the blood-brain-barrier that releases serum components into the normally serum-free brain parenchyma, whereas injuries that do not result in serum release do not induce significant glial scarring [170;252-255]. Without serum, glial precursors do not migrate to an injury site in vitro when a portion of the culture is scraped free of cells ([4] and unpublished observations) and in vivo models have shown a strong NPC [271] and inflammatory cytokine [103] response to injuries that involve BBB breakdown but a minimal response to those that do not. Furthermore, serum is often used as a differentiating factor within culture models studying neural and glial precursor cells, with serum driving the differentiation into an astrocytic cell type at the expense of other neural cell fates like oligodendrocytes or even neurons [71;256-258]. If serum is released with every round of device micromotion, it may generate a thicker and thicker scar, pushing away healthy neurons even as nearby neurons are damaged by the electrode motion[166]. The heparin sulfate proteoglycans in the basal lamina concentrate and present neural precursor cell growth factors such as bFGF and PDGF, so each round of damage through micromotion may create a more potent concentration of growth factors and thus a thicker scar [185]. There was no interaction between bFGF and serum as shown in Figure 22 so they may be acting independently of each other (i.e. serum may spurs migration while bFGF leads to proliferation) or together on the same pathway (i.e. both encourage migration).

There are several factors such as those in the BMP family (BMP-2 and BMP-4), as well as those in the IL-6 family acting through surface receptor gp-130, which drive the differentiation of neural precursor cells into astrocytes or the transformation of resting astrocytes into scar astrocytes. We had expected to see an increase in scar formation with these factors at a higher

level than what was observed (only BMP-2 addition resulted in an increase when bFGF was in the media and none of these factors made a difference when bFGF was not present). However, only the *number* of cells accumulating on the hydrogel was measured in this study, not the differentiation state of the cells or the level of GFAP expression. Future studies will look into cell identity and protein expression levels (i.e. GFAP, precursor cell markers) in the cells responding to the injury. Also, because neurons were not routinely stained for, the health of the cultures after soluble factor addition was not measured. However, through routine GFAP measurement, it was clear that some factors changed the environment of the culture as a whole and may have created conditions that were not healthy for the growth of neurons or microglia, although a confluent layer of astrocytes was present with each factor at the concentration tested. Specifically, IL-1α seemed to create an unhealthy looking culture with activated astrocytes throughout the culture and cavitation commonly seen in inflammatory environments in vitro [272].

Taken together, Figures 23 and 24 suggest that few of the factors tested could significantly raise the level of scarring beyond the already high level when bFGF was in the culture medium. Furthermore, although there was a slight non-significant decrease in scarring in the presence of anti-inflammatory factors and the gp-130 pathway blocker, in general the anti-inflammatory, anti-BMP, anti-Notch, or anti-gp-130 factors tested could not significantly lower that high level (presumably because inflammation, BMP's, Notch, or IL-6-family cytokines were not responsible for a large portion of the scarring). The FGF-receptor 1 blocker SU5402 was the only factor capable of blocking bFGF induced scarring in the culture model. bFGF is a necessary growth factor for the proliferation and maintenance of neural precursor cells, is upregulated in injury, and induces migration [124-126;128]. The data supports a conclusion that increasing NPC growth results in a larger, more robust glial scar. Such a conclusion is well supported by recent reports of

NG2+ NPC's and other undifferentiated, multipotent cells migrating to injury sites and differentiating into scar astrocytes, a notion that is at odds with the previously established view that it is the nearby mature astrocytes that proliferate, become reactive, and form the glial scar [73;76;78]. Astrocytes exposed to IL-1α and bFGF have been shown to help support NPC migration [127]. bFGF, PDGF, and an inflammatory environment may be sufficient for the proliferation and migration of precursor cells and scar astrocytes while BMP's, Notch, and IL-6 family cytokines are necessary for scar maturation and precursor cell differentiation once the scar is populated with enough immature cells. Future studies will explore the differentiation state of the cells within the scar in vitro as a result of different factors and will also explore the effect of multiple factors acting together.

## *5.5 Conclusions*

In this study, we used a previously developed and optimized in vitro model of glial scarring to further explore the biological mechanisms involved in glial scarring. Through the addition of a basal-lamina-like hydrogel as a coating to the metal microwires placed in the culture we were able to explore the cellular response to an implant injury after the initial microglial response subsides and a chronic astroglial response begins. Under conditions that supported glial scarring in our model (serum, bFGF, conditions favorable to neural precursor cell maintenance and growth), the hydrogels were covered in GFAP and Vimentin expressing cells. The number of cells responding to the inserted hydrogels rose with rising concentrations of serum and bFGF. Inflammatory cytokines IL-1β and IL-1α increased the level of scarring beyond that seen with just serum and bFGF, but most soluble factors tested (except for PDGF and SU5402, a bFGF inhibitor) had little to no effect, suggesting bFGF and serum are the key drivers of cell migration

and proliferation of cells responding to injury by forming a glial scar, with inflammation serving to accelerate the process. Future studies will explore the differentiation state of the cells within the scar in vitro as a result of local and global release of different factors.

# Chapter 6: Contributions, New Perspectives, and Future Directions.

## *6.1 Summary and Contributions*

This dissertation work began when a neuroscientist conducting regular neural recordings with custom made microwire electrodes (Dr. Miguel Nicolelis) approached Dr. Reichert for help with the problem of signal stability in chronic recording applications. A review of the literature, published as [3] and now cited over 70 times, revealed that this biocompatibility problem was indeed the true bottleneck between experiments on animals in the lab and broader clinical use. The review also highlighted how little was know about the biological mechanisms behind the tissue response (thought to cause the signal degradation), and revealed an overemphasis on material science strategies and in vivo implantation models in developing solutions. It was thought that an in vivo model of glial scarring would enable the type of rapid, mechanistic, iterative experiments needed to gain a better understanding of the deleterious tissue response.

Model development began with astrocyte and microglial cell lines, although this direction did not yield any experimental findings as the cell lines were unable to recreate the cellular and molecular responses to injury previously seen in vivo. However, working with the cell lines did allow a collaboration to form between the lab of Dr. J.S. Hong at the National Institutes of Environmental Health Sciences and the Reichert lab. Over time, it was discovered that the neuron-glia culture currently used in the Hong lab to study neuroinflammation could be adapted to display many hallmarks of the glial scarring response previously only seen in vivo. The development and characterization of the model was published as [4] and represented the first in

vitro model of glial scarring that recreated microglial migration and attachment to a foreign body and the upregulation of GFAP by nearby astrocytes. These early experiments also revealed the role of precursor cells that do not stain for GFAP but are very quick to respond to injury and differentiate into GFAP expressing scar astrocytes.

However, there was a problem with the initial model. While it recreated many aspects of the glial scar in vitro, it was highly variable. Although this variability was not surprising given the variability know to occur in vivo, it frustrated the use of the model to explore biological mechanisms because no strong positive control was present. A two year process of continuous, iterative model optimization ensued to find the factors that affected glial scar formation in the culture and those that would create a glial scar in every of the culture. After trying hundreds of variations, it was found that culture conditions that encouraged neural stem cell maintenance and growth resulted in greater scars. Specifically, it was found that serum, bFGF, and Neurobasal media with B27 supplement generated scarring in every culture, thus providing a strong positive control. Controlled experiments on six different culture dimensions also revealed that the scar matures after 4-5 days in the culture, that even low amounts of serum can drastically increase scarring, and that bFGF should be present in the media both at seeding and at treatment time for the most robust scars. This optimized culture protocol and the biological insights gained in the process of model optimization were recently accepted for publication as [5].

Finally, with a strong positive control and some insights into factors affecting glial scarring, the model was put to use to get a better understanding of the biological mechanisms behind glial scarring. First, a hydrogel coating that resembled the basal lamina typically found in the glial scar was added to the microwires placed in the culture. This allowed the observation of events

following the microglial response, namely the response of neural precursor cells and astrocytes forming the glial scar. Adding the hydrogel also allowed the removal of all the cells responding to injury from the culture for further processing. It also allows for future studies that incorporate local release of proteins. Experiments looking at the effect of serum and bFGF concentration revealed a strong increase in scarring (as measured by the number of cells in and on top of the hydrogel) with increasing concentrations of serum and bFGF, although the two did not interact. Further experiments with a battery of soluble factors thought to be involved in glial scarring revealed that inflammatory cytokines IL-1α and IL-1β increase scarring beyond that seen with just bFGF (and serum), and these same cytokines along with BMP-2 and PDGF can increase the level of scarring from a low baseline level when bFGF is not present (but with serum). Only an FGF receptor inhibitor was able to significantly reduce the level of scarring produced by the positive control (bFGF + serum) (manuscript in preparation). These results further highlight the role of serum and bFGF in glial scar formation and suggest further experiments looking at the differentiation state of the cells responding to the hydrogel coated microwires. Since only cell presence was measured, not cell identity (although most of the cells were observed to be GFAP+, many were non GFAP+ precursor cells), the effect of cytokines such as BMP's and IL-6 on the differentiation of precursors may offer further mechanistic insight into the glial scarring process.

Ultimately, the glial scarring model that was developed allowed the high throughput testing of hypotheses and the fine grained mechanistic insight that is impossible with in vivo studies. It can be a useful tool for neuroscientists in the future. These insights also point to a bigger role for micromotion that induces successive rounds of serum and bFGF release in the failure of chronically implanted recording electrodes.

## *6.2 A new perspective on neuroelectrode failure*

In the course of developing the in vitro model of glial scarring described in the preceding chapters, a new perspective on the tissue response to implanted electrodes began to take shape. This perspective was also shaped by a summer-long internship at Cyberkinetics, the only company thus far to have attempted (and ultimately failed) human clinical trials on chronically implanted recording electrodes [12]. Because most of the experiments developing and optimizing the in vitro model have been biological in nature, the perspective is also a biological look at the events following electrode insertion. Although this project started with the desire to find a biological solution to the stability of recording electrodes, surprisingly, the end result has been to suggest that the culprit is a very non-biological, non-cellular or molecular mechanism: device micromotion. This section briefly describes this new perspective on the tissue response and device failure.

### 6.2.1 Cellular and Soluble Factor Reaction to Injury

For electrode insertion to occur, the stiffness of the electrode must be much higher than the stiffness of the brain, which is similar to that of loose gelatin. Since current generation recording electrodes are made of metals or silicon, the mismatch in stiffness means that the insertion is similar to that of a shard of glass or a needle into a block of gelatin. The insertion causes tissue damage, including neuronal and glial cell death, and more importantly, breakdown of the BBB as blood vessels are broken [137]. The localized BBB breakdown releases blood components that are not normally seen in the brain, and these components signal that there has been tissue injury, and therefore initiate inflammation and wound healing. These components are soluble serum

factors, platelets, and cells such as neutrophils and macrophages. While blood components may be quickly removed or absorbed by immune cells clearing debris, it takes a healthy BBB to keep blood proteins out of the brain, a process that may take several days. The ECM in the brain, primarily made of proteoglycans, may also capture and present protein factors released during injury long after the wound is closed. However, it may be easiest to imagine serum release as the early stimulus that initiates the cascade of cellular and molecular processes that result in the glial scar.

The serum factors either cause the immediate release of chemoattractants (i.e. MCP-1 and MIP-1) from cellular stores or they themselves act as chemoattractants, instantly initiating large-scale microglial and NPC migration to the injured area [273]. The migration of cells to the site of injury plays a dominant role in glial scarring [130;274] and thus the extent of healing can be impaired by inhibiting cell migration machinery like aquaporins [273]. Nearby cells are directed to upregulate neurotrophins to keep neurons alive and ECM deposition to promote wound healing [175]. The ECM deposited at the site of injury collects, concentrates, and presents bFGF (and EGF) to the NPC's arriving at the injury site to induce their proliferation.

Microglia arrive to the site of insertion within hours and help participate in the cleanup and inflammatory reaction already begun by the blood leukocytes concentrated at the injury site. Upon reaching the site of injury several hours after the microglia, NPC's join microglia in releasing cytokines like IL-1β, TNF-α, and IL-6 to help with orchestrating inflammation and wound healing, release neuroprotective factors to help protect against secondary damage to neurons caused by inflammation, produce the proteoglycans and basal lamina proteins as part of the wound ECM, and NPC's begin their several day long process of differentiation into activated

scar astrocytes. Over the course of several days, if the implant is not moving relative to the brain, the cell debris is cleared out and damaged neurons die while less damaged neurons recover and recorded signals become more stable. Microglia and macrophages coat the foreign material of the electrode and try to degrade it with proteolytic enzymes. Although these enzymes could be harmful to bystander neurons, it is likely that the enzymes are only present within tightly controlled compartments that form between the microglia/macrophages and the implant material [275]. Over time, the microglia may fuse into giant cells in order to better engulf the much larger implant.

A new basal lamina composed of laminin, collagen IV, proteoglycans, and other ECM proteins forms between the layer of microglia sitting on the surface of the electrode and the surrounding brain tissue. The basal lamina contains many ECM proteins known to sequester and present growth factors such as TGF-β, BMP's and bFGF to surrounding cells [185].

As NPC's differentiate through the action of IL-6 cytokines acting through STAT3 and BMP cytokines acting through SMAD released at the injury site, a layer of GFAP expressing astrocytes form the region directly adjacent to the basal lamina and the microglia coating the surface. The only areas of the brain that naturally have astrocytes expressing such high levels of GFAP are at the intersection of brain tissue and "non brain" regions like blood vessels or meningeal connective layers. At each of these intersections, a basal lamina is present and strongly GFAP expressing astrocyte processes, called "end feet" terminate at these regions, forming the glia limitans [46;164]. Therefore, it is not surprising to see astrocyte processes expressing high levels of GFAP contacting the basal lamina around the implant and creating a barrier between a "non-brain" region (the implant) and the brain parenchyma. This was observed in the in vitro model as

described in Chapter 5. In a stable environment without further injury, a "non-brain" microglia coated implanted electrode, surrounded by GFAP+ reactive astrocytes with a thin basal lamina in between becomes the new "normal" state. Some neuron death did occur during the initial insertion injury, but the dead cells have been removed, brain integrity has been restored, and action potentials from nearby neurons can be recorded.

### 6.2.2 Device Failure

A discussion about device failure must begin with a description of what neuroscientists working on animal and human subjects experience. There seems to be a disconnect between the three groups involved in the brain machine interface: electrode engineers, cell and molecular biologists studying glial scarring and biocompatibility, and neurophysiologists making recordings. A term commonly used by the biocompatibility community is a "gradual decline" in the number of units recorded. However, neuroscientists making recordings will note that the declines they see are only gradual over the long term and on average. Each individual recording channel is highly dynamic [214]. Large units will enter one day but be gone the next day. A channel may record a single unit for months, only to see the unit disappear overnight while another unit may appear the same day on a different channel. There may be discrete drops in recording, where dozens of units are present one day with almost no units present the next day, but many units returning within a week. There is often a gradual decrease in signal to noise ratio such that large single units become low amplitude multi-unit clusters, and eventually the noise becomes larger than the signal. However, this gradual decline in SNR occurs in parallel to the drastic changes between and

among units on individual electrodes and it is the disappearance of units, not necessarily the overall decrease in SNR that is the cause of device failure.

What causes these sudden changes in the number of recorded units? A tethered electrode that is undergoing micro- or macromotion relative to the brain because of animals moving their head is like a shard of glass inside a cup of gelatin that is being shaken. The gelatin is highly deformable and will move around, while the shard of glass cuts up the surrounding gelatinous tissue. This motion of a hard, non-deformable electrode relative to the very soft, highly deformable brain creates further damage which begins the scarring cycle all over again. Even normal breathing results in surface micromotion of the brain on the order of 10-30 μm [206]. Vasculature is broken, serum is once again released, immune cells create an inflammatory environment, surrounding cells migrate and proliferate in the area and lay down more ECM, and the scar becomes thicker. In addition to killing more neurons in the region with each round of damage, the scar pushes living neurons further away, turning single units into low SNR multi-unit clusters. The inflammatory environment may silence neurons in the area, which only return to normal firing patterns several days or weeks later, but now fewer in numbers and farther away. The motion may also move the electrode to a new location with healthy neurons, especially with electrode designs such as microwires and the UEA which have tip electrodes (as opposed to Michigan electrodes which record from the shank surface), although eventually the entire area becomes devoid of neurons. Sharp declines in units, possibly caused by traumatic events (i.e. monkey hitting its head on its cage) are often later followed by later sharp increases in units, except the number of units that return are fewer and have a lower SNR, until after several such cycles too few units remain to provide a control signal. As evidence for the dominant role of micromotion, electrodes tethered to the skull generate significantly thicker scars than untethered

electrodes [34] and tethering resulted in massive neurofilament loss (and presumable neuronal death) within 100 μm of the electrode [166], precisely the distance from which electrodes must record.

A cycle of injury and repair may result in a state of constant activation for cells in the glial scar. The chronic presence of microglia on the surface of the electrode may also keep the scar astrocytes in a chronic "activated state", whereas they might have lowered their GFAP immunoreactivity had the microglia ceased to release factors such as IL-6 and IL-1β. Chapter 5 presented evidence that inflammatory cytokines such as IL-1α and IL-1β can increase the already high levels of scarring obtained with serum release and bFGF. However, the mere presence of a basal lamina may result in an astrocytic response that involves GFAP immunoreactivity, similar to the response around blood vessels and meningeal cell layers [46;164]. The long-term presence of bFGF and NPC's at the site of injury may result in a chronically activated, non-differentiated state for the NPC's adjacent to the electrode [102].

### 6.2.3 Possible solutions to problems with micromotion

One solution to the biocompatibility issue may lie in creating electrodes that have the same modulus as the brain and will not cause further injury due to sharp brain movements or simple micromotion. Of course an electrode must be able to pierce the pia, but there has been some work on polymers that change their modulus after hydration or changes in temperature [276]. Alternatively, a biodegradable rigid backbone can be used for the initial insertion, or a microwire can be inserted first and removed, creating a hole for the flexible electrode. Because the initial

insertion doesn't seem to cause enough damage to kill or silence all nearby electrodes, making a hole may be an easy way overcome the rigidity issue.

### 6.2.4 Conclusions

This perspective on the progression of the tissue response to chronically implanted recording electrodes and its effect on electrode failure is similar to the generally accepted view presented in Chapter 2. However, the focus is shifted from the role of microglia, astrocytes, and inflammatory molecules to a focus on micromotion, serum release, and the role of NPC's to migrate, proliferate and differentiate at the site of injury. The glial scar that forms after the initial insertion is not deleterious enough to affect recordings and probably even stabilizes the electrode and maintains a healthy environment for surrounding neurons through neurotrophin release. However, as the hard electrode pistons up and down (or laterally) relative to the soft tissue, more and more neurons are killed, the glial scar thickens with further serum release and NPC migration/proliferation, and the number of healthy neurons near the recording sites decreases. A strategy that removes the mechanical mismatch (i.e. through modulus changing polymers or a degradable electrode that only leaves the recording leads) should overcome the recording problems experienced thus far without the need to drastically modify the body's normal wound healing response in the brain – the glial scar.

## *6.3 Future Work*

The first 5.5 out of 6 years of this study was spent developing an in vitro model to study glial scarring. This model was characterized and optimized and shown to recreate many of the hallmarks of this tissue response to implanted biomaterials. The final model was so powerful and

versatile that it was used to generate more data regarding the biological triggers of glial scarring in the last six months than many in vivo studies implanting mock electrodes have generated up to this point. What was developed was a tool to look at these triggers and to give neuroscientists and biomedical engineers insight into how to make functional electrodes and how to treat injuries that create a glial scar (i.e. spinal cord injuries). While it is true that the process of *developing* this tool allowed insights into the biological mechanisms behind glial scarring that could not have been achieved otherwise, the real insights are yet to come by *using* the tool. This last section proposes future studies to take advantage of the unique capabilities of the in vitro model described in this dissertation.

### 6.3.1 Cell Identity and Differentiation

Chapter 5 described cells responding to a hydrogel coated microwire placed into the culture model. The cells that had accumulated on the basal lamina-like coating were stained and removed from the culture for cell counts. The final end points measured were the number of cells on the microwires for each culture condition. This study only looked at cell accumulation, via migration and proliferation, not cell identity. Casual observation revealed that in the positive control conditions, many of the cells on the coated microwire were GFAP+ scar astrocytes, none were neurons, few were microglia, and many were unstained for microglial, asotrcyte, or neuronal markers and were presumably NPC's. A study that quantified this staining along with cell identity would be the logical next step for this model. Instead of results that generated the bar graphs in Chapter 5 that looked like the following:

| **Condition** | **Control** | **LIF** | **IL-1β** | **SU5402** | **IL-1α** | **Dex** |
|---|---|---|---|---|---|---|
| **Normalized Cell Count** | 72 | 91 | 126 | 16 | 179 | 47 |

The new set of experiments would allow a more in depth look at the effect of the various treatments on NPC differentiation into scar astrocytes and at their effect on microglia (hypothetical data):

| | **Condition** | | | | | |
|---|---|---|---|---|---|---|
| | **Control** | **LIF** | **IL-1β** | **SU5402** | **IL-1α** | **Dex** |
| **GFAP+ Astrocytes** | 45 | 80 | 30 | 8 | 30 | 45 |
| **OX-42+ Microglia** | 6 | 5 | 20 | 6 | 55 | 0 |
| **MAP-2+ Neurons** | 0 | 0 | 0 | 0 | 0 | 0 |
| **NG2+ NPC's** | 18 | 0 | 65 | 1 | 75 | 2 |
| **Unstained Cells** | 3 | 0 | 11 | 1 | 16 | 0 |
| **Total Cell Count** | **72** | **85** | **126** | **16** | **176** | **47** |

For example, this hypothetical data would point out that although there was no significant change in the total number of cells between Control and LIF (as found in Chapter 5), the LIF had a strong differentiating effect on the NPC's that had arrived at the coated microwire. In this hypothetical data set, the increase in cell numbers from the inflammatory cytokines is due to higher numbers of microglia and more undifferentiated NPC's, which is blocked by the Dexamethasone treatment. BrdU staining can also identify which cells are proliferating and therefore dissect the cells migrating vs. proliferating at the site of injury, unlike the data presented in Chapter 5, which combined these modes of accumulation. The ability to test specific hypotheses regarding how the glial scar is formed and how it responds to different cytokines would be extraordinary.

### 6.3.2 Combinations of Factors

In Chapter 5 only single factors were added into the media to test their effect. However, it is well known that not only are there dozens of factors released by cells after injury and within the glial scar, but many factors work together to achieve the behavior seen in vivo. For example, BMP's and IL-6 cytokines act synergistically to differentiate NPC's into astrocytes. Dexamethasone may not have any function unless IL-1β is stimulating the microglia or other cells in the culture. Combinatorial testing can easily be accomplished with this model system as each plate contains 24 wells for 24 separate experiments. Other factors or conditions (i.e. TGF-β, temperature, pH) can also be tested. Clearly there is a practical limit (cell counting time) to the number of factor combinations that can be tested, but the most promising combinations can be easily tested.

### 6.3.3 Incorporation of Factors into the Hydrogel

All of the factors tested in Chapter 5 were delivered globally into the media. Therefore, every cell in the culture experienced the effect of the added factors and therefore no concentration gradients or localized presentation of ECM-based growth factors could be achieved. There are numerous ways to create a hydrogel that incorporates proteins or small molecules for burst or delayed release, and even the present formulation allows for soluble factor incorporation. The effect of chemotaxis and cell migration to the site of injury as a result of soluble factors can be studied through local release. Different ECM proteins can be incorporated or covalently linked to the hydrogel to measure the specific contributions of, for example, perlecan vs. neurocan, on the behavior of cells responding to injury. The role of ECM proteins to present growth factors like bFGF can also be explored.

### 6.3.4 Adding the Time Dimension

One of the benefits of being able to run many experiments in vitro is the ability to create time courses. A time course was presented in Chapter 3 that uncovered the role of precursor cells to migrate into a wound region and differentiate into scar astrocytes. Time courses in Chapter 4 showed that it took the GFAP+ scar approximately 5 days to form, which is consistent with the amount of time it takes for NPC's to fully differentiate into astrocytes. The time course can follow this differentiation process as well as gather more fine-grained information about migration to the site. The microscope setup in the Reichert Lab has the ability to perform videomicroscopy on living cells in culture over a week. Movies of the cells accumulating on the hydrogel, or of cells migrating to the coated microwire can be made. By staining certain cells with fluorescent markers and adding them to the culture, or by transfecting certain cell types with fluorescent proteins driven by specific promoters, movies of microglia migrating to the site of injury or of NPC's migrating and differentiating, or of scar astrocytes upregulating GFAP can be obtained. Because cells don't express NG2 and GFAP at the same time, the differentiation of NG2+ NPC's into GFAP+ astrocytes is incredibly difficult to observe in vivo and has yet to be unequivocally demonstrated, but it can easily be done with videomicroscopy in vitro with this model.

### 6.3.5 In Vivo Validation

An in vitro model is only useful if the lessons learned in vitro can be translated and validated in vivo. Using the insights gained in Chapters 4 and 5, such as the role of serum, NPC's and bFGF

in glial scar formation, implants that deliver therapies to block glial scar formation can be implanted in vivo. For example, the bFGF blocker SU5402 that completely blocked cell accumulation can be delivered during implantation or through a minipump. Other molecules or therapies, such as STAT, SMAD, Notch, ECM, or cytokine blockers can also be used. Coatings for implants that elute drugs have been developed. What this model can contribute is the mechanistic insights that allow researchers to know *which* drug should be delivered.

One of the insights already gained through the development and use of the model is the possibility that micromotion plays a central role in signal degradation. Implants that are specifically designed to minimize micromotion can be implanted and either assayed for glial scarring or used for recording. One such implant design is presented in Figure 25. Open architecture like that proposed by the "via hole" has recently been shown to reduce scarring around an electrode:[211].

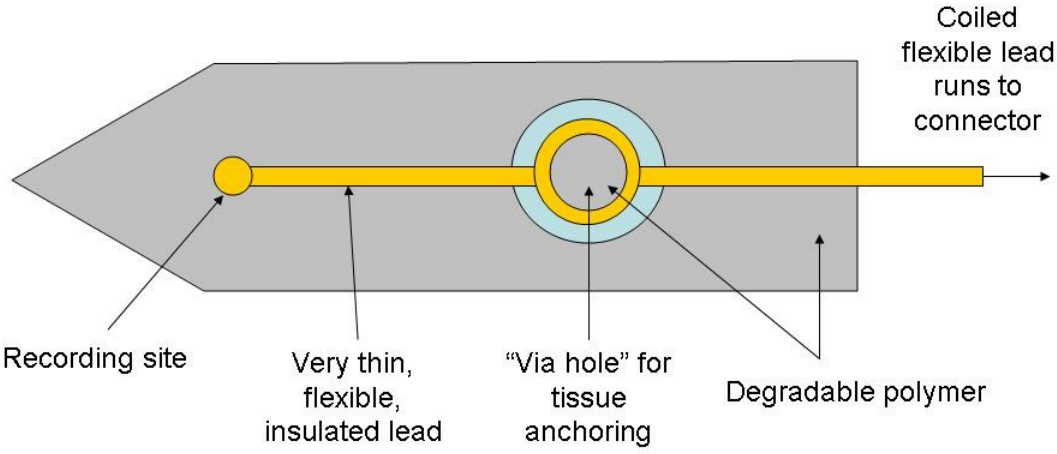


**Figure 25: Electrode designed to minimize micromotion-induced glial scarring in vivo. Some micromotion and glial scarring may occur around the "via hole", but the recording site should be unaffected.**

# Appendix A: In Vitro Models of Neuroelectrode Biocompatibility

{Originally published as [277])

## *The Importance of In Vitro Models*

Currently, the detailed mechanisms responsible for the electrode-tissue interactions leading to the formation of the glial scar around chronically implanted neuron-recording electrodes are poorly understood. As a consequence, the long-term use of electrodes for human prosthetics largely remains an untapped therapeutic resource. This chapter briefly summarize the currently available *in vitro* models which have the potential to uncover how the glial scar impedes brain electrode function and which provide a test bed to screen potential therapeutic compounds. Also presented is a discussion the strengths and weaknesses of each of the *in vitro* models and how this line of inquiry could advance the field.

Multiple cell types interact to result in normal brain physiology and the formation of the glial scar. Through *in vitro* ("in glass") studies, as opposed to *in vivo* ("in life") experiments, we may begin to directly address the effects of electrodes and foreign objects at a cellular and molecular level, clarifying the respective contribution of individual cell types and basic mechanisms. Specifically, cell culture studies offer the potential for detailed inquiry into how electrodes initiate the glial scar, what drives glial scar formation, and the glial scar mechanisms responsible for electrode signal degradation. Ideally, this process will reveal novel therapeutic strategies capable of extending the viability and utility of brain electrodes.

## Relative advantages of in vitro models

The primary advantage of *in vitro* studies is that they offer a controlled environment to test specific cellular and molecular hypotheses (Table 3). Tissue culture controls for environmental influences (e.g. temperature) and physiologic conditions of the animal (e.g. hormones, illness, nutrition), resulting in reduced experimental variation and assisting in the ease of experimental replication [278]. By using controlled combinations of relevant and specific cell types, it is possible to obtain valuable insight into how these critical cells interact. For example, using reconstituted cultures, it has been shown that LPS is toxic to dopaminergic neurons only in the presence of microglia, the resident innate immune cell in the brain. While mixed cultures comprised of neurons, astrocytes, and microglia resulted in neuron damage, those cultures containing only neurons showed no LPS effect. However, addition of microglia back in to neuron-enriched cultures reinstated the LPS-induced neurotoxicity while addition of astrocytes did not result in any LPS-induced effect [242]. Thus, using cell culture, it becomes possible to identify critical cell types responsible for glial scar formation and reveal essential cell-cell interactions. In addition to extracellular interactions, culture allows inquiry into the biochemical processes responsible for electrode failure.

Another great advantage of tissue culture is the ease of experimental procedures, experimental designs, and shortened experimental time scales. Although animal dissections are required to acquire primary tissue, the time, expense, and animal treatment stress associated with *in vivo* work on electrode biocompatibility is eliminated by *in vitro* models. In addition, treatment (agonists, antagonists, or potential therapeutic compounds) is applied in lower volumes (milliliters), drastically reducing the cost of compounds when compared to whole animal

exposures. Together, these characteristics add to the convenience of *in vitro* experiments and work to attenuate the traditionally excessive expense associated with *in vivo* studies of biocompatibility.

## In vitro model limitations

All models are wrought with limitations which must be considered in overall experimental design (Table 3). The most widely recognized limitation of tissue culture is based on the fact that the cells grown *in vitro* are not the exact dissociated replicates of their *in vivo* counterparts. For example, dissociation may (or may not) change cell identity or function. In primary culture, often embryonic cells are used and younger less differentiated cells may have different phenotypes than mature in vivo counterparts. Further, there is a known genetic and phenotypic instability in many cell lines and primary cultures. Finally, the artificial and controlled environment is not the same as what the cells experience in *vivo* and could have an effect, depending upon the measure being assessed. Whether tissue culture experiments will accurately mimic in vivo behavior will vary based on the cell types tested, the treatment being investigated, and the endpoints measured. However, the potential experimental downfalls can be identified and consequently accounted for with the proper use of both positive and negative controls to discern that the tissue culture model is functioning consistently with *in vivo* physiology. In addition, critical components of novel *in vitro* findings must be confirmed *in vivo*. Thus, while *in vitro* models are a powerful tool of mechanistic diagnosis and a convenient, cost effective method of screening, they can not completely replace the use of animal and human studies.

**Table 4: General Benefits & Disadvantages of In Vitro Models**

| **Benefits of Tissue Culture** | **Examples** |
|---|---|
| **Control of Environment** | Temperature, pH, hormone & nutrient concentrations |
| **Control of Cellular Constitution** | Defined cellular identity and controlled cellular interactions |
| **Less Time** | Time measured in days to weeks, rather than months. |
| **Scale: Less Reagent Required** | Distribution of compounds in milliliter volumes compared to systemic distribution. |
| **Less expensive than *in vivo* experiments** | After initial equipment acquisition, the costs of consumables and media are significantly less expensive than animal husbandry |
| **Replicates and Variability** | Traditionally easy to replicate and less variability than *in vivo* studies. |
| **Reduction of Animal Use** | Treatment is administered to cell lines or primary cultures/tissue rather than in the in tact animal. Animals stress due to treatment is reduced. |
| | |

| Table 4, continued | |
|---|---|
| **Disadvantages of Tissue Culture** | **Examples** |
| **Lack of Systemic Input from the Periphery** | Brain pathology receives input from the peripheral system. |
| **Sterile Technique/Expertise** | The process of cell culture requires knowledge about sterile technique and the cell types of interest. |
| **Potential for Dedifferentiation and Selection** | The cells types may not be identical to cells in the intact system. |
| **Three Dimensional Structure Lost** | The effects of tissue and organ structure are not present. |

*Adapted from [278]

## *Types of Models*

A variety of in vitro models involving living cells have been employed to look at material-tissue interactions that might occur in the brain. These models range widely in complexity from very simple single cell lines to complex organotypic brain slices. As the complexity of the model increases, the relevance of the data to the actual in vivo conditions also increases, but the tradeoff is a loss of predictability, simplicity, and control. One possible decision tree with this tradeoff in mind is presented as Figure 26. The decision of which in vitro model to employ should be made with the aim of the experiment and the limitations of each system in mind. For example, cytotoxicity studies looking at the effect of monomer leaching from a polymeric implant would be better served by a fibroblast cell line rather than primary cell culture comprised of many interacting cell types. The fibroblast cell line is easier to culture, cheaper, and has an established experimental protocol that has been used in hundreds of cytotoxicity studies, resulting in established controls. On the other hand, if neurons are known to be more sensitive to a particular pharmacological insult (such as the leaching monomer) than fibroblasts, then primary neuronal cultures may be more appropriate. However, if a new protocol is chosen over an established design, the new design requires greater characterization and validation of controls. In the rest of this chapter, we will review the different in vitro systems employed by investigators to study neuroelectrode-tissue interactions and attempt to offer insights into future models currently being developed within our own lab. We begin the review with simple cell line models, then proceed to primary single cell models, then more complex primary culture systems with interacting cell types, and finally end with organotypic tissue slices, which represent an intermediate model between dissociated cell culture and in vivo.

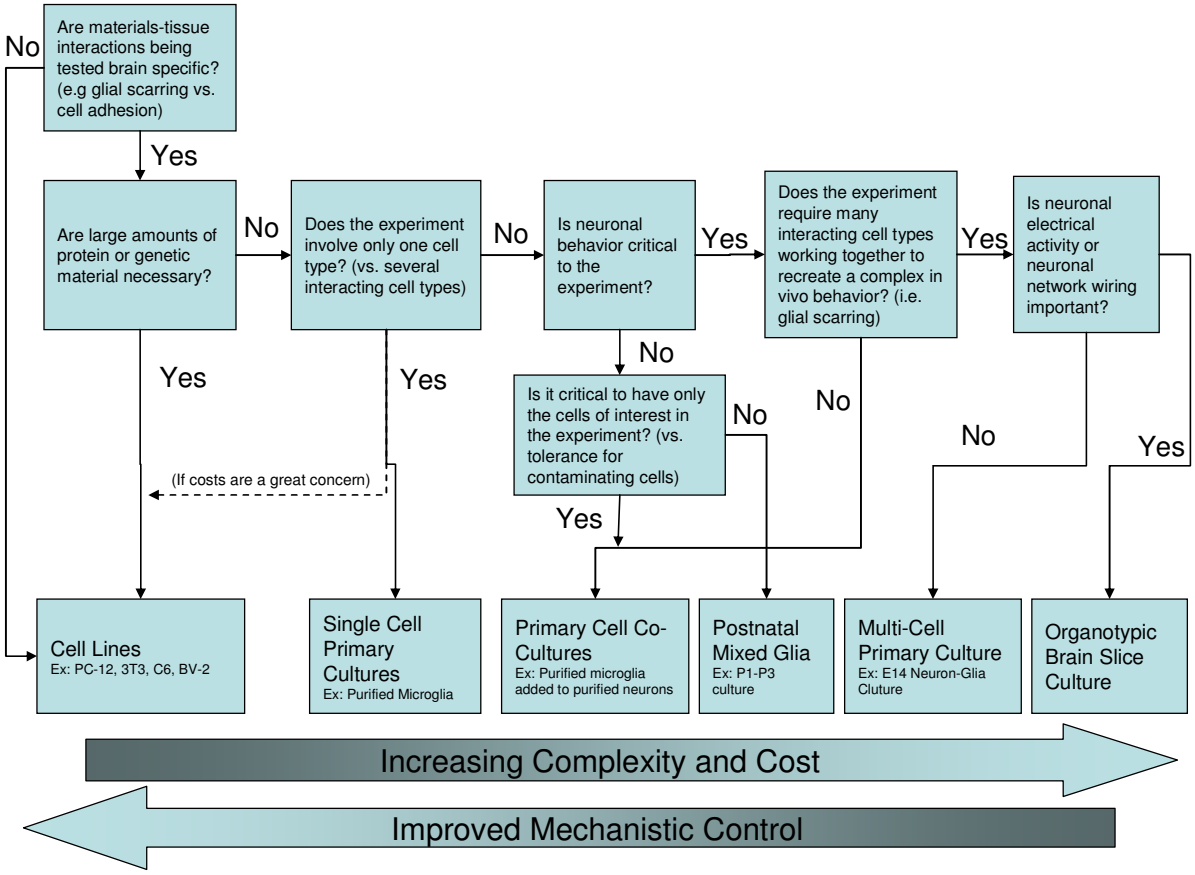


**Figure 26: One of many possible decision trees that can be used to determine the best in vitro model to use when planning an experiment**

## Cell Lines

The simplest in vitro models involve cultures of immortalized cell lines. There are several advantages to the use of cell lines: they are easy to culture, easy to grow and maintain indefinitely, inexpensive relative to primary cultures, and generate highly reproducible results. For example, it is much easier to obtain large amounts of protein or mRNA for analysis, particularly when compared to primary cultures. Furthermore, cell lines are derived from a single

cell type, so there is no danger of contamination by other confounding cell types. However, the limitations of cell lines are severe, and must be well appreciated to accurately interpret experimental results. Since cell lines are derived from tumors or other genetically unstable cells, the cell line phenotype will only approximate the normal, genetically stable cell population. For example, the emphasis of the cell line's metabolism may have shifted to growth and proliferation rather than the resting, fully differentiated function of the cell type that the cell line is approximating [279]. The genetic instability of cell lines also contributes to a loss in reproducibility and relevance over multiple passages. In addition to noting the source of your cells and the passage number, it is usually best practice to keep the passage number variance to a minimum in experiments. When these limitations are combined with the more general limitations of two-dimensional dissociated cell cultures, it is often difficult to place much faith in those results observed in cell line studies but not yet confirmed in vivo or in primary culture. However, as long as the limitations of immortalized cells are kept in mind, cell lines can be a powerful tool in the in vitro arsenal.

**Fibroblast Cell Lines**

The simplest biocompatibility experiments that can be conducted are cytotoxicity and non-specific cell adhesion assays. Stephen Massia's group regularly uses the 3T3 fibroblast cell line to evaluate the cytotoxicity of new neuroelectrode materials and coatings [202;205;280]. This cell line is among a set of well characterized lines mandated for use by the FDA as part of the cytotoxicity testing protocols for approving new medical devices. 3T3 fibroblasts are grown in a monolayer and exposed to materials such as polyimide and silicon based neuroelectrodes [205], diamond-like carbon coatings [202], or bioactive dextran/peptide coatings on a model substrate

[280] (Figure 27). A standard live/dead assay is conducted after 24 hours to see if the material tested caused any cytotoxicity. For adhesion studies, cells are seeded on top of materials and the number of cells adhering to the material after 24 hours is counted and compared to a base material or tissue culture polystyrene. Fibroblast cell lines are often used because they are easy to grow and maintain. However, since the meninges contain fibroblast-like cells, sometimes fibroblast cell properties are desired when comparing adhesion to brain cell types such as neurons and astrocytes. For example, 3T3 fibroblast adhesion was compared to astrocyte and neuronal cell line adhesion on various substrates. The degree of fibroblast cell line adhesion was found to be significantly different from that of a neuronal cell line on RGD adhesion peptide modified surfaces, but similar to that of a glial cell line [280]. In contrast, a different group using a different fibroblast cell line derived from rat skin (CRL-1213; American Type Culture Collection (ATCC)) did show a significant difference in adhesive properties between the fibroblast and glial cell lines on RGDS modified surfaces [212], underscoring the variability in responses between different cell lines.

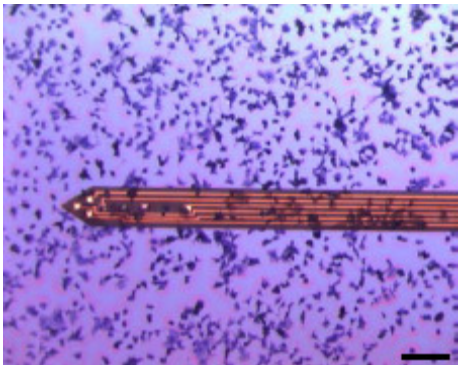

**Figure 27: Photomicrograph depicting morphology of adherent 3T3 cells on PI electrode shank and surrounding wafer surface, scale bar = 100 $\mu$m. Adapted from [205]**

**Neuronal Cell Lines**

One line of neuroelectrode research has focused on finding materials that attract neuronal processes and/or stimulate neurite growth. For these experiments, neuronal cell lines have often been used and their responses to various materials compared to other cell types found in the brain. The most widely used neuronal cell line in the neurobiology community is the PC-12 cell line, which exhibits many neuronal behaviors, especially reversible differentiation and neurite growth in response to NGF. A typical experiment with this cell line involves coating the substrate of interest with laminin or another molecule to promote adhesion, seeding the cells on the substrate, waiting for cell growth and differentiation (typically 1-3 days), and then fixing the cells and using immunostaining to image cell bodies and neurites. To measure adhesion, the number of cells is counted in random microscope fields to obtain a cell number or cell coverage ratio. A more sensitive measure to look at how the electrode material (cell culture substrate) affects neuronal growth involves counting the neurites and even measuring average neurite length as the immortalized neuronal cells differentiate. In two such experiments, PC-12 cell neurite growth was found to be more robust on textured silicon neuroelectrodes than on non-porous silicon by Moxon et al. [198], and PC-12 cells were found to adhere to IKVAV peptide modified polyimide and silicon oxide surfaces to a much greater extent than fibroblast or glial cell lines [280]. David Martin's group is attempting to integrate a conducting polymer grown from the neuroelectrode recording sites with neurons around the electrode to try to establish a more reliable and robust signal. They found that after seeding the cells on top of several different substrates, the human neuroblastoma SH-SY5Y cell line preferentially grew on top of the polypyrrole/CDPGYIGSR polymer/peptide blend "grown" from the recording sites of a silicon electrode [197]. Over a

dozen well characterized neuronal cell lines are available as a result of the decades of cell line experiments in the neurosciences [279].

**Astrocyte Cell Lines**

Because of the widespread understanding that the biocompatibility of neuroelectrodes is a function of the glial response to the implanted material, the majority of cell line-based experiments have been conducted using cell lines that approximate microglial or astroglial function. None of the astrocyte cell lines are perfect in recreating primary astrocyte behavior, but they are seen as more relevant than fibroblast cell lines in studying brain biocompatibility. As with neuronal cell lines, the most common experiment measures cell adhesion and growth of cells on a specific substrate. Cells are seeded in tissue culture plates containing the substrate of interest and allowed to adhere and growth for 1-3 days. The cells are then fixed, rinsed, and stained to assess the number of cells adhering to the substrate (as compared to other substrates or tissue culture plastic control). Cell spreading can also be measured to identify materials that promote a specific type of behavior (whether one desires spreading or no spreading depends on the objectives of the experiment). One of the most common astroglial cell lines is the C6 line derived from a rat N-nitrosomethylurea-induced glioma. The cell line expresses one stereotypical astroglial marker, S100, but not the most specific astrocyte marker, GFAP. C6 cells were used to show preferential glial cell adhesion to polypyrrole/SLPF polymer/peptide blend on a silicon electrode [197] (Figure 28). The DITNC1 astrocyte cell line (ATCC CRL-2005) expresses GFAP and appears to be similar in phenotype to Type 1 astrocytes in culture (Type 1 astrocytes are more physiologically relevant, while Type 2 astrocytes are thought to be an in vitro phenomenon). This cell line showed lower adhesion to textured neuroelectrodes than to smooth silicon electrodes

[198], which together with the neurite outgrowth data presented above, suggests texturing as a possible strategy to improve biocompatibility. Stephen Massia's group uses another Fischer rat glioma line, F98 (ATCC #CRL-1690) in experiments testing astrocyte adhesion to different surfaces [202;280].

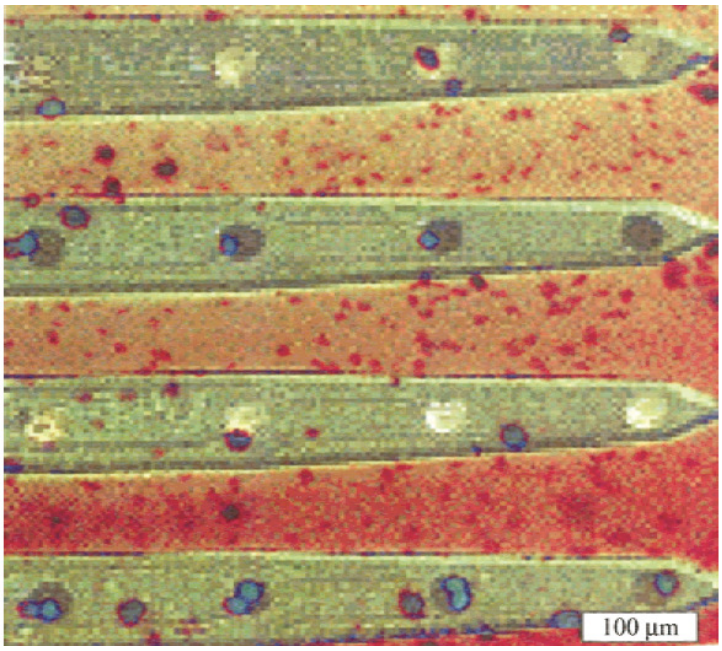


**Figure 28: PPy/SLPF coated 4-shank 16-channel neural probe cultured with C6 cells. Cells were stained using Hoechst 33342, and the blue spots correspond to individual cells. Adapted from [197]**

Several groups working on neuroelectrode biocompatibility at Cornell University, the Wadsworth Center, and Rensselaer Polytechnic Institute have used the LRM55 astroglial cell line to test new materials and modifications. A transformed rat glioma cell line originally developed by Martin and Shain [281], this cell type has been shown to exhibit several important astrocyte metabolic features. Investigators have used this cell line to show adhesion and spreading on micropatterned hydrophilic hexagonal DETA surfaces of varying sizes [218], an LRM55 preference for microfabricated silicon pillars and wells [220], the cell line preference for microcontact printed

surfaces over traditional photolithographic pattered surfaces [282], and a preference of smooth chemically etched regions over roughened "silicon grass" regions [217] (Figure 29). Contradictory behavior from primary astrocytes, which favor roughened "silicon grass" regions, underscores the limited ability to make definitive conclusions from cell line experiments [220].

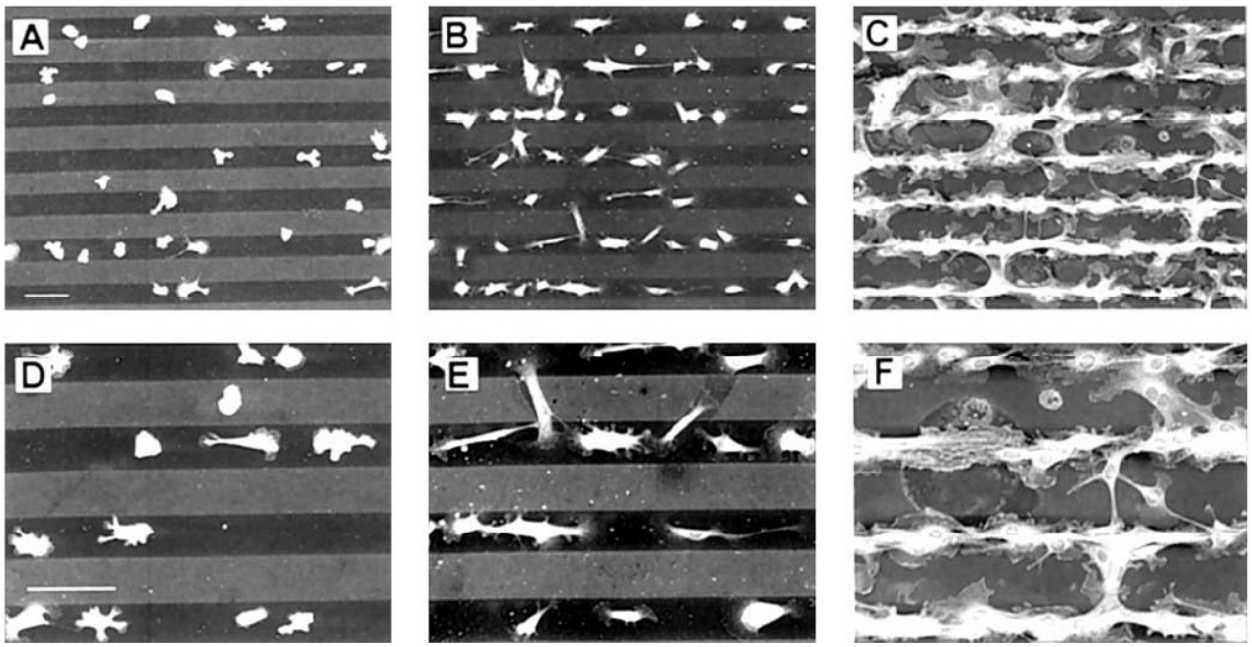


**Figure 29: Time course of LRM55 astroglial cell attachment to surfaces patterned by microcontact printing. Cells were plated and fixed after 2 h (A and D), 6 h (B and E), and 24 h (C and F). Bar, 100 mm for both low magnification (10_ objective, A–C) and high magnification (20 X objective, D–F) images. Dark regions are a permissive DETA (a hydrophobic organosilane self assembled monolayer) while the light stripes are layers of inhibitory OTS (a hydrophobic organosilane). Adapted from [282].**

### Microglia Cell Lines

Microglia based cell lines are commonly used to study neuroinflammatory processes, but only recently have biocompatibility studies recognized the dominant role of microglial cells. Often cell lines are employed to better understand processes already known to occur in vivo or in primary cells. For example, Tzeng and Huang used the immortalized mouse microglial BV-2 cell line to

probe the effect of neurotrophin-3 (NT-3) on the cytokines and inflammatory molecules released by microglia after an LPS immune challenge [283], a process suggested by in vivo observations. Kremlev et. al. used the BV-2 cell line as well as the HAPI microglial-like rat cell line to assay for the release of chemokines and the expression of chemokine receptors after an immune challenge after in vivo data suggested the involvement of chemokines in inflammation-mediated brain injury [284]. Both the BV-2 and HAPI cell lines are commonly used in the Hong lab to further explore behaviors observed in vivo or in primary cultures [285]. Once the cell lines show the same behavior as we earlier observed in vivo (i.e. release of a certain cytokine after immune challenge), we can then use the cell lines to examine the details of that behavior (i.e. the signal transduction pathway of cytokine expression). Another example where microglial cell lines were advantageous over primary culture is in the case of studying LPS internalization in microglia. All microglia, including cell lines, phagocytose LPS and it was simpler to use the cell line, because they were less sensitive than primary cultures to the lower density seeding that was necessary to get single cell images for confocal microscopy (Figure 30) [286].

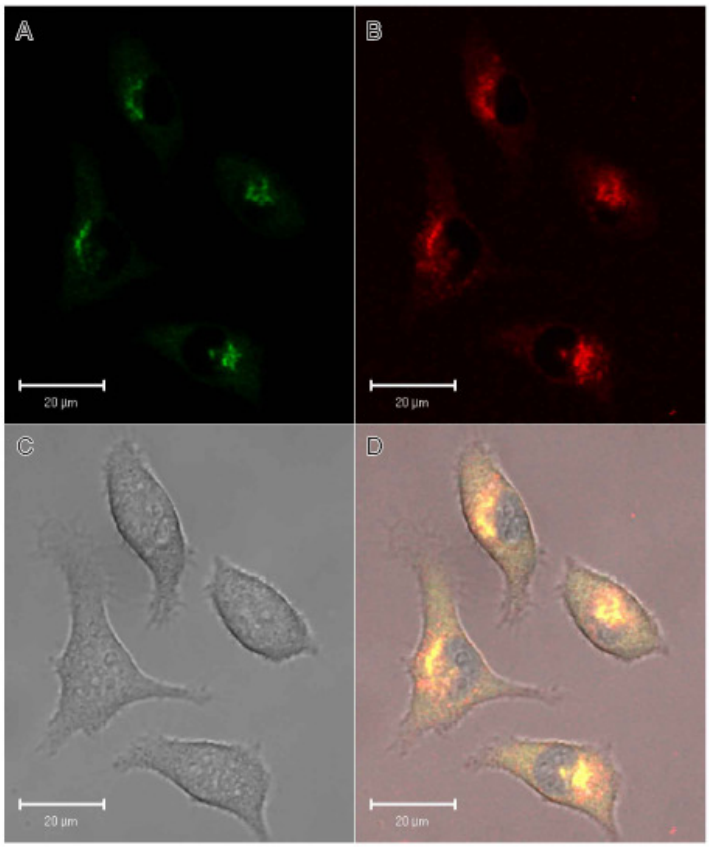


**Figure 30: Internalized LPS is localized in the golgi. HAPI microglial cells were exposed to 10 ug/ml labeled LPS an 1µM NBD-ceramide for 1 h at 37º C. Perinuclear colocalization of NBD-ceramide (A) and Alexa568-LPS (B) in HAPI microglia. (C) Shows the transmitted light image and (D) the overlay of transmitted light and fluorescence images. The scale bars indicate 20 µm.**

## Primary Cells

The step up in complexity from cell lines to primary cultures is significant. Primary cells are genetically stable and are often the actual cells taking part in the in vivo process, so the results from primary culture experiments are much more trustworthy. However, in exchange for the increase in relevance comes significant new challenges, including additional costs of animal purchase and husbandry, isolation difficulties, and increased culture variability. One also looses

the ability to easily culture and proliferate cells through many generations. As primary cells proliferate and are passaged, the phenotype may change to a point where the cells no longer behave in the same way that the initially isolated cells behaved. For this reason, only the first or the first few passages of primary cells can be used, and the actual number of valid passages depends on the cell type and behavior being investigated.

Even with greater relevance to the in vivo situation, primary cell culture is still not a perfect model of the in vivo environment as the isolation procedure often injures or activates the cell, resulting in an altered phenotype, and the two-dimensional culture system without vasculature, extracellular matrix (ECM), and other supporting cells further alters cellular behavior. Furthermore, as with any phenotypically diverse biological system, the results obtained with primary cultures will show a higher degree of variability than the results from genetically identical cell line cultures.

Primary cultures can be subdivided further into increasing levels of complexity. The least complex cultures are single cell type primary cultures. These are the primary cell equivalent of cell lines, where the researcher is interested in the response of a single cell type to the experimental conditions. By combining two independently isolated sets of primary cells together (i.e. primary astrocytes and primary neurons), a more complex co-culture can be used, thus allowing analysis of cell-cell interactions. Finally, if two or more cell types are isolated together from the same tissue in the same procedure (i.e. a culture of astrocytes and microglia from postnatal rat cortex), this is an additional step towards the more complex conditions of the in vivo environment.

**Single Cell Type Primary Cultures: Primary Neurons**

Because of their unique electrical properties relative to other cells, and their varied phenotypes within the CNS and PNS, neurons are not well represented by cell lines in culture. While a few neuronal cell lines, like the PC-12 line, exhibit limited neuronal behavior, the vast majority of neurobiological studies in the past several decades have used primary neuronal cultures. Neurons are highly varied in form and in behavior depending on their age, location, and function in the brain, but commonly share negligible to no proliferative potential, making cell culture quite difficult. Still, several isolation protocols have been established that consistently produce highly pure, electrophysiologically active neuronal cultures.

Because of the limited proliferative potential of adult neurons and their relative sensitivity to injury, neurons are usually isolated from embryonic or early postnatal animals, while they are still differentiating from the hardier, dividing neuronal precursor cells. Cells are mechanically or enzymatically dissociated, plated on poly-D-lysine or laminin coated polystyrene and maintained in specially defined, serum-free media. Dobbertin et al used a standard cortical neuronal culture from embryonic day 17 (E17) Sprague-Dawley rats to study the growth of neurites on RPTPβ/phosphacan, a condroitin sulphate proteoglycan upregulated after injury to the CNS [287]. After removing the striatum and hippocampus, the cerebral cortices were freed of meninges and cut into small pieces before enzymatic treatment with trypsin. By seeding at low density ($10^4$ cells/$cm^2$ and using specially defined growth media (1:1 mixture of DMEM and Ham's F12 with 1% N2 supplement), the investigators were able to get a cell culture that was 98% pure neurons. Ravenscroft et al used a similar procedure to isolate E18-19 hippocampal neurons in their studies and patterned them on silane modified surfaces [288]. They were then

able to engineer circuits of aligned neurons on glass coated with a patterned silane film. In this case, cells were dissociated with papain and layered over a step gradient to remove cellular debris before resuspension in serum-free Neurobasal medium supplemented with B27, glutamine, and glutamate.

Postnatal derived neuronal cultures have a lower neuronal yield since most neurons perish in the isolation process and require more stringent precautions for removing non-neuronal cells, such as a nylon mesh to remove meninges and treatment with mitotic inhibitors to prevent the culture from being overgrown by proliferating glia [289]. Other neuronal cultures include embryonic spinal motorneuron cultures, embryonic or perinatal rodent sympathetic ganglia cultures, and embryonic dorsal root ganglion cultures [279].

If neurons are cultured alone without glia, they will become spontaneously electrophysiologically active within a week of the dissection and can remain viable and active in culture with the proper maintenance for many weeks to months. Potter's group and others have cultured neurons on microelectrode array (MEA) recording systems for over a year by maintaining the osmolality of the culture within a narrow range [290]. However, while much of the neuroscience community uses primary neuronal cultures, neuroelectrode engineers have not used them for biocompatibility studies because there is little need for accurate electrophysiological behavior when straightforward cytotoxicity and cell attachment assays are being performed. As greater emphasis is placed on more complex in vitro models (i.e. simultaneous observation of signal degradation and glial scar formation in vitro), and electrically active electrodes are used in culture, primary neurons will need to replace neuronal cell lines in future biocompatibility studies.

**Single Cell Type Primary Cultures: Primary Glia**

Primary glial cultures are easier to generate than primary neuronal cultures because glia have much higher proliferative abilities and are more likely to be part of the approximately 1% of cells that survive the isolation procedure [279]. Furthermore, since the diversity of astrocytes, microglia, and oligodendrocytes is not well understood, unlike the much greater appreciation for neuronal phenotype differences (i.e. dorsal root ganglion versus motorneuron isolation), researchers typically use heterogeneous cultures of glia. A procedure to isolate glia initially established by McCarthy and de Vellis in 1980 has been modified by various groups but has roughly remained intact for over 25 years [291]. In this procedure, perinatal (Postnatal Day 1-4) rat or mouse cerebral brain cells are plated at high density ($2x\ 10^5$ /$cm^2$) in serum supplemented medium after removal of the meninges and mechanical or enzymatic dissociation. At this point, glia are still dividing, and with the help of serum and endogenously produced cytokines, will create a confluent layer of astrocytes, glial precursor cells, and microglia within 6 days. The astrocytes in these cultures tend to form a confluent layer on top of the poly-D-lysine coated polystyrene with the loosely adherent microglia resting on top of the astrocyte layer. To isolate primary cultures of microglia, researchers take advantage of these differences in adherence and shake the cultures two weeks after plating, and then again three weeks after plating. Although the culture can be shaken further, the microglia from additional shakes are no longer used in order to avoid experimental error derived from clonal expansion of particularly adherent microglia. The media is collected after each shake and centrifuged, resulting in microglia that are around 95% pure and an astrocyte layer that is more than 98 % pure. Shaking occurs on a standard rotary shaker at room temperature, although the times and speeds vary from lab to lab (our lab shakes for less than 3 hours at 180 RPM). The longer and faster the cells are shaken, the purer the

astrocyte culture will be. However, shaking also activates the microglia, so longer shake times may result in more basal microglial activation. Astrocytes grown this way can survive for many weeks and can be subcultured several times, while microglia cannot survive for more than a few days without the supporting astrocyte layer. This method by McCarthy and de Vellis forms the basis for the primary glial cell isolation procedure, but each research group tends to make adjustments based on their own experience. Each group varies details such as the shake date, duration, speed, and frequency, the media and serum formulation.

**Single Cell Type Primary Cultures: Primary Microglia**

Our laboratory routinely maintains primary enriched-microglia cultures, which are prepared from the whole brains of 1-day-old Fisher 344 rat pups or mice according to a variation of the McCarthy and de Vellis procedure [238]. After removing meninges and blood vessels, the brain tissue (minus olfactory bulbs and cerebellum) is gently triturated and seeded ($5x10^7$, approximately 2.5 rat pup brains or 4 mouse pup brains) in 150 $cm^3$ flasks. The culture medium consists of DMEM-F12 media supplemented with 10% heat-inactivated fetal bovine serum (FBS), 2 mM L-glutamine, 1 mM sodium pyruvate, 100 mM non-essential amino acids, 50 U/mL penicillin, and 50 lg/mL streptomycin. Cultures are maintained at 37C in a humidified atmosphere of 5% CO2 and 95% air. One week after seeding, the media is replaced. Two weeks after seeding, when the cells reach a confluent monolayer of glial cells, microglia are shaken off. Afterward, cells are resuspended in a treatment media (DMEM-F12 media supplemented with 2%FBS, 50 U/mL penicillin, and 50 ug/mL streptomycin) and replated at 1 $x10^5$ in a 96-well plate. Cells are treated 12-24 h after seeding the enriched microglia. Media can be replaced in

the original 150 $cm^3$ flask of mixed glia and a week later, an additional shake of microglia can be harvested.

Other than this standard culture preparation, there are other preparations that are less commonly used. Microglia that are 92-97% pure can be bulk isolated from older rats, as described Basu et al, where the investigators used a series of digestive incubations, nylon meshes, and centrifugation steps to isolate microglia from 8-12 week Sprague Dawley rats [292]. Other cells known to participate in the glial scarring reaction, such as meningeal cells [289] and O2A precursor cells [287] can be isolated, but have not yet been used widely in biocompatibility experiments.

**Single Cell Type Primary Cultures: Primary Astrocytes**

The astrocyte isolation procedure is the inverse of the microglia isolation procedure since microglia are shaken off and discarded while the astrocytes are maintained and subcultured. Dobbertin et al used 2 day old Sprague Dawley rats, enzymatically triturated small pieces of tissue using 0.1% trypsin in HBSS for 20 minutes, and seeded poly-D-lysine coated flasks with 10% fetal calf serum in DMEM [287]. The cultures were shaken between the $8^{th}$ and $12^{th}$ days and the cells were subcultured and treated with 20$\mu$M of the antimitotic cytosine -1-β-D arabinofuranosid (Ara-C) in serum free media to remove any remaining proliferating glial precursors. Remaining microglia were removed by treatment with 10mM L-leucine methyl ester (LME) which is a phagocyte toxin.

The more shakings that the astrocytes go through, the more microglia are removed and a purer astrocyte culture is generated. After weekly shakings for 6 weeks, a 98% pure astrocyte culture

remains. However, this method will produce a significant number of Type 2 astrocytes, thus our group prefers to acquire astrocytes using a primary cortical astrocytes method, as previously described [293] with a slight modifications [294]. Again, whole brains from one day old rats are isolated and the meninges are removed. However, for astrocytes, the cerebral cortices are dissected and subjected to enzymatic digestion for 15 min in D-MEM/F-12 containing 2.0 mg/ml porcine trypsin and 0.005% DNase I. The tissue is then mechanically disaggregated using a 60 µm cell dissociation kit (Sigma-Aldrich, St. Louis, MO) to yield a mixed glial cell suspension. The cell suspension is centrifuged for 10 min at 300 g and resuspended in fresh culture medium: D-MEM/F-12 supplemented with 10% fetal bovine serum, 100 µM nonessential amino acids, 100 µM sodium pyruvate, 200 µM L-glutamine, 50 U/ml penicillin, and 50 µg/ml streptomycin. The cells are plated on 75 $cm^2$ polystyrene tissue culture flasks and maintained at 37°C, 5% CO2 and 95% air until confluency for two weeks. Fresh medium is replenished every 3-4 days. Following confluency, the cells are placed on an orbital shaker at 150 rev/min for 6 hrs to remove contaminating cells (mostly microglia). The cells are harvested with 0.1% trypsin/EDTA in Hank's Balanced Salt Solution and plated in either T25 flasks or 100 mm Petri dishes at a density of $0.35\text{-}1 \times 10^6$ cells. Experimental studies are performed within 3-4 weeks of initial plating. Specifically, cells are treated when they are confluent, approximately 1 week after the last seeding. Upon treatment, cultures are switched to fresh medium containing 2% of heat-inactivated FBS, 2 mM L-glutamine, 1 mM sodium pyruvate, 50 U/mL penicillin, and 50 µg/mL streptomycin.

**Primary Cell Co-Culture**

A further step up in complexity from primary cultures of a single cell type is co-cultures where two different cell types from two different sources are combined together. The result is a culture that allows the study of cell-cell interactions between two cell types and is not limited by the different sensitivities of two different cell types to one isolation procedure. For example, sensitive neurons can be isolated by one procedure in an embryonic animal while hardier astrocytes can be isolated by a different procedure in an adult animal. The two cell suspensions are seeded together, or one atop the other, and neuron-astrocyte interactions can be observed, or behaviors only observed in the presence of both cell types together can be tested. Although these cultures may be more relevant to the in vivo situation since cells are combined with other cell types that they normally interact with in vivo, relevance may be lost if different sources and isolation procedures result in behavior that is not physiologically relevant.

To test the effect of different materials in influencing cortical *astrocyte* ability to promote *neuronal* growth, Biran et al seeded cerebellar granule neurons isolated from 7 day old rats through a panning procedure atop a layer of astrocytes isolated from P-1 rat cerebral cortex that had been purified away from microglia and other cells by shaking (as described in the previous section) [216]. Since the P-1 dissection procedure does not yield neurons, yet neurons were important in assessing the growth promoting properties of cortical astrocytes, the co-culture was necessary to answer the question of biocompatibility posed by the researchers. They were able to use the culture to find no difference in astrocyte growth promoting ability between different materials. In one of the few attempts to look at astrogliosis in vitro, Guenard and colleagues used dorsal root ganglion (DRG) neurons prepared from E15 Rats plated on top of astrocytes from E21 rat cortex or 2-3 month old rat spinal cord to study the effect of mechanical axonal injury on astrocyte proliferation, GFAP expression, ECM deposition, and process orientation [295]. DRG

neuron explants provide long-living neurons with large axons to study axonal damage and regrowth after injury whereas smaller neurons from the cortex (the astrocyte cell source) may have been difficult to isolate or analyze. Hirsch and Bahr seeded retinal explants from E16 rat embryos on top of adult optic nerve astrocytes or P-1 to P-3 cortical astrocyte layers to find that the retinal ganglion cell axons preferred to grow on astrocyte regions of the culture rather than the contaminating meningeal cell regions, putatively because of the different mix of inhibitory ECM expressed by the different basal layer cell types [296]. In another study, cortical neonatal astrocytes that were grown on a stretchable substrate, and thus aligned in specific orientations because of continuous mechanical strain in one direction were used as the base layer to culture P-1 DRG neurons [215]. The study showed that aligned astrocytes also resulted in aligned ECM deposition and aligned neuronal process growth, thus potentially laying the groundwork for engineered glial substrates for spinal cord repair. Although astrocyte-neuron co-cultures are most common, neurons can also be co-cultured with other cell types, such as Schwann cells [295] and meningeal cells [296].

**Multi-cell Primary Cultures: An in vitro model of glial scarring**

The glial scarring response to implanted biomaterials involves at least three interacting cell types: neurons, astrocytes, and microglia. To keep the in vitro cell culture system as relevant to the in vivo environment as possible, all three cell types should optimally be isolated in the same isolation procedure from the same animal at the same time. Unlike experimenters who go to great lengths to isolate a specific cell type and remove “contaminating” cells, our approach has been to isolate and culture these interacting cell types together, thus more closely reproducing the in vivo environment. The benefit is that the complicated glial scarring response, which requires cell-cell

interaction between at least three cell types, can be reproduced in vitro (Figure 31) [4]. We have been able to reproduce the glial scarring response to biomaterials placed in such culture and the in vitro approach allows us to create a time course of events leading to glial scarring while potentially recording from the culture at the same time. We plan to further use the in vitro model to explore the mechanisms behind glial scar formation and further develop the model as a way to test new biocompatibility approaches that become available in the neuroprosthetics field.

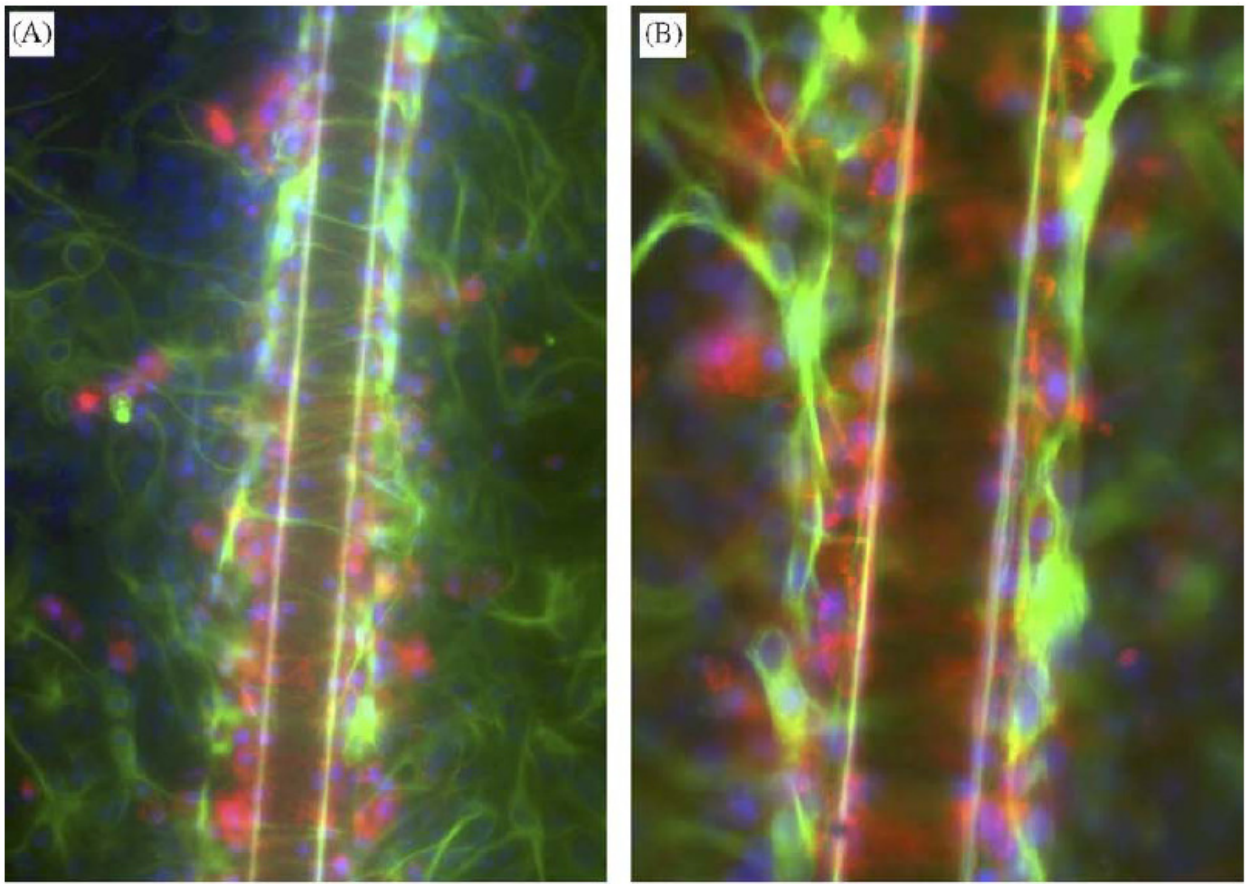


**Figure 31: (A–B) Triple fluorescent labeling of a model electrode in neuron-glia culture with DAPI staining nuclei blue, GFAP staining green, and OX-42 staining microglia red shows the relative positions of different cells near the wire after 10 days in culture. Just as observed in vivo, there is a layer of microglia (Red) adjacent to the microwire and astrocytes (Green) outside of the microglial layer showing upregulated GFAP. The image in (B) shows the glial scarring at a higher magnification, clearly visualizing the prevalence of microglia around the microwire. For reference, the wire diameter is 50um in all images. Adapted from [4]**

The increased complexity also comes with several drawbacks as compared to simpler cell line or single cell type primary cell culture. First, the variability between culture preparations and experimenters is greater as more parameters can potentially be varied. The cell-cell interactions are more difficult to observe and analyze as there are now seven interactions possible between the three different cell types (A-A, B-B, C-C, A-B, A-C, B-C, A-B-C), whereas only one interaction is present in single cell type cultures (A-A), or three possible interactions are present in less complex co-cultures cultures (A-A, B-B, A-B). Furthermore, since all the cell types have to be present in one isolation procedure, early embryonic (E14-E17) cells are used to keep neurons alive, thus potentially reducing the culture's relevance to adult in vivo behavior.

Understanding the tradeoffs involved in using a more complex culture, we have decided that the benefits – namely the re-creation of the glial scar around electrode materials in vitro – outweigh the limitations in the system described above. The neuron-glia cell culture system contains all of the cell types relevant to glial scar formation. It is an embryonic day 14 midbrain culture that contains the physiologically relevant mix of approximately 40% neurons, 10% microglia, and 50% astrocytes [236]. To generate the culture, first, the midbrain is dissected out and the meninges removed. Then, the cells are mechanically triturated with various sized pipette tips and seeded at 5 x $10^5$/well into poly-D-lysine-coated 24-well plates. Cells are maintained at 37°C in a humidified atmosphere of 5% $CO_2$ and 95% air, in minimal essential medium (MEM) containing 10% fetal bovine serum (FBS), 10% horse serum (HS), 1 g/L glucose, 2 mM L-glutamine, 1 mM sodium pyruvate, 100 µM nonessential amino acids, 50 U/mL penicillin, and 50 µg/mL streptomycin. Seven-day-old cultures are used for treatment after a media change to MEM

containing 2% FBS, 2% HS, 2 mM L-glutamine, 1 mM sodium pyruvate, 50 U/mL penicillin, and 50 µg/mL.

Treatment involves several different interventions to induce the culture to reproduce the scarring or inflammatory behavior that leads to recording electrode failure in vivo [4]. One simple treatment option is to add 10 ng/ml of LPS into the culture, which results in microglial activation, inflammatory cytokine release, and neuronal bystander damage. To simulate physical damage and cell death characteristic of the mechanical injury sustained during device insertion, a scrape model is used (Figure 32a). In this model, an area of the confluent cell layer is scraped off with a cell scraper or a pipette tip and cells are monitored as they repopulate the damaged region. A treatment to reproduce the foreign body response and glial scarring around an implant that occurs as a result of chronic electrode implantation involves the placement of short (2-5 mm) pieces of microwire into the culture and observe the cell reaction to the foreign body (Figure 32b). We use stainless steel wire because it is inexpensive, easy to sterilize, and is used in some microwire recording arrays, although we have used other materials with little observable difference in cellular response. Each culture is fixed at a certain time point after treatment and immunostained for different cell markers to differentiate neuronal (MAP-2, NeuN cell markers), microglial (IBA-1, OX-42), and astrocyte (GFAP) behavior. For the LPS treatment, fixation is usually done in the first 3 days since the maximal cytokine response is at 24 hours. The scrape is looked at with a time course ranging from several hours to 7 days (when the "wound" is filled), and the microwire treatment is extended as long as the culture is stable, typically 10 days.

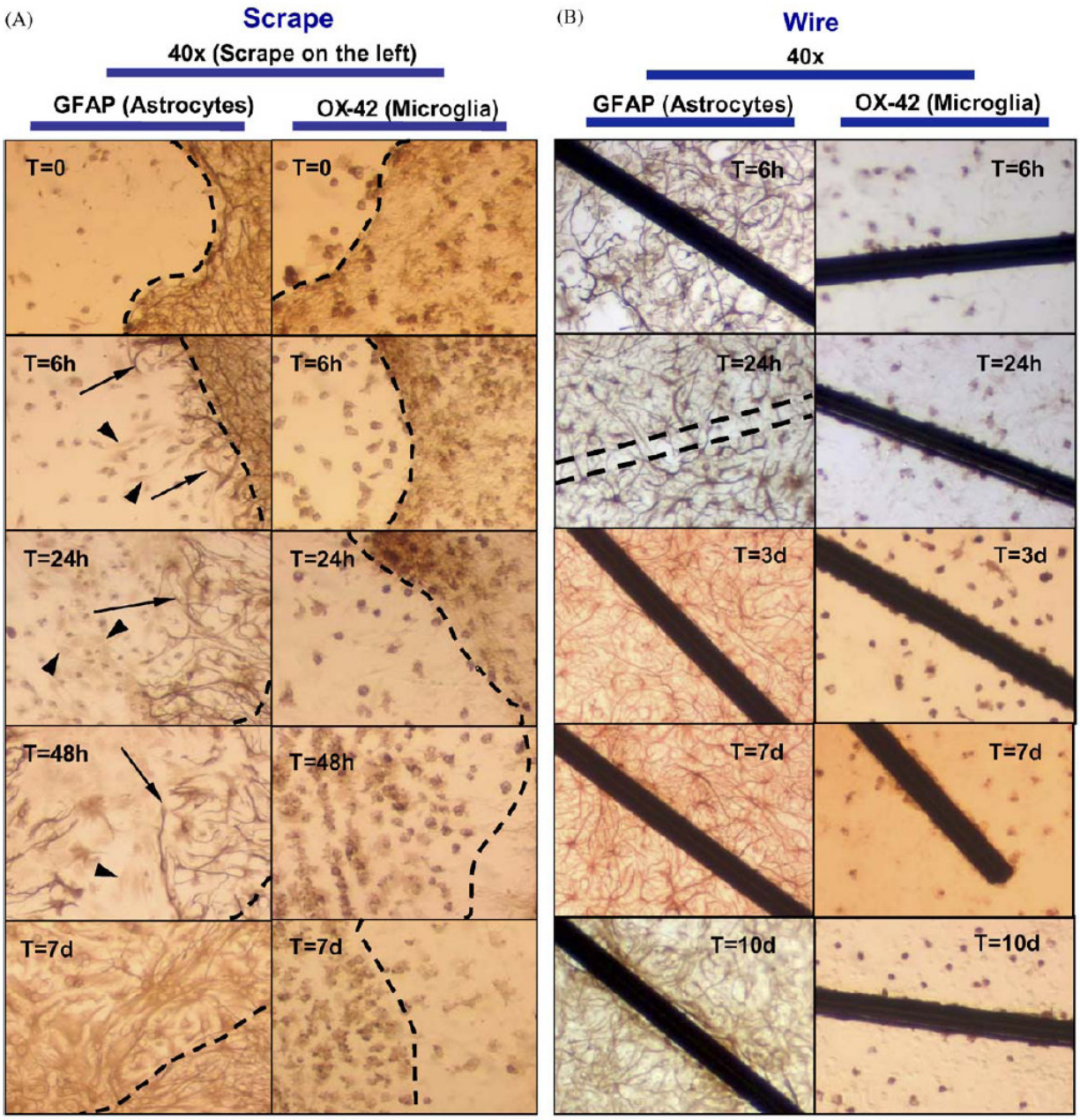


**Figure 32: (A) Time course of cellular events in response to the Scrape wound. The area scraped free of cell is on the left of the dotted line. The left panel shows the time course of astrocytes as stained for GFAP and the right panel shows the microglial response over time as stained for MAC-1 (OX-24 antibody). Astrocytes are seen to send processes (arrows) into the wound beginning at 6 h and continuing through 48 h, and completely re-colonize the wound by 7 days. GFAP negative spindle-shaped precursor cells (arrowheads) that do not stain for microglial markers but stain for vimentin (not shown) migrate into and colonize the wound ahead of the GFAP positive processes. Microglia migrate to and spread out within the wound by 24 h and their numbers increase over time, until by 7 days there are more microglia inside the wound than in the surrounding culture. (B) Time course of cellular events in response to the Wire placement. Microglia attach to the wire as early as 6 h and**

**increase in numbers until a layer of microglia 1–2 cells thick is formed covering the length of the wire. This layer remains through 10 days in culture. Astrocytes show now response to the microwire until 7 days after treatment, when the beginnings of a response may be seen. By 10 days after treatment, a layer of activated astrocytes with upregulated GFAP forms around the microwire, mimicking the glial scarring seen in vivo. Adapted from [4]**

This culture system has been used routinely to study the neuroinflammatory processes underlying progressive neurological diseases such as Parkinson's disease and Alzheimer's disease [168;236-238;241;242;249;250;297-300]. Removal of each of the different cell types destroys our ability to follow these processes as each cell type contributes something to the overall disease process. We encounter the same logic with reproducing glial scarring behavior around biomaterials placed in culture. To recreate the microglial migration and attachment to the wire, the astrocyte upregulation of GFAP and glial scar, and the neuronal isolation from the recording surface, we need to have microglia, astrocytes and neurons in the culture. A culture without microglia would potentially survive for longer periods than the 3 weeks we can maintain neuronal survival and a culture without neurons could potentially be isolated from postnatal or even adult animals, yet critical cell types would not be present in these situations. To our knowledge, ours is the first and only demonstration of this scarring behavior to be published in vitro, due in part to the specific presence of all three cell types known to participate in the brain's response to implanted foreign materials. The system certainly has its drawbacks, whether it is the use of embryonic cells, the short-lived viability of the cells, or the non-cortical cell source, yet no other system has produced in vitro behavior that so closely mimics the characteristics of the in vivo response. We have begun to look at E17-E18 cortical cultures that also contain a relevant mix of neurons, astrocytes and microglia, and initial results suggest a similar glial scarring response is present in these cultures as well (unpublished results).

Other multi-cell culture employed in our lab is the P-1 mixed glia culture. Primary mixed glia cultures are prepared from the whole brains of 1-day-old Fisher 344 rat pups or mice. After removing meninges and blood vessels, the brain tissue (minus olfactory bulbs and cerebellum) is gently triturated and.5 x $10^6$ cells/well are seeded in a 24 well plate or .5 x $10^5$ cells/well in a 96 well plate. The culture medium consists of DMEM-F12 supplemented with 10% heat-inactivated fetal bovine serum (FBS), 2 mM L-glutamine, 1 mM sodium pyruvate, 100 lM non-essential amino acids, 50 U/mL penicillin, and 50 lg/mL streptomycin. Cultures are maintained at 37C in a humidified atmosphere of 5% CO2 and 95% air. Three days after initial seeding, cultures are replenished with 0.5 mL/well fresh medium (24 well plate) or 0.1mL/well (96 well plate). At seven days post seeding, cultures are treated. Upon treatment, cultures are switched to fresh medium containing 2% of heat-inactivated FBS ), 2 mM L-glutamine, 1 mM sodium pyruvate, 50 U/mL penicillin, and 50 µg/mL streptomycin. The P-1 mixed glia system could be a useful tool to study glial responses to foreign materials even without the presence of neurons.

## *Brain Slices: Complexity approaching in vivo*

Another way to model the brain environment is to use organotypic brain slice cultures. In contrast to primary cultures, these slices, as their name suggests, provide a three-dimensional representation of the cellular environment and preserve cell-to-cell interactions. The preparation of these slices minimally raises the basal level of activation and thereby allows for a more sensitive model. In addition, fewer animals are required to create these cultures since many slices can be obtained from one brain and each slice can be maintained for months [35;301]. Finally, slices of mature animals, up to postnatal day 21-23, can be grown in culture whereas primary cultures can only be produced from embryonic or neonatal animals [279]. The drawbacks to

increasing the complexity are that the culture approaches the uncontrolled nature of the in vivo environment. Furthermore, while the slices are well suited for generating acute and chronic recordings of neurons in preserved circuits, the staining and fixation protocols necessary to perform immunocytochemical analysis on the cellular response to biomaterials is more difficult than in 2-d cultures or even in vivo, where tissue sections are easily cut and stained. The thin slices attach to growth membrane in tissue culture and are difficult to fix, section, and stain. The complexity of these models presents its own challenges. Preserving the cellular environment eliminates the ability to produce uniformly dissociated cultures and thus increases the difficulty of attributing an observed response to a specific cell type. To assess the overall response of a particular agent, the selective vulnerability of cells in different regions of the brain, which may not be readily identifiable, must be taken into account. Further, the presence of extensive networks impedes examining and tracking of individual cells. Primary dissociated cultures, in contrast, allow for easy perfusion of agents without problems of tissue absorption or interaction from neighboring cells or tissues. Finally, many studies have shown that slice cultures have not consistently replicated *in vivo* responses [302]. Thus the slice models may provide a promising alternative or addition to current primary models, however, the individual challenges they pose warrant caution for their use.

In a typical isolation procedure, the tissue slice is placed onto a semiporous membrane that is attached to a removable insert and the assembly is placed into a media-filled well. The membrane prevents direct contact of the media to the tissue. A diagram of the basic components and an image of the interface setup are shown in Figure 33. Typically, slices from the brains of postnatal animals, in particular rats and mice, are used. Multiple slices of uniform thickness can be prepared at once by using a vibrating microtome or a less complex manual tissue chopper. Fresh

slices of approximately 300 to 400 µm thick are cultured for two to three weeks to allow cells to stabilize before treatment with chemical or mechanical injuries. The slices can be observed for many weeks afterwards.

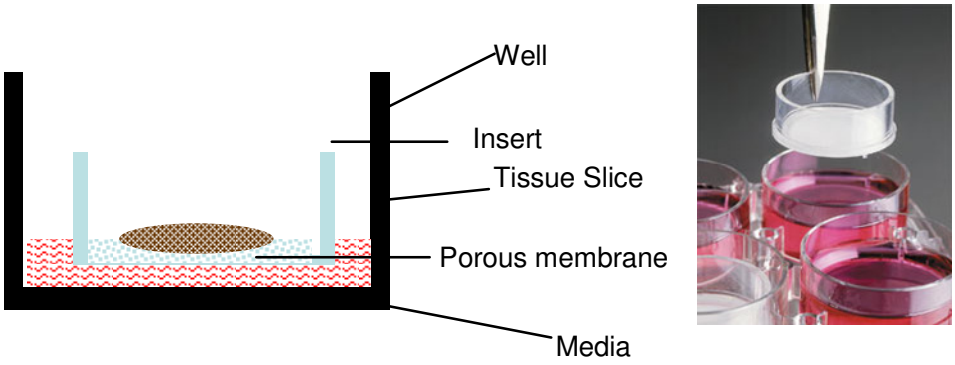


**Figure 33: Diagram and image (Millipore) of the Stoppini method for culturing tissue slices. The tissue is placed on an insert and positioned in a media-containing well without direct contact by the tissue to the media.**

Although few in the neuroprosthetics community have used brain slices to study biocompatibility, the literature abounds with studies to support the use of slices as culture models. The use of multiple techniques to characterize the behavior and morphology of cells has provided documentation for numerous in vivo events, including immediate and long-term responses, activated and resting state transitions, and cellular reactions to mechanical, excitotoxic, and bacterial injuries. In other studies, slices have been co-cultured with dissociated cells to examine the interactions between specific cell types. The versatility that slice cultures offer indicates that they may be used to isolate and study a broad range of disease mechanisms.

## Brain Slices: Biocompatibility studies

Studies using this model to assess the biocompatibility of implants and prosthetics are limited. Within the field of biocompatibility, there are only a handful of studies examining the response to neural electrodes. Koeneman and colleagues conducted one of the first studies, embedding single polybenzylcyclobutene implants in rat brain slices and studying the tissue response over a two-week period [301]. Using cell specific markers to simultaneously visualize the number, morphology, and localization of different cell types near the implant, they showed that glia and neurons made extensive contact with the implants and further, that the implants did not promote cell death (Figure 34). These observations suggested that the electrodes were biocompatible. Although quantitative assays are needed to support their conclusions, the study showed that brain slice models could be used as an alternative to assess neural electrode biocompatibility and provided techniques in which such assessments could be performed.

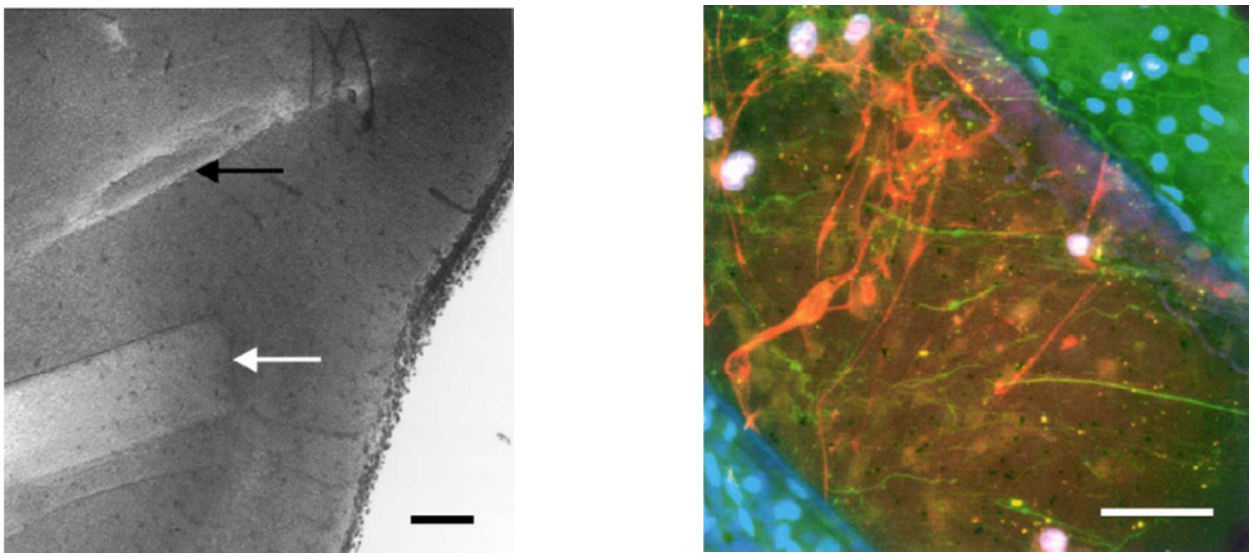

**Figure 34: Electrode implanted in 300 µm coronal slice: black arrow = insertion only, white implant. Right: Confocal image of the electrode after 7 days: Blue = nuclei, orange = GFAP, green = neurons. Adapted from [301]**

Using a different technique, Kristensen et al. assessed neural implant biocompatibility by growing hippocampal slices directly on microelectrode arrays and analyzing the structural interaction between the array and native cells [36]. Although they observed formation of a glial scar at the base of the electrode, though not at the tip, the histological patterns in slices grown on arrays were comparable to those grown on standard membranes. Furthermore, slices grown on arrays did not become more susceptible to excitotoxins and neurotoxins. These results, in addition to the possibility that the scar may have resulted from initial tissue injury, led them to conclude the arrays are biocompatible with tissue slices.

Bypassing traditional methods of slice culture that maintains neuronal elecrophysiological activity, Bjornsson et al have recently used 500 μm thick cortical slices to measure the effects of electrode insertion parameters on tissue strain [303]. In this case, the experimenters needed the 3-dimensional structure and vascular features that are unavailable in cell culture, but needed an ex-vivo setup to conduct quantitative analysis on the tissue response to insertion. Their analysis found that a faster insertion results in lower tissue deformation, although large variability was found between insertions and this variability was heavily influenced by cortical surface features such as vascular elements.

## *Conclusion*

In vivo studies have always been, and will continue to be, the gold standard in evaluating device-tissue interactions. However, in vivo studies are costly, time consuming, and often cannot provide the mechanistic insight necessary to understand the underlying problems causing device failure. Without the cellular and molecular mechanisms that controlled in vitro cell culture experiments

can provide, the quest for a non-fouling, non-scarring electrode design may continue to progress through the slow, seemingly random path that subcutaneous devices such as implantable glucose sensors have taken. However, the variety and richness of the in vitro cell culture models available for the brain may accelerate or help guide the in vivo experiments and novel electrode designs. Simple cell line experiments that cost on the order of several hundreds of dollars can prevent costly problems of in vivo material cytotoxicity while primary cell cultures can help to explain why one material attracts neurite growth when another repels neuronal attachment and elongation. Cell cultures involving multiple interacting cell types or even slices of brain tissue can reproduce glial scarring and electrode failure under controlled, observable conditions and potentially eliminate the need for in vivo experiments except as a validation of in vitro results. At all times with in vitro experimentation, one must keep in mind that cell cultures are an imperfect model of in vivo behavior and as the in vitro system becomes more rigid and controlled, it moves away from the uncontrolled, complicated in vivo environment the model is emulating. However, by keeping the limitations of in vitro analysis in mind, and verifying in vitro findings in vivo, one can make great strides in the understanding of the tissue reaction to implanted electrodes and in the design of biocompatible devices by utilizing an appropriately chosen in vitro cell culture system.

# Reference List


[1] Nobunaga,A.I., Go,B.K., Karunas,R.B., Recent demographic and injury trends in people served by the model spinal cord injury care systems, Arch. Phys. Med. Rehabil., 80 (1999) 1372-1382.

[2] Hochberg,L.R., Serruya,M.D., Friehs,G.M., Mukand,J.A., Saleh,M., Caplan,A.H., Branner,A., Chen,D., Penn,R.D., Donoghue,J.P., Neuronal ensemble control of prosthetic devices by a human with tetraplegia, Nature, 442 (2006) 164-171.

[3] Polikov,V.S., Tresco,P.A., Reichert,W.M., Response of brain tissue to chronically implanted neural electrodes, J. Neurosci. Methods, 148 (2005) 1-18.

[4] Polikov,V.S., Block,M.L., Fellous,J.M., Hong,J.S., Reichert,W.M., In vitro model of glial scarring around neuroelectrodes chronically implanted in the CNS, Biomaterials, 27 (2006) 5368-5376.

[5] Polikov,V.S., Su,E.C., Ball,M.A., Hong,J.S., Reichert,W.M., Control protocol for robust in vitro glial scar formation around microwires: Essential roles of bFGF and serum in gliosis, J. Neurosci. Methods, (2009).

[6] Carmena,J.M., Lebedev,M.A., Crist,R.E., O'Doherty,J.E., Santucci,D.M., Dimitrov,D.F., Patil,P.G., Henriquez,C.S., Nicolelis,M.A.L., Learning to control a brain-machine interface for reaching and grasping by primates, Plos Biology, 1 (2003) 193-208.

[7] Taylor,D.M., Tillery,S.I.H., Schwartz,A.B., Direct cortical control of 3D neuroprosthetic devices, Science, 296 (2002) 1829-1832.

[8] Wessberg,J., Stambaugh,C.R., Kralik,J.D., Beck,P.D., Laubach,M., Chapin,J.K., Kim,J., Biggs,J., Srinivasan,M.A., Nicolelis,M.A.L., Real-time prediction of hand trajectory by ensembles of cortical neurons in primates, Nature, 408 (2000) 361-365.

[9] Williams,J.C., Rennaker,R.L., Kipke,D.R., Stability of chronic multichannel neural recordings: Implications for a long-term neural interface, Neurocomputing, 26-7 (1999) 1069-1076.

[10] Rousche,P.J., Pellinen,D.S., Pivin,D.P., Williams,J.C., Vetter,R.J., Kipke,D.R., Flexible polyimide-based intracortical electrode arrays with bioactive capability, IEEE Trans. Biomed. Eng., 48 (2001) 361-371.

[11] Maynard,E.M., Fernandez,E., Normann,R.A., A technique to prevent dural adhesions to chronically implanted microelectrode arrays, J. Neurosci. Methods, 97 (2000) 93-101.

[12] Hochberg,L.R., Serruya,M.D., Friehs,G.M., Mukand,J.A., Saleh,M., Caplan,A.H., Branner,A., Chen,D., Penn,R.D., Donoghue,J.P., Neuronal ensemble control of prosthetic devices by a human with tetraplegia, Nature, 442 (2006) 164-171.

[13] Williams,J.C., Rennaker,R.L., Kipke,D.R., Long-term neural recording characteristics of wire microelectrode arrays implanted in cerebral cortex, Brain Research Protocols, 4 (1999) 303-313.

[14] Kralik,J.D., Dimitrov,D.F., Krupa,D.J., Katz,D.B., Cohen,D., Nicolelis,M.A.L., Techniques for long-term multisite neuronal ensemble recordings in behaving animals, Methods, 25 (2001) 121-150.

[15] Drake,K.L., Wise,K.D., Farraye,J., Anderson,D.J., Bement,S.L., Performance of Planar Multisite Microprobes in Recording Extracellular Single-Unit Intracortical Activity, IEEE Trans. Biomed. Eng., 35 (1988) 719-732.

[16] Campbell,P.K., Jones,K.E., Huber,R.J., Horch,K.W., Normann,R.A., A Silicon-Based, 3-Dimensional Neural Interface - Manufacturing Processes for An Intracortical Electrode Array, IEEE Trans. Biomed. Eng., 38 (1991) 758-768.

[17] Schwartz,A.B., Cortical neural prosthetics, Annu. Rev. Neurosci., 27 (2004) 487-507.

[18] Cyberkinetics,I. Form SB2. 2007.
Ref Type: Report

[19] Nicolelis,M.A.L., Ribeiro,S., Multiellectrode recordings: the next steps, Curr. Opin. Neurobiol., 12 (2002) 602-606.

[20] Nicolelis,M.A.L., Dimitrov,D., Carmena,J.M., Crist,R., Lehew,G., Kralik,J.D., Wise,S.P., Chronic, multisite, multielectrode recordings in macaque monkeys, Proc. Natl. Acad. Sci. U. S. A., 100 (2003) 11041-11046.

[21] Rousche,P.J., Normann,R.A., Chronic recording capability of the Utah Intracortical Electrode Array in cat sensory cortex, J. Neurosci. Methods, 82 (1998) 1-15.

[22] Liu,X., McCreery,D.B., Carter,R.R., Bullara,L.A., Yuen,T.G.H., Agnew,W.F., Stability of the Interface Between Neural Tissue and Chronically Implanted Intracortical Microelectrodes, IEEE Trans. Rehabil. Eng., 7 (1999) 315-326.

[23] Landis,D.M.D., The Early Reactions of Nonneuronal Cells to Brain Injury, Annu. Rev. Neurosci., 17 (1994) 133-151.

[24] Berry,M., Butt,A., Logan,A., Cellular Responses to Penetrating CNS Injury. In Berry,M, Loughlin,AJ (Eds.), CNS Injuries: Cellular Responses and Pharmacological Strategies CRC Press, Boca Raton, Fla, 1999, pp. 1-18.

[25] Biran,R., Martin,D.C., Tresco,P.A., Neuronal cell loss accompanies the brain tissue response to chronically implanted silicon microelectrode arrays, Exp. Neurol., 195 (2005) 115-126.

[26] Szarowski,D.H., Andersen,M.D., Retterer,S., Spence,A.J., Isaacson,M., Craighead,H.G., Turner,J.N., Shain,W., Brain responses to micro-machined silicon devices, Brain Res., 983 (2003) 23-35.

[27] Turner,J.N., Shain,W., Szarowski,D.H., Andersen,M., Martins,S., Isaacson,M., Craighead,H., Cerebral astrocyte response to micromachined silicon implants, Exp. Neurol., 156 (1999) 33-49.

[28] Edell,D.J., Toi,V.V., Mcneil,V.M., Clark,L.D., Factors Influencing the Biocompatibility of Insertable Silicon Microshafts in Cerebral-Cortex, IEEE Trans. Biomed. Eng., 39 (1992) 635-643.

[29] Menei,P., Croue,A., Daniel,V., Pouplardbarthelaix,A., Benoit,J.P., Fate and Biocompatibility of 3 Types of Microspheres Implanted Into the Brain, J. Biomed. Mater. Res., 28 (1994) 1079-1085.

[30] Thomas,W.E., Brain Macrophages - Evaluation of Microglia and Their Functions, Brain Research Reviews, 17 (1992) 61-74.

[31] Cui,X.Y., Wiler,J., Dzaman,M., Altschuler,R.A., Martin,D.C., In vivo studies of polypyrrole/peptide coated neural probes, Biomaterials, 24 (2003) 777-787.

[32] Yuen,T.G.H., Agnew,W.F., Histological-Evaluation of Polyesterimide-Insulated Gold Wires in Brain, Biomaterials, 16 (1995) 951-956.

[33] Khan,A.S., Michael,A.C., Invasive consequences of using micro-electrodes and microdialysis probes in the brain, Trac-Trends in Analytical Chemistry, 22 (2003) 503-508.

[34] Kim,Y.T., Hitchcock,R.W., Bridge,M.J., Tresco,P.A., Chronic response of adult rat brain tissue to implants anchored to the skull, Biomaterials, 25 (2004) 2229-2237.

[35] Kunkler,P.E., Kraig,R.P., Reactive astrocytosis from excitotoxic injury in hippocampal organ culture parallels that seen in vivo, J. Cereb. Blood Flow Metab., 17 (1997) 26-43.

[36] Kristensen,B.W., Noraberg,J., Thiebaud,P., Koudelka-Hep,M., Zimmer,J., Biocompatibility of silicon-based arrays of electrodes coupled to organotypic hippocampal brain slice cultures, Brain Res., 896 (2001) 1-17.

[37] Eaton,K.P., Henriquez,C.S., Confounded spikes generated by synchrony within neural tissue models, Neurocomputing, 65 (2005) 851-857.

[38] Henze,D.A., Borhegyi,Z., Csicsvari,J., Mamiya,A., Harris,K.D., Buzsaki,G., Intracellular features predicted by extracellular recordings in the hippocampus in vivo, J. Neurophysiol., 84 (2000) 390-400.

[39] Rosenthal,F., Extracellular potential fields of single PT-neurons, Brain Res., 36 (1972) 251-263.

[40] Rall,W., Electrophysiology of a dendritic neuron model, Biophys. J., 2(2)Pt 2 (1962) 145-167.

[41] Mountcastle,V.B., Modality and topographic properties of single neurons of cat's somatic sensory cortex, J. Neurophysiol., 20 (1957) 408-434.

[42] Purves,D., Augustine,G.J., Fitzpatrick,D., Katz,L.C., LaMantia,A., McNamara,J.O., Williams,S.M., Neuroscience, Sinauer Associates, Sunderland, 2001.

[43] Nathaniel,E.J.H., Nathaniel,D.R., The Reactive Astrocyte. In Federoff,S (Ed.), Advances in Cellular Neurobiology, Vol. 2, Academic Press, Orlando, 1981, pp. 249-301.

[44] Astrocytes: Pharmacology and Function, Academic Press, San Diego, CA, 1993.

[45] Neuroglia, Oxford University Press, New York, 1995.

[46] Sievers,J., Pehlemann,F.W., Gude,S., Berry,M., Meningeal Cells Organize the Superficial Glia Limitans of the Cerebellum and Produce Components of Both the Interstitial Matrix and the Basement-Membrane, J. Neurocytol., 23 (1994) 135-149.

[47] Eng,L.F., DeArmond,S.J., Immunohistochemical Studies of Astrocytes in Normal Development and Disease. In Federoff,S (Ed.), Advances in Cellular Neurobiology, Vol. 3, Academic Press, Orlando, 1982, pp. 145-171.

[48] Bignami,A., Dahl,D., Reuger,D.C., Glial Fibrillary Acidic Protein (GFA) in Normal Neural Cells and in Pathological Conditions. In Federoff,S (Ed.), Advances in Cellular Neurobiology, Vol. 1, Academic Press, Orlando, 1980, pp. 285-310.

[49] Ling,E., The Origin and Nature of Microglia. In Federoff,S (Ed.), Advances in Cellular Neurobiology, Vol. 2, Academic Press, Orlando, 1981, pp. 33-82.

[50] Streit,W.J., Microglial Cells. In Kettenmann,H, Ransom,BR (Eds.), Neuroglia Oxford University Press, New York, 1995, pp. 85-95.

[51] Banati,R.B., Gehrmann,J., Schubert,P., Kreutzberg,G.W., Cytotoxicity of Microglia, Glia, 7 (1993) 111-118.

[52] Babcock,A.A., Kuziel,W.A., Rivest,S., Owens,T., Chemokine expression by glial cells directs leukocytes to sites of axonal injury in the CNS, J. Neurosci., 23 (2003) 7922-7930.

[53] Giulian,D., Li,J., Leara,B., Keenen,C., Phagocytic Microglia Release Cytokines and Cytotoxins That Regulate the Survival of Astrocytes and Neurons in Culture, Neurochem. Int., 25 (1994) 227-233.

[54] Woodroofe,M.N., Sarna,G.S., Wadhwa,M., Hayes,G.M., Loughlin,A.J., Tinker,A., Cuzner,M.L., Detection of Interleukin-1 and Interleukin-6 in Adult-Rat Brain, Following Mechanical Injury, by Invivo Microdialysis - Evidence of A Role for Microglia in Cytokine Production, J. Neuroimmunol., 33 (1991) 227-236.

[55] Giulian,D., Li,J., Li,X., George,J., Rutecki,P.A., The Impact of Microglia-Derived Cytokines Upon Gliosis in the Cns, Dev. Neurosci., 16 (1994) 128-136.

[56] Sheng,W.S., Hu,S.X., Kravitz,F.H., Peterson,P.K., Chao,C.C., Tumor-Necrosis-Factor-Alpha Up-Regulates Human Microglial Cell Production of Interleukin-10 In-Vitro, Clin. Diagn. Lab. Immunol., 2 (1995) 604-608.

[57] Chabot,S., Williams,G., Yong,V.W., Microglial production of TNF-alpha is induced by activated T lymphocytes - Involvement of VLA-4 and inhibition by interferon beta-1b, J. Clin. Invest., 100 (1997) 604-612.

[58] Nakajima,K., Honda,S., Tohyama,Y., Imai,Y., Kohsaka,S., Kurihara,T., Neurotrophin secretion from cultured microglia, Journal of Neuroscience Research, 65 (2001) 322-331.

[59] Elkabes,S., DiCiccoBloom,E.M., Black,I.B., Brain microglia macrophages express neurotrophins that selectively regulate microglial proliferation and function, J. Neurosci., 16 (1996) 2508-2521.

[60] Giulian,D., Corpuz,M., Chapman,S., Mansouri,M., Robertson,C., Reactive Mononuclear Phagocytes Release Neurotoxins After Ischemic and Traumatic Injury to the Central-Nervous-System, J. Neurosci. Res., 36 (1993) 681-693.

[61] Giulian,D., Vaca,K., Corpuz,M., Brain Glia Release Factors with Opposing Actions Upon Neuronal Survival, J. Neurosci., 13 (1993) 29-37.

[62] Auger,M.J., Ross,J.A., The Biology of the Macrophage. In Lewis CE, McGee JO'D (Eds.), The Macrophage. The Natural Immune System IRL Press at Oxford University Press, Oxford, 1992, pp. 3-74.

[63] Giulian,D., Baker,T.J., Characterization of Ameboid Microglia Isolated from Developing Mammalian Brain, J. Neurosci., 6 (1986) 2163-2178.

[64] Minghetti,L., Levi,G., Microglia as effector cells in brain damage and repair: Focus on prostanoids and nitric oxide, Prog. Neurobiol., 54 (1998) 99-125.

[65] Zielasek,J., Muller,B., Hartung,H.P., Inhibition of cytokine-inducible nitric oxide synthase in rat microglia and murine macrophages by methyl-2,5-dihydroxycinnamate, Neurochem. Int., 29 (1996) 83-87.

[66] Weldon,D.T., Rogers,S.D., Ghilardi,J.R., Finke,M.P., Cleary,J.P., O'Hare,E., Esler,W.P., Maggio,J.E., Mantyh,P.W., Fibrillar beta-amyloid induces microglial phagocytosis, expression of inducible nitric oxide synthase, and loss of a select population of neurons in the rat CNS in vivo, J. Neurosci., 18 (1998) 2161-2173.

[67] Nishiyama,A., Polydendrocytes: NG2 cells with many roles in development and repair of the CNS, Neuroscientist, 13 (2007) 62-76.

[68] Nishiyama,A., Yang,Z.S., Butt,A., Astrocytes and NG2-glia: what's in a name?, Journal of Anatomy, 207 (2005) 687-693.

[69] Baracskay,K.L., Kidd,G.J., Miller,R.H., Trapp,B.D., NG2-positive cells generate A2B5-positive oligodendrocyte precursor cells, Glia, 55 (2007) 1001-1010.

[70] Belachew,S., Chittajallu,R., Aguirre,A.A., Yuan,X.Q., Kirby,M., Anderson,S., Gallo,V., Postnatal NG2 proteoglycan-expressing progenitor cells are intrinsically multipotent and generate functional neurons, J. Cell Biol., 161 (2003) 169-186.

[71] Kondo,T., Raff,M., Oligodendrocyte precursor cells reprogrammed to become multipotential CNS stem cells, Science, 289 (2000) 1754-1757.

[72] Wang,K., Bekar,L.K., Furber,K., Walz,W., Vimentin-expressing proximal reactive astrocytes correlate with migration rather than proliferation following focal brain injury, Brain Res., 1024 (2004) 193-202.

[73] Alonso,G., NG2 proteoglycan-expressing cells of the adult rat brain: Possible involvement in the formation of glial scar astrocytes following stab wound, Glia, 49 (2005) 318-338.

[74] Kernie,S.G., Erwin,T.M., Parada,L.F., Brain remodeling due to neuronal and astrocytic proliferation after controlled cortical injury in mice, J. Neurosci. Res., 66 (2001) 317-326.

[75] Wang,Y., Moges,H., Bharucha,Y., Symes,A., Smad3 null mice display more rapid wound closure and reduced scar formation after a stab wound to the cerebral cortex, Exp. Neurol., 203 (2007) 168-184.

[76] Hampton,D.W., Rhodes,K.E., Zhao,C., Franklin,R.J.M., Fawcett,J.W., The responses of oligodendrocyte precursor cells, astrocytes and microglia to a cortical stab injury, in the brain, Neuroscience, 127 (2004) 813-820.

[77] Cao,Q.L., Benton,R.L., Whittemore,S.R., Stem cell repair of central nervous system injury, J. Neurosci. Res., 68 (2002) 501-510.

[78] Magnus,T., Coksaygan,T., Korn,T., Xue,H.P., Arumugam,T.V., Mughal,M.R., Eckley,D.M., Tang,S.C., DeTolla,L., Rao,M.S., Cassiani-Ingoni,R., Mattson,M.P., Evidence that nucleocytoplasmic Olig2 translocation mediates brain-injury-induced differentiation of glial precursors to astrocytes, J. Neurosci. Res., 85 (2007) 2126-2137.

[79] Kondo,T., Raff,M.C., A role for Noggin in the development of oligodendrocyte precursor cells, Developmental Biology, 267 (2004) 242-251.

[80] Morrow,T., Song,M.R., Ghosh,A., Sequential specification of neurons and glia by developmentally regulated extracellular factors, Development, 128 (2001) 3585-3594.

[81] Sriram,K., Benkovic,S.A., Hebert,M.A., Miller,D.B., O'Callaghan,J.P., Induction of gp130-related cytokines and activation of JAK2/STAT3 pathway in astrocytes precedes up-regulation of glial fibrillary acidic protein in the 1-methyl-4-phenyl-1,2,3,6-tetrahydropyridine model of neurodegeneration - Key signaling pathway for astrogliosis in vivo?, J. Biol. Chem., 279 (2004) 19936-19947.

[82] Rajan,P., Panchision,D.M., Newell,L.E., Mckay,R.D.G., BMPs signal alternately through a SMAD or FRAP-STAT pathway to regulate fate choice in CNS stem cells, J. Cell Biol., 161 (2003) 911-921.

[83] Turnley,A.M., Bartlett,P.F., Cytokines that signal through the leukemia inhibitory factor receptor-beta complex in the nervous system, J. Neurochem., 74 (2000) 889-899.

[84] Deleyrolle,L., Marchal-Victorion,S., Dromard,C., Fritz,V., Saunier,M., Sabourin,J.C., Van Ba,C.T., Privat,A., Hugnot,J.P., Exogenous and fibroblast growth factor 2/epidermal growth factor-regulated endogenous cytokines regulate neural precursor cell growth and differentiation, Stem Cells, 24 (2006) 748-762.

[85] Nakashima,K., Taga,T., Mechanisms underlying cytokine-mediated cell-fate regulation in the nervous system, Molecular Neurobiology, 25 (2002) 233-244.

[86] Nakashima,K., Yanagisawa,M., Arakawa,H., Kimura,N., Hisatsune,T., Kawabata,M., Miyazono,K., Taga,T., Synergistic signaling in fetal brain by STAT3-Smad1 complex bridged by p300, Science, 284 (1999) 479-482.

[87] Chang,M.Y., Son,H., Lee,Y.S., Lee,S.H., Neurons and astrocytes secrete factors that cause stem cells to differentiate into neurons and astrocytes, respectively, Molecular and Cellular Neuroscience, 23 (2003) 414-426.

[88] Streit,W.J., Hurley,S.D., Mcgraw,T.S., Semple-Rowland,S.L., Comparative evaluation of cytokine profiles and reactive gliosis supports a critical role for interleukin-6 in neuron-glia signaling during regeneration, J. Neurosci. Res., 61 (2000) 10-20.

[89] Nakanishi,M., Niidome,T., Matsuda,S., Akaike,A., Kihara,T., Sugimoto,H., Microglia-derived interleukin-6 and leukaemia inhibitory factor promote astrocytic differentiation of neural stem/progenitor cells, Eur. J. Neurosci., 25 (2007) 649-658.

[90] Van Wagoner,N.J., Benveniste,E.N., Interleukin-6 expression and regulation in astrocytes, J. Neuroimmunol., 100 (1999) 124-139.

[91] Fukuda,S., Abematsu,M., Mori,H., Yanagisawa,M., Kagawa,T., Nakashima,K., Yoshimura,A., Taga,T., Potentiation of astrogliogenesis by STAT3-mediated activation of bone morphogenetic protein-Smad signaling in neural stem cells, Mol. Cell. Biol., 27 (2007) 4931-4937.

[92] Kondo,T., Raff,M., Chromatin remodeling and histone modification in the conversion of oligodendrocyte precursors to neural stem cells, Genes & Development, 18 (2004) 2963-2972.

[93] Mi,H.Y., Haeberle,H., Barres,B.A., Induction of astrocyte differentiation by endothelial cells, J. Neurosci., 21 (2001) 1538-1547.

[94] Kahn,M.A., Huang,C.J., Caruso,A., Barresi,V., Nazarian,R., Condorelli,D.F., Devellis,J., Ciliary neurotrophic factor activates JAK/Stat signal transduction cascade and induces transcriptional expression of glial fibrillary acidic protein in glial cells, J. Neurochem., 68 (1997) 1413-1423.

[95] Takizawa,T., Ochiai,W., Nakashima,K., Taga,T., Enhanced gene activation by Notch and BMP signaling cross-talk, Nucleic Acids Research, 31 (2003) 5723-5731.

[96] Hermann,A., Maisel,M., Wegner,F., Liebau,S., Kim,D.W., Gerlach,M., Schwarz,J., Kim,K.S., Storch,A., Multipotent neural stem cells from the adult tegmentum with dopaminergic potential develop essential properties of functional neurons, Stem Cells, 24 (2006) 949-964.

[97] Dailey,L., Ambrosetti,D., Mansukhani,A., Basilico,C., Mechanisms underlying differential responses to FGF signaling, Cytokine & Growth Factor Reviews, 16 (2005) 233-247.

[98] Clarke,W.E., Berry,M., Smith,C., Kent,A., Logan,A., Coordination of fibroblast growth factor receptor 1 (FGFR1) and fibroblast growth factor-2 (FGF-2) trafficking to nuclei of reactive astrocytes around cerebral lesions in adult rats, Molecular and Cellular Neuroscience, 17 (2001) 17-30.

[99] Nagao,M., Sugimori,M., Nakafuku,M., Cross talk between Notch and growth factor/cytokine signaling pathways in neural stem cells, Mol. Cell. Biol., 27 (2007) 3982-3994.

[100] Wu,Y.Y., Liu,Y., Levine,E.M., Rao,M.S., Hes1 but not Hes5 regulates an astrocyte versus oligodendrocyte fate choice in glial restricted precursors, Dev. Dyn., 226 (2003) 675-689.

[101] Zhou,Y.X., Armstrong,R.C., Interaction of fibroblast growth factor 2 (FGF2) and notch signaling components in inhibition of oligodendrocyte progenitor (OP) differentiation, Neurosci. Lett., 421 (2007) 27-32.

[102] Cassiani-Ingoni,R., Coksaygan,T., Xue,H.P., Reichert-Scrivner,S.A., Wiendl,H., Rao,M.S., Magnus,T., Cytoplasmic translocation of Olig2 in adult glial progenitors marks the generation of reactive astrocytes following autoimmune inflammation, Exp. Neurol., 201 (2006) 349-358.

[103] Streit,W.J., Semple-Rowland,S.L., Hurley,S.D., Miller,R.C., Popovich,P.G., Stokes,B.T., Cytokine mRNA profiles in contused spinal cord and axotomized facial nucleus suggest a beneficial role for inflammation and gliosis, Exp. Neurol., 152 (1998) 74-87.

[104] Huang,D.R., Han,Y.L., Rani,M.R.S., Glabinski,A., Trebst,C., Sorensen,T., Tani,M., Wang,J.T., Chien,P., O'Bryan,S., Bielecki,B., Zhou,Z.L., Majumder,S., Ransohoff,R.M., Chemokines and chemokine receptors in inflammation of the nervous system: manifold roles and exquisite regulation, Immunol. Rev., 177 (2000) 52-67.

[105] Acarin,L., Gonzalez,B., Castellano,B., Neuronal, astroglial and microglial cytokine expression after an excitotoxic lesion in the immature rat brain, Eur. J. Neurosci., 12 (2000) 3505-3520.

[106] Liberto,C.M., Albrecht,P.J., Herx,L.M., Yong,V.W., Levison,S.W., Pro-regenerative properties of cytokine-activated astrocytes, J. Neurochem., 89 (2004) 1092-1100.

[107] Winter,C.G., Saotome,Y., Levison,S.W., Hirsh,D., A Role for Ciliary Neurotrophic Factor As An Inducer of Reactive Gliosis, the Glial Response to Central-Nervous-System Injury, Proc. Natl. Acad. Sci. U. S. A., 92 (1995) 5865-5869.

[108] Kalehua,A.N., Nagel,J.E., Whelchel,L.M., Gides,J.J., Pyle,R.S., Smith,R.J., Kusiak,J.W., Taub,D.D., Monocyte chemoattractant protein-1 and macrophage inflammatory protein-2 are involved in both excitotoxin-induced neurodegeneration and regeneration, Exp. Cell Res., 297 (2004) 197-211.

[109] Rohl,C., Lucius,R., Sievers,J., The effect of activated microglia on astrogliosis parameters in astrocyte cultures, Brain Res., 1129 (2007) 43-52.

[110] Giulian,D., Woodward,J., Young,D.G., Krebs,J.F., Lachman,L.B., Interleukin-1 Injected Into Mammalian Brain Stimulates Astrogliosis and Neovascularization, J. Neurosci., 8 (1988) 2485-2490.

[111] Liesi,P., Kauppila,T., Induction of type IV collagen and other basement-membrane-associated proteins after spinal cord injury of the adult rat may participate in formation of the glial scar, Exp. Neurol., 173 (2002) 31-45.

[112] Bugga,L., Gadient,R.A., Kwan,K., Stewart,C.L., Patterson,P.H., Analysis of neuronal and glial phenotypes in brains of mice deficient in leukemia inhibitory factor, Journal of Neurobiology, 36 (1998) 509-524.

[113] Nakashima,K., Wiese,S., Yanagisawa,M., Arakawa,H., Kimura,N., Hisatsune,T., Yoshida,K., Kishimoto,T., Sendtner,M., Taga,T., Developmental requirement of gp130 signaling in neuronal survival and astrocyte differentiation, J. Neurosci., 19 (1999) 5429-5434.

[114] Okada,S., Nakamura,M., Katoh,H., Miyao,T., Shimazaki,T., Ishii,K., Yamane,J., Yoshimura,A., Iwamoto,Y., Toyama,Y., Okano,H., Conditional ablation of Stat3 or Socs3 discloses a dual role for reactive astrocytes after spinal cord injury, Nature Medicine, 12 (2006) 829-834.

[115] Barnabe-Heider,F., Wasylnka,J.A., Fernandes,K.J.L., Porsche,C., Sendtner,M., Kaplan,D.R., Miller,F.D., Evidence that embryonic the onset of cortical neurons regulate gliogenesis via cardiotrophin-1, Neuron, 48 (2005) 253-265.

[116] Faijerson,J., Tinsley,R.B., Aprico,K., Thorsell,A., Nodin,C., Nilsson,M., Blomstrand,F., Eriksson,P.S., Reactive astrogliosis induces astrocytic differentiation of adult neural stem/progenitor cells in vitro, J. Neurosci. Res., 84 (2006) 1415-1424.

[117] Levison,S.W., Ducceschi,M.H., Young,G.M., Wood,T.L., Acute exposure to CNTF in vivo induces multiple components of reactive gliosis, Exp. Neurol., 141 (1996) 256-268.

[118] Hudgins,S.N., Levison,S.W., Ciliary neurotrophic factor stimulates astroglial hypertrophy in vivo and in vitro, Exp. Neurol., 150 (1998) 171-182.

[119] Tilgner,J., Volk,B., Kaltschmidt,C., Continuous interleukin-6 application in vivo via macroencapsulation of interleukin-6-expressing COS-7 cells induces massive gliosis, Glia, 35 (2001) 234-245.

[120] Levison,S.W., Jiang,F.J., Stoltzfus,O.K., Ducceschi,M.H., IL-6-type cytokines enhance epidermal growth factor-stimulated astrocyte proliferation, Glia, 32 (2000) 328-337.

[121] Martin,A., Hofmann,H.D., Kirsch,M., Glial reactivity in ciliary neurotrophic factor-deficient mice after optic nerve lesion, J. Neurosci., 23 (2003) 5416-5424.

[122] Setoguchi,T., Nakashima,K., Takizawa,T., Yanagisawa,M., Ochiai,W., Okabe,M., Yone,K., Komiya,S., Taga,T., Treatment of spinal cord injury by transplantation of fetal neural precursor cells engineered to express BMP inhibitor, Exp. Neurol., 189 (2004) 33-44.

[123] Hampton,D.W., Asher,R.A., Kondo,T., Steeves,J.D., Ramer,M.S., Fawcett,J.W., A potential role for bone morphogenetic protein signalling in glial cell fate determination following adult central nervous system injury in vivo, Eur. J. Neurosci., 26 (2007) 3024-3035.

[124] Ben Hur,T., Ben Menachem,O., Furer,V., Einstein,O., Mizrachi-Kol,R., Grigoriadis,N., Effects of proinflammatory cytokines on the growth, fate, and motility of multipotential neural precursor cells, Molecular and Cellular Neuroscience, 24 (2003) 623-631.

[125] Kornblum,H.I., Introduction to neural stem cells, Stroke, 38 (2007) 810-816.

[126] Joy,A., Moffett,J., Neary,K., Mordechai,E., Stachowiak,E.K., Coons,S., RankinShapiro,J., Florkiewicz,R.Z., Stachowiak,M.K., Nuclear accumulation of FGF-2 is

associated with proliferation of human astrocytes and glioma cells, Oncogene, 14 (1997) 171-183.

[127] Fok-Seang,J., DiProspero,N.A., Meiners,S., Muir,E., Fawcett,J.W., Cytokine-induced changes in the ability of astrocytes to support migration of oligodendrocyte precursors and axon growth, Eur. J. Neurosci., 10 (1998) 2400-2415.

[128] Ferretti,P., Zhang,F., O'Neill,P., Changes in spinal cord regenerative ability through phylogenesis and development: Lessons to be learnt, Dev. Dyn., 226 (2003) 245-256.

[129] Smith,C., Berry,M., Clarke,W.E., Logan,A., Differential expression of fibroblast growth factor-2 and fibroblast growth factor receptor 1 in a scarring and nonscarring model of CNS injury in the rat, Eur. J. Neurosci., 13 (2001) 443-456.

[130] FaberElman,A., Solomon,A., Abraham,J.A., Marikovsky,M., Schwartz,M., Involvement of wound-associated factors in rat brain astrocyte migratory response to axonal injury: In vitro simulation, J. Clin. Invest., 97 (1996) 162-171.

[131] Engele,J., Bohn,M.C., The Neurotrophic Effects of Fibroblast Growth-Factors on Dopaminergic-Neurons Invitro Are Mediated by Mesencephalic Glia, J. Neurosci., 11 (1991) 3070-3078.

[132] Eves,E.M., Skoczylas,C., Yoshida,K., Alnemri,E.S., Rosner,M.R., FGF induces a switch in death receptor pathways in neuronal cells, J. Neurosci., 21 (2001) 4996-5006.

[133] Eclancher,F., Kehrli,P., Labourdette,G., Sensenbrenner,M., Basic fibroblast growth factor (bFGF) injection activates the glial reaction in the injured adult rat brain, Brain Res., 737 (1996) 201-214.

[134] Hermanson,O., Jepsen,K., Rosenfeld,M.G., N-CoR controls differentiation of neural stem cells into astrocytes, Nature, 419 (2002) 934-939.

[135] Boilly,B., Vercoutter-Edouart,A.S., Hondermarck,H., Nurcombe,V., Le Bourhis,X., FGF signals for cell proliferation and migration through different pathways, Cytokine & Growth Factor Reviews, 11 (2000) 295-302.

[136] Klapka,N., Muller,H.W., Collagen matrix in spinal cord, Journal of Neurotrauma, 23 (2006) 422-435.

[137] Bjornsson,C.S., Oh,S.J., Al Kofahi,Y.A., Lim,Y.J., Smith,K.L., Turner,J.N., De,S., Roysam,B., Shain,W., Kim,S.J., Effects of insertion conditions on tissue strain and vascular damage during neuroprosthetic device insertion, Journal of Neural Engineering, 3 (2006) 196-207.

[138] Schmidt,S., Horch,K., Normann,R., Biocompatibility of Silicon-Based Electrode Arrays Implanted in Feline Cortical Tissue, J. Biomed. Mater. Res., 27 (1993) 1393-1399.

[139] Fujita,T., Yoshimine,T., Maruno,M., Hayakawa,T., Cellular dynamics of macrophages and microglial cells in reaction to stab wounds in rat cerebral cortex, Acta Neurochir. (Wien)., 140 (1998) 275-279.

[140] Giordana,M.T., Attanasio,A., Cavalla,P., Migheli,A., Vigliani,M.C., Schiffer,D., Reactive Cell-Proliferation and Microglia Following Injury to the Rat-Brain, Neuropathol. Appl. Neurobiol., 20 (1994) 163-174.

[141] Stensaas,S.S., Stensaas,L.J., The Reaction of the Cerebral Cortex to Chronically Implanted Plastic Needles, Acta Neuropathol. (Berl)., 35 (1976) 187-203.

[142] Csicsvari,J., Henze,D.A., Jamieson,B., Harris,K.D., Sirota,A., Bartho,P., Wise,K.D., Buzsaki,G., Massively parallel recording of unit and local field potentials with silicon-based electrodes, J. Neurophysiol., 90 (2003) 1314-1323.

[143] Stensaas,S.S., Stensaas,L.J., Histopathological Evaluation of Materials Implanted in Cerebral-Cortex, Acta Neuropathol. (Berl)., 41 (1978) 145-155.

[144] Winn,S.R., Aebischer,P., Galletti,P.M., Brain-Tissue Reaction to Permselective Polymer Capsules, J. Biomed. Mater. Res., 23 (1989) 31-44.

[145] Mofid,M.M., Thompson,R.C., Pardo,C.A., Manson,P.N., VanderKolk,C.A., Biocompatibility of fixation materials in the brain, Plast. Reconstr. Surg., 100 (1997) 14-20.

[146] Emerich,D.F., Tracy,M.A., Ward,K.L., Figueiredo,M., Qian,R.L., Henschel,C., Bartus,R.T., Biocompatibility of poly (DL-lactide-co-glycolide) microspheres implanted into the brain, Cell Transplant., 8 (1999) 47-58.

[147] Mokry,J., Karbanova,J., Lukas,J., Paleckova,V., Dvorankova,B., Biocompatibility of HEMA copolymers designed for treatment of CNS diseases with polymer-encapsulated cells, Biotechnol. Prog., 16 (2000) 897-904.

[148] Shain,W., Spataro,L., Dilgen,J., Haverstick,K., Retterer,S., Isaacson,M., Saltzman,M., Turner,J.N., Controlling cellular reactive responses around neural prosthetic devices using peripheral and local intervention strategies, Ieee Transactions on Neural Systems and Rehabilitation Engineering, 11 (2003) 186-188.

[149] Reier,P.J., Stensaas,L.J., Guth,L., The Astrocytic Scar as an Impediment to Regeneration in the Central Nervous System. In Kao,CC, Bunge,RP, Reier,PJ (Eds.), Spinal Cord Regeneration Raven Press, New York, 1983, pp. 163-195.

[150] Bush,T.G., Puvanachandra,N., Horner,C.H., Polito,A., Ostenfeld,T., Svendsen,C.N., Mucke,L., Johnson,M.H., Sofroniew,M.V., Leukocyte infiltration, neuronal degeneration, and neurite outgrowth after ablation of scar-forming, reactive astrocytes in adult transgenic mice, Neuron, 23 (1999) 297-308.

[151] Myer,D.J., Gurkoff,G.G., Lee,S.M., Hovda,D.A., Sofroniew,M.V., Essential protective roles of reactive astrocytes in traumatic brain injury, Brain, 129 (2006) 2761-2772.

[152] Faulkner,J.R., Herrmann,J.E., Woo,M.J., Tansey,K.E., Doan,N.B., Sofroniew,M.V., Reactive astrocytes protect tissue and preserve function after spinal cord injury, J. Neurosci., 24 (2004) 2143-2155.

[153] Scherbel,U., Raghupathi,R., Nakamura,M., Saatman,K.E., Trojanowski,J.Q., Neugebauer,E., Marino,M.W., McIntosh,T.K., Differential acute and chronic responses of tumor necrosis factor-deficient mice to experimental brain injury, Proc. Natl. Acad. Sci. U. S. A., 96 (1999) 8721-8726.

[154] Penkowa,M., Giralt,M., Lago,N., Camats,J., Caffasco,J., Hernandez,J., Molinero,A., Campbell,I.L., Hidalgo,J., Astrocyte-targeted expression of IL-6 protects the CNS against a focal brain injury, Exp. Neurol., 181 (2003) 130-148.

[155] Schultz,R.L., Willey,T.J., The ultrastructure of the sheath around chronically implanted electrodes in brain, J. Neurocytol., 5 (1976) 621-642.

[156] Schmidt,E.M., Bak,M.J., McIntosh,J.S., Long-term chronic recording from cortical neurons, Exp. Neurol., 52 (1976) 496-506.

[157] Agnew,W.F., Yuen,T.G.H., McCreery,D.B., Bullara,L.A., Histopathologic Evaluation of Prolonged Intracortical Electrical-Stimulation, Exp. Neurol., 92 (1986) 162-185.

[158] Carter,R.R., Houk,J.C., Multiple Single Unit Recordings from the CNS Using Thin-Film Electrode Arrays, IEEE Trans. Rehabil. Eng., 1 (1993) 175-184.

[159] Schmidt,C.E., Shastri,V.R., Vacanti,J.P., Langer,R., Stimulation of neurite outgrowth using an electrically conducting polymer, Proc. Natl. Acad. Sci. U. S. A., 94 (1997) 8948-8953.

[160] McCreery,D.B., Yuen,T.G.H., Agnew,W.F., Bullara,L.A., A characterization of the effects on neuronal excitability due to prolonged microstimulation with chronically implanted microelectrodes, IEEE Trans. Biomed. Eng., 44 (1997) 931-939.

[161] Roitbak,T., Sykova,E., Diffusion barriers evoked in the rat cortex by reactive astrogliosis, Glia, 28 (1999) 40-48.

[162] Williams,J.C., Hippensteel,J.A., Dilgen,J., Shain,W., Kipke,D.R., Complex impedance spectroscopy for monitoring tissue responses to inserted neural implants, Journal of Neural Engineering, 4 (2007) 410-423.

[163] Stichel,C.C., Muller,H.W., The CNS lesion scar: new vistas on an old regeneration barrier, Cell Tissue Res., 294 (1998) 1-9.

[164] Fawcett,J.W., Asher,R.A., The glial scar and central nervous system repair, Brain Res. Bull., 49 (1999) 377-391.

[165] Bovolenta,P., Fernaud-Espinosa,I., Nervous system proteoglycans as modulators of neurite outgrowth, Prog. Neurobiol., 61 (2000) 113-132.

[166] Biran,R., Martin,D.C., Tresco,P.A., The brain tissue response to implanted silicon microelectrode arrays is increased when the device is tethered to the skull, Journal of Biomedical Materials Research Part A, 82A (2007) 169-178.

[167] Wu,V.W., Schwartz,J.P., Cell culture models for reactive gliosis: New perspectives, J. Neurosci. Res., 51 (1998) 675-681.

[168] Mcmillian,M.K., Thai,L., Hong,J.S., Ocallaghan,J.P., Pennypacker,K.R., Brain Injury in A Dish - A Model for Reactive Gliosis, Trends Neurosci., 17 (1994) 138-142.

[169] Wu,V.W., Nishiyama,N., Schwartz,J.P., A culture model of reactive astrocytes: Increased nerve growth factor synthesis and reexpression of cytokine responsiveness, J. Neurochem., 71 (1998) 749-756.

[170] Balasingam,V., Tejadaberges,T., Wright,E., Bouckova,R., Yong,V.W., Reactive Astrogliosis in the Neonatal Mouse-Brain and Its Modulation by Cytokines, J. Neurosci., 14 (1994) 846-856.

[171] Smith,G.M., Miller,R.H., Silver,J., Changing-Role of Forebrain Astrocytes During Development, Regenerative Failure, and Induced Regeneration Upon Transplantation, J. Comp. Neurol., 251 (1986) 23-43.

[172] Silver,J., Ogawa,M.Y., Postnatally Induced Formation of the Corpus-Callosum in Acallosal Mice on Glia-Coated Cellulose Bridges, Science, 220 (1983) 1067-1069.

[173] Mckeon,R.J., Schreiber,R.C., Rudge,J.S., Silver,J., Reduction of Neurite Outgrowth in A Model of Glial Scarring Following Cns Injury Is Correlated with the Expression of Inhibitory Molecules on Reactive Astrocytes, J. Neurosci., 11 (1991) 3398-3411.

[174] Rudge,J.S., Smith,G.M., Silver,J., An Invitro Model of Wound-Healing in the Cns - Analysis of Cell Reaction and Interaction at Different Ages, Exp. Neurol., 103 (1989) 1-16.

[175] Fitch,M.T., Silver,J., Activated macrophages and the blood-brain barrier: Inflammation after CNS injury leads to increases in putative inhibitory molecules, Exp. Neurol., 148 (1997) 587-603.

[176] Fitch,M.T., Silver,J., CNS injury, glial scars, and inflammation: Inhibitory extracellular matrices and regeneration failure, Exp. Neurol., 209 (2008) 294-301.

[177] Silver,J., Miller,J.H., Regeneration beyond the glial scar, Nature Reviews Neuroscience, 5 (2004) 146-156.

[178] Ness,R., David,S., Leptomeningeal cells modulate the neurite growth promoting properties of astrocytes in vitro, Glia, 19 (1997) 47-57.

[179] Stichel,C.C., Niermann,H., D'Urso,D., Lausberg,F., Hermanns,S., Muller,H.W., Basal membrane-depleted scar in lesioned CNS: Characteristics and relationships with regenerating axons, Neuroscience, 93 (1999) 321-333.

[180] Buss,A., Pech,K., Kakulas,B.A., Martin,D., Schoenen,J., Noth,J., Brook,G.A., Growth-modulating molecules are associated with invading Schwann cells and not astrocytes in human traumatic spinal cord injury, Brain, 130 (2007) 940-953.

[181] Logan,A., Baird,A., Berry,M., Decorin attenuates gliotic scar formation in the rat cerebral hemisphere, Exp. Neurol., 159 (1999) 504-510.

[182] Hermanns,S., Klapka,N., Muller,H.W., The collagenous lesion scar - an obstacle for axonal regeneration in brain and spinal cord injury, Restorative Neurology and Neuroscience, 19 (2001) 139-148.

[183] Shearer,M.C., Niclou,S.P., Brown,D., Asher,R.A., Holtmaat,A.J.G.D., Levine,J.M., Verhaagen,J., Fawcett,J.W., The astrocyte/meningeal cell interface is a barrier to neurite outgrowth which can be overcome by manipulation of inhibitory molecules or axonal signalling pathways, Molecular and Cellular Neuroscience, 24 (2003) 913-925.

[184] Pasterkamp,R.J., Giger,R.J., Ruitenberg,M.J., Holtmaat,A.J.G.D., De Wit,J., De Winter,F., Verhaagen,J., Expression of the gene encoding the chemorepellent semaphorin III is induced in the fibroblast component of neural scar tissue formed following injuries of adult but not neonatal CNS, Molecular and Cellular Neuroscience, 13 (1999) 143-166.

[185] Cool,S.M., Nurcombe,V., Heparan sulfate regulation of progenitor cell fate, J. Cell. Biochem., 99 (2006) 1040-1051.

[186] Smith,G.M., Hale,J.H., Macrophage/microglia regulation of astrocytic tenascin: Synergistic action of transforming growth factor-beta and basic fibroblast growth factor, J. Neurosci., 17 (1997) 9624-9633.

[187] Stichel,C.C., Hermanns,S., Luhmann,H.J., Lausberg,F., Niermann,H., D'Urso,D., Servos,G., Hartwig,H.G., Muller,H.W., Inhibition of collagen IV deposition promotes regeneration of injured CNS axons, Eur. J. Neurosci., 11 (1999) 632-646.

[188] Geller,H.M., Fawcett,J.W., Building a bridge: Engineering spinal cord repair, Exp. Neurol., 174 (2002) 125-136.

[189] Yurchenco,P.D., Schittny,J.C., Molecular Architecture of Basement-Membranes, FASEB J., 4 (1990) 1577-1590.

[190] Mcnaughton,B.L., Okeefe,J., Barnes,C.A., The Stereotrode - A New Technique for Simultaneous Isolation of Several Single Units in the Central Nervous-System from Multiple Unit Records, J. Neurosci. Methods, 8 (1983) 391-397.

[191] Gray,C.M., Maldonado,P.E., Wilson,M., McNaughton,B., Tetrodes markedly improve the reliability and yield of multiple single-unit isolation from multi-unit recordings in cat striate cortex, J. Neurosci. Methods, 63 (1995) 43-54.

[192] Branner,A., Stein,R.B., Normann,R.A., Selective stimulation of cat sciatic nerve using an array of varying-length microelectrodes, J. Neurophysiol., 85 (2001) 1585-1594.

[193] Kipke,D.R., Vetter,R.J., Williams,J.C., Hetke,J.F., Silicon-substrate intracortical microelectrode arrays for long-term recording of neuronal spike activity in cerebral cortex, Ieee Transactions on Neural Systems and Rehabilitation Engineering, 11 (2003) 151-155.

[194] Kewley,D.T., Hills,M.D., Borkholder,D.A., Opris,I.E., Maluf,N.I., Storment,C.W., Bower,J.M., Kovacs,G.T.A., Plasma-etched neural probes, Sensors and Actuators A-Physical, 58 (1997) 27-35.

[195] Bai,Q., Wise,K.D., Single-unit neural recording with active microelectrode arrays, IEEE Trans. Biomed. Eng., 48 (2001) 911-920.

[196] Chen,J.K., Wise,K.D., Hetke,J.F., Bledsoe,S.C., A multichannel neural probe for selective chemical delivery at the cellular level, IEEE Trans. Biomed. Eng., 44 (1997) 760-769.

[197] Cui,X.Y., Lee,V.A., Raphael,Y., Wiler,J.A., Hetke,J.F., Anderson,D.J., Martin,D.C., Surface modification of neural recording electrodes with conducting polymer/biomolecule blends, J. Biomed. Mater. Res., 56 (2001) 261-272.

[198] Moxon,K.A., Kalkhoran,N.M., Markert,M., Sambito,M.A., McKenzie,J.L., Webster,J.T., Nanostructured surface modification of ceramic-based microelectrodes to enhance biocompatibility for a direct brain-machine interface, IEEE Trans. Biomed. Eng., 51 (2004) 881-889.

[199] Moxon,K.A., Leiser,S.C., Gerhardt,G.A., Barbee,K.A., Chapin,J.K., Ceramic-based multisite electrode arrays for chronic single-neuron recording, IEEE Trans. Biomed. Eng., 51 (2004) 647-656.

[200] Muthuswamy,J., Okandan,M., Jackson,N., Single neuronal recordings using surface micromachined polysilicon microelectrodes, J. Neurosci. Methods, 142 (2005) 45-54.

[201] Kennedy,P.R., The Cone Electrode - A Long-Term Electrode That Records from Neurites Grown Onto Its Recording Surface, J. Neurosci. Methods, 29 (1989) 181-193.

[202] Singh,A., Ehteshami,G., Massia,S., He,J.P., Storer,R.G., Raupp,G., Glial cell and fibroblast cytotoxicity study on plasma-deposited diamond-like carbon coatings, Biomaterials, 24 (2003) 5083-5089.

[203] Ignatius,M.J., Sawhney,N., Gupta,A., Thibadeau,B.M., Monteiro,O.R., Brown,I.G., Bioactive surface coatings for nanoscale instruments: Effects on CNS neurons, J. Biomed. Mater. Res., 40 (1998) 264-274.

[204] Sanchez,J.C., Alba,N., Nishida,T., Batich,C., Carney,P.R., Structural modifications in chronic microwire electrodes for cortical neuroprosthetics: A case study, Ieee Transactions on Neural Systems and Rehabilitation Engineering, 14 (2006) 217-221.

[205] Lee,K.K., He,J.P., Singh,A., Massia,S., Ehteshami,G., Kim,B., Raupp,G., Polyimide-based intracortical neural implant with improved structural stiffness, Journal of Micromechanics and Microengineering, 14 (2004) 32-37.

[206] Gilletti,A., Muthuswamy,J., Brain micromotion around implants in the rodent somatosensory cortex, Journal of Neural Engineering, 3 (2006) 189-195.

[207] Wisniewski,N., Moussy,F., Reichert,W.M., Characterization of implantable biosensor membrane biofouling, Fresenius Journal of Analytical Chemistry, 366 (2000) 611-621.

[208] Sharkawy,A.A., Klitzman,B., Truskey,G.A., Reichert,W.M., Engineering the tissue which encapsulates subcutaneous implants. II. Plasma-tissue exchange properties, J. Biomed. Mater. Res., 40 (1998) 586-597.

[209] Sharkawy,A.A., Klitzman,B., Truskey,G.A., Reichert,W.M., Engineering the tissue which encapsulates subcutaneous implants. III. Effective tissue response times, J. Biomed. Mater. Res., 40 (1998) 598-605.

[210] Sharkawy,A.A., Klitzman,B., Truskey,G.A., Reichert,W.M., Engineering the tissue which encapsulates subcutaneous implants .1. Diffusion properties, J. Biomed. Mater. Res., 37 (1997) 401-412.

[211] Seymour,J.P., Kipke,D.R., Neural probe design for reduced tissue encapsulation in CNS, Biomaterials, 28 (2007) 3594-3607.

[212] Kam,L., Shain,W., Turner,J.N., Bizios,R., Selective adhesion of astrocytes to surfaces modified with immobilized peptides, Biomaterials, 23 (2002) 511-515.

[213] Yang,J.Y., Martin,D.C., Microporous conducting polymers on neural microelectrode arrays II. Physical characterization, Sensors and Actuators A-Physical, 113 (2004) 204-211.

[214] Ludwig,K.A., Uram,J.D., Yang,J.Y., Martin,D.C., Kipke,D.R., Chronic neural recordings using silicon microelectrode arrays electrochemically deposited with a poly(3,4-ethylenedioxythiophene) (PEDOT) film, Journal of Neural Engineering, 3 (2006) 59-70.

[215] Biran,R., Noble,M.D., Tresco,P.A., Directed nerve outgrowth is enhanced by engineered glial substrates, Exp. Neurol., 184 (2003) 141-152.

[216] Biran,R., Noble,M.D., Tresco,P.A., Characterization of cortical astrocytes on materials of differing surface chemistry, J. Biomed. Mater. Res., 46 (1999) 150-159.

[217] Craighead,H., Turner,S.W., Davis,R.C., James,C.D., Perez,A.M., St.John,P.M., Isaacson,M., Kam,L., Shain,W., Turner,J.N., Banker,G., Chemical and Topographical Surface Modification for Control of Central Nervous sytem Cell Adhesion, Journal of Biomedical Microdevices, 1 (1998) 49-64.

[218] Kam,L., Shain,W., Turner,J.N., Bizios,R., Correlation of astroglial cell function on micro-patterned surfaces with specific geometric parameters, Biomaterials, 20 (1999) 2343-2350.

[219] Stjohn,P.M., Kam,L., Turner,S.W., Craighead,H.G., Issacson,M., Turner,J.N., Shain,W., Preferential glial cell attachment to microcontact printed surfaces, Journal of Neuroscience Methods, 75 (1997) 171-177.

[220] Turner,A.M.P., Dowell,N., Turner,S.W.P., Kam,L., Isaacson,M., Turner,J.N., Craighead,H.G., Shain,W., Attachment of astroglial cells to microfabricated pillar arrays of different geometries, J. Biomed. Mater. Res., 51 (2000) 430-441.

[221] Stichel,C.C., Muller,H.W., Experimental strategies to promote axonal regeneration after traumatic central nervous system injury, Prog. Neurobiol., 56 (1998) 119-148.

[222] Yoon,J.J., Kim,J.H., Park,T.G., Dexamethasone-releasing biodegradable polymer scaffolds fabricated by a gas-foaming/salt-leaching method, Biomaterials, 24 (2003) 2323-2329.

[223] Hickey,T., Kreutzer,D., Burgess,D.J., Moussy,F., In vivo evaluation of a dexamethasone/PLGA microsphere system designed to suppress the inflammatory tissue response to implantable medical devices, J. Biomed. Mater. Res., 61 (2002) 180-187.

[224] Zhong,Y.H., Bellamkonda,R.V., Dexamethasone-coated neural probes elicit attenuated inflammatory response and neuronal loss compared to uncoated neural probes, Brain Res., 1148 (2007) 15-27.

[225] Purcell,E.K., Seymour,J.P., Yandamuri,S., Kipke,D.R., In vivo evaluation of a neural stem cell-seeded prosthesis, Journal of Neural Engineering, 6 (2009).

[226] Schmidt,E.M., Single Neuron Recording from Motor Cortex As A Possible Source of Signals for Control of External Devices, Ann. Biomed. Eng., 8 (1980) 339-349.

[227] Mckeon,R.J., Hoke,A., Silver,J., Injury-Induced Proteoglycans Inhibit the Potential for Laminin-Mediated Axon Growth on Astrocytic Scars, Exp. Neurol., 136 (1995) 32-43.

[228] Yu,X.J., Bellamkonda,R.V., Dorsal root ganglia neurite extension is inhibited by mechanical and chondroitin sulfate-rich interfaces, J. Neurosci. Res., 66 (2001) 303-310.

[229] Tom,V.J., Steinmetz,M.P., Miller,J.H., Doller,C.M., Silver,J., Studies on the development and behavior of the dystrophic growth cone, the hallmark of regeneration failure, in an in vitro model of the glial scar and after spinal cord injury, J. Neurosci., 24 (2004) 6531-6539.

[230] Klaver,C.L., Caplan,M.R., Bioactive surface for neural electrodes: Decreasing astrocyte proliferation via transforming growth factor-beta 1, Journal of Biomedical Materials Research Part A, 81A (2007) 1011-1016.

[231] Kornyei,Z., Czirok,A., Vicsek,T., Madarasz,E., Proliferative and migratory responses of astrocytes to in vitro injury, J. Neurosci. Res., 61 (2000) 421-429.

[232] Yu,A.C.H., Lee,Y.L., Eng,L.F., Astrogliosis in Culture .1. the Model and the Effect of Antisense Oligonucleotides on Glial Fibrillary Acidic Protein-Synthesis, J. Neurosci. Res., 34 (1993) 295-303.

[233] Seniuk,N.A., Henderson,J.T., Tatton,W.G., Roder,J.C., Increased Cntf Gene-Expression in Process-Bearing Astrocytes Following Injury Is Augmented by R(-)-Deprenyl, J. Neurosci. Res., 37 (1994) 278-286.

[234] Maynard,E.M., Nordhausen,C.T., Normann,R.A., The Utah Intracortical Electrode Array: A recording structure for potential brain-computer interfaces, Electroencephalogr. Clin. Neurophysiol., 102 (1997) 228-239.

[235] Jones,K.E., Campbell,P.K., Normann,R.A., A Glass Silicon Composite Intracortical Electrode Array, Ann. Biomed. Eng., 20 (1992) 423-437.

[236] Li,G.R., Cui,G., Tzeng,N.S., Wei,S.J., Wang,T.G., Block,M.L., Hong,J.S., Femtomolar concentrations of dextromethorphan protect mesencephalic dopaminergic neurons from inflammatory damage, FASEB J., 19 (2005) 489-496.

[237] Liu,B., Jiang,J.W., Wilson,B.C., Du,L., Yang,S.N., Wang,J.Y., Wu,G.C., Cao,X.D., Hong,J.S., Systemic infusion of naloxone reduces degeneration of rat substantia nigral dopaminergic neurons induced by intranigral injection of lipopolysaccharide, J. Pharmacol. Exp. Ther., 295 (2000) 125-132.

[238] Liu,B., Du,L.N., Hong,J.S., Naloxone protects rat dopaminergic neurons against inflammatory damage through inhibition of microglia activation and superoxide generation, J. Pharmacol. Exp. Ther., 293 (2000) 607-617.

[239] Pennypacker,K.R., Hong,J.S., Mullis,S.B., Hudson,P.M., Mcmillian,M.K., Transcription factors in primary glial cultures: Changes with neuronal interactions, Mol. Brain Res., 37 (1996) 224-230.

[240] Koschwanez,H.E., Reichert,W.M., In vitro, in vivo and post implantation testing of glucose-detecting biosensors: current methods and recommendations. In Narayan,R (Ed.), Biomaterials: Processing and Characterization Cambridge University Press, 2006.

[241] Li,G.R., Liu,Y.X., Tzeng,N.S., Cui,G., Block,M.L., Wilson,B., Qin,L.Y., Wang,T.G., Liu,B., Liu,J., Hong,J.S., Protective effect of dextromethorphan against endotoxic shock in mice, Biochem. Pharmacol., 69 (2005) 233-240.

[242] Gao,H.M., Jiang,J., Wilson,B., Zhang,W., Hong,J.S., Liu,B., Microglial activation-mediated delayed and progressive degeneration of rat nigral dopaminergic neurons: relevance to Parkinson's disease, J. Neurochem., 81 (2002) 1285-1297.

[243] Rezaie,P., Trillo-Pazos,G., Greenwood,J., Everall,I.P., Male,D.K., Motility and ramification of human fetal microglia in culture: An investigation using time-lapse video microscopy and image analysis, Exp. Cell Res., 274 (2002) 68-82.

[244] Nimmerjahn,A., Kirchhoff,F., Helmchen,F., Resting microglial cells are highly dynamic surveillants of brain parenchyma in vivo, Science, 308 (2005) 1314-1318.

[245] Spataro,L., Dilgen,J., Retterer,S., Spence,A.J., Isaacson,M., Turner,J.N., Shain,W., Dexamethasone treatment reduces astroglia responses to inserted neuroprosthetic devices in rat neocortex, Exp. Neurol., 194 (2005) 289-300.

[246] Morrow,T., Song,M.R., Ghosh,A., Sequential specification of neurons and glia by developmentally regulated extracellular factors, Development, 128 (2001) 3585-3594.

[247] Liu,A.X., Han,Y.R., Li,J.D., Sun,D.M., Ouyang,M., Plummer,M.R., Casaccia-Bonnefil,P., The glial or neuronal fate choice of oligodendrocyte progenitors is modulated by their ability to acquire an epigenetic memory, J. Neurosci., 27 (2007) 7339-7343.

[248] Yang,Z.S., Watanabe,M., Nishiyama,A., Optimization of oligodendrocyte progenitor cell culture method for enhanced survival, J. Neurosci. Methods, 149 (2005) 50-56.

[249] Wang,T.G., Pei,Z., Zhang,W., Liu,B., Langenbach,R., Lee,C., Wilson,B., Reece,J.M., Miller,D.S., Hong,J.S., MPP+-induced COX-2 activation and subsequent dopaminergic neurodegeneration, FASEB J., 19 (2005).

[250] Qin,L.Y., Liu,Y.X., Wang,T.G., Wei,S.J., Block,M.L., Wilson,B., Liu,B., Hong,J.S., NADPH oxidase mediates lipopolysaccharide-induced neurotoxicity and proinflammatory gene expression in activated microglia, J. Biol. Chem., 279 (2004) 1415-1421.

[251] Gao,H.M., Liu,B., Zhang,W.Q., Hong,J.S., Critical role of microglial NADPH oxidase-derived free radicals in the in vitro MPTP model of Parkinson's disease, FASEB J., 17 (2003) 1954-+.

[252] Raivich,G., Bohatschek,M., Kloss,C.U.A., Werner,A., Jones,L.L., Kreutzberg,G.W., Neuroglial activation repertoire in the injured brain: graded response, molecular mechanisms and cues to physiological function, Brain Research Reviews, 30 (1999) 77-105.

[253] Nadal,A., Fuentes,E., Pastor,J., Mcnaughton,P.A., Plasma albumin induces calcium waves in rat cortical astrocytes, Glia, 19 (1997) 343-351.

[254] Nadal,A., Fuentes,E., Pastor,J., McNaughton,P.A., Plasma-Albumin Is A Potent Trigger of Calcium Signals and Dna-Synthesis in Astrocytes, Proc. Natl. Acad. Sci. U. S. A., 92 (1995) 1426-1430.

[255] Skoff,R.P., Fine-Structure of Pulse Labeled (H-3-Thymidine Cells) in Degenerating Rat Optic-Nerve, J. Comp. Neurol., 161 (1975) 595-611.

[256] Magnus,T., Coksaygan,T., Korn,T., Xue,H.P., Arumugam,T.V., Mughal,M.R., Eckley,D.M., Tang,S.C., DeTolla,L., Rao,M.S., Cassiani-Ingoni,R., Mattson,M.P., Evidence that nucleocytoplasmic Olig2 translocation mediates brain-injury-induced differentiation of glial precursors to astrocytes, J. Neurosci. Res., 85 (2007) 2126-2137.

[257] Hermann,A., Maisel,M., Wegner,F., Liebau,S., Kim,D.W., Gerlach,M., Schwarz,J., Kim,K.S., Storch,A., Multipotent neural stem cells from the adult tegmentum with dopaminergic potential develop essential properties of functional neurons, Stem Cells, 24 (2006) 949-964.

[258] Kahn,M.A., Huang,C.J., Caruso,A., Barresi,V., Nazarian,R., Condorelli,D.F., Devellis,J., Ciliary neurotrophic factor activates JAK/Stat signal transduction cascade and induces transcriptional expression of glial fibrillary acidic protein in glial cells, J. Neurochem., 68 (1997) 1413-1423.

[259] Biederer,T., Scheiffele,P., Mixed-culture assays for analyzing neuronal synapse formation, Nature Protocols, 2 (2007) 670-676.

[260] Kleinman,H.K., Mcgarvey,M.L., Liotta,L.A., Robey,P.G., Tryggvason,K., Martin,G.R., Isolation and Characterization of Type-Iv Procollagen, Laminin, and Heparan-Sulfate Proteoglycan from the Ehs Sarcoma, Biochemistry, 21 (1982) 6188-6193.

[261] Herx,L.M., Rivest,S., Yong,V.W., Central nervous system-initiated inflammation and neurotrophism in trauma: IL-1 beta is required for the production of ciliary neurotrophic factor, J. Immunol., 165 (2000) 2232-2239.

[262] Hamilton,T.A., Tannenbaum,C.S., Tebo,J.M., Cytokine-Initiated Intracellular Signaling Pathways. In Ransohoff,RM, Benveniste,EN (Eds.), Cytokines and the CNS CRC Press, Boca Raton, 1996, pp. 25-45.

[263] Rostworowski,M., Balasingam,V., Chabot,S., Owens,T., Yong,V.W., Astrogliosis in the neonatal and adult murine brain post-trauma: Elevation of inflammatory cytokines and the lack of requirement for endogenous interferon-gamma, J. Neurosci., 17 (1997) 3664-3674.

[264] Woiciechowsky,C., Schoning,B., Stoltenburg-Didinger,G., Stockhammer,F., Volk,H.D., Brain-IL-1 beta triggers astrogliosis through induction of IL-6: Inhibition by propranolol and IL-10, Medical Science Monitor, 10 (2004) BR325-BR330.

[265] St.Pierre,B.A., Merrill,J.E., Dopp,J.M., Effects of Cytokines on CNS Cells: Glia. In Ransohoff,RM, Benveniste,EN (Eds.), Cytokines and the CNS CRC Press, Boca Raton, 1996, pp. 151-167.

[266] Anderson,J.M., Biological responses to materials, Annual Review of Materials Research, 31 (2001) 81-110.

[267] Schmidt,C.E., Leach,J.B., Neural tissue engineering: Strategies for repair and regeneration, Annual Review of Biomedical Engineering, 5 (2003) 293-347.

[268] Levitzki,A., Protein tyrosine kinase inhibitors as novel therapeutic agents, Pharmacology & Therapeutics, 82 (1999) 231-239.

[269] Norris,J.G., Tang,L.P., Sparacio,S.M., Benveniste,E.N., Signal-Transduction Pathways Mediating Astrocyte Il-6 Induction by Il-1-Beta and Tumor-Necrosis-Factor-Alpha, J. Immunol., 152 (1994) 841-850.

[270] Kao,W.J., Hubbell,J.A., Anderson,J.M., Protein-mediated macrophage adhesion and activation on biomaterials: a model for modulating cell behavior, Journal of Materials Science-Materials in Medicine, 10 (1999) 601-605.

[271] Rhodes,K.E., Raivich,G., Fawcett,J.W., The injury response of oligodendrocyte precursor cells is induced by platelets, macrophages and inflammation-associated cytokines, Neuroscience, 140 (2006) 87-100.

[272] Fitch,M.T., Doller,C., Combs,C.K., Landreth,G.E., Silver,J., Cellular and molecular mechanisms of glial scarring and progressive cavitation: In vivo and in vitro analysis of inflammation-induced secondary injury after CNS trauma, J. Neurosci., 19 (1999) 8182-8198.

[273] Saadoun,S., Papadopoulos,M.C., Watanabe,H., Yan,D.H., Manley,G.T., Verkman,A.S., Involvement of aquaporin-4 in astroglial cell migration and glial scar formation, J. Cell Sci., 118 (2005) 5691-5698.

[274] Papadopoulos,M.C., Saadoun,S., Verkman,A.S., Aquaporins and cell migration, Pflugers Archiv-European Journal of Physiology, 456 (2008) 693-700.

[275] Anderson,J.M., Defife,K., Mcnally,A., Collier,T., Jenney,C., Monocyte, macrophage and foreign body giant cell interactions with molecularly engineered surfaces, Journal of Materials Science-Materials in Medicine, 10 (1999) 579-588.

[276] Capadona,J.R., Shanmuganathan,K., Tyler,D.J., Rowan,S.J., Weder,C., Stimuli-responsive polymer nanocomposites inspired by the sea cucumber dermis, Science, 319 (2008) 1370-1374.

[277] Polikov,V.S., Block,M.L., Zhang,C., Reichert,W.M., Hong,J.S., In Vitro Models for Neuroelectrodes: A Paradigm for Studying Tissue-materials Interactions in the Brain. In Reichert,WM (Ed.), Indwelling Neural Implants: Strategies for Contending with the In Vivo Environment CRC Press, Boca Raton, FL, 2008, pp. 89-115.

[278] Freshney,I., Application of cell cultures to toxicology, Cell Biol. Toxicol., 17 (2001) 213-230.

[279] Protocols for Neural Cell Culture, Humana Press, Totowa, N.J., 2001.

[280] Massia,S.P., Holecko,M.M., Ehteshami,G.R., In vitro assessment of bioactive coatings for neural implant applications, Journal of Biomedical Materials Research Part A, 68A (2004) 177-186.

[281] Martin,D.L., Shain,W., High-Affinity Transport of Taurine and Beta-Alanine and Low Affinity Transport of Gamma-Aminobutyric Acid by A Single Transport-System in Cultured Glioma-Cells, J. Biol. Chem., 254 (1979) 7076-7084.

[282] St.John,P.M., Kam,L., Turner,S.W., Craighead,H.G., Issacson,M., Turner,J.N., Shain,W., Preferential glial cell attachment to microcontact printed surfaces, J. Neurosci. Methods, 75 (1997) 171-177.

[283] Tzeng,S.F., Huang,H.Y., Downregulation of inducible nitric oxide synthetase by neurotrophin-3 in microglia, J. Cell. Biochem., 90 (2003) 227-233.

[284] Kremlev,S.G., Roberts,R.L., Palmer,C., Differential expression of chemokines and chemokine receptors during microglial activation and inhibition, J. Neuroimmunol., 149 (2004) 1-9.

[285] Wang,T.G., Liu,B., Zhang,W., Wilson,B., Hong,J.S., Andrographolide reduces inflammation-mediated dopaminergic neurodegeneration in mesencephalic neuron-glia cultures by inhibiting microglial activation, J. Pharmacol. Exp. Ther., 308 (2004) 975-983.

[286] Pei,Z., Pang,H., Qian,L., Yang,S.N., Wang,T.G., Zhang,W., Wu,X.F., Dallas,S., Wilson,B., Reece,J.M., Miller,D.S., Hong,J.S., Block,M.L., MAC1 mediates LPS-induced superoxide from microglia: the role of phagocytosis receptors in dopaminergic neurotoxicity, Glia, (2007).

[287] Dobbertin,A., Rhodes,K.E., Garwood,J., Properzi,F., Heck,N., Rogers,J.H., Fawcett,J.W., Faissner,A., Regulation of RPTP beta/phosphacan expression and glycosaminoglycan epitopes in injured brain and cytokine-treated glia, Molecular and Cellular Neuroscience, 24 (2003) 951-971.

[288] Ravenscroft,M.S., Bateman,K.E., Shaffer,K.M., Schessler,H.M., Jung,D.R., Schneider,T.W., Montgomery,C.B., Custer,T.L., Schaffner,A.E., Liu,Q.Y., Li,Y.X., Barker,J.L., Hickman,J.J., Developmental neurobiology implications from fabrication and analysis of hippocampal neuronal networks on patterned silane-modified surfaces, J. Am. Chem. Soc., 120 (1998) 12169-12177.

[289] Takano,M., Horie,M., Narahara,M., Miyake,M., Okamoto,H., Expression of kininogen mRNAs and plasma kallikrein mRNA by cultured neurons, astrocytes and meningeal cells in the rat brain, Immunopharmacology, 45 (1999) 121-126.

[290] Potter,S.M., DeMarse,T.B., A new approach to neural cell culture for long-term studies, J. Neurosci. Methods, 110 (2001) 17-24.

[291] Mccarthy,K.D., Devellis,J., Preparation of Separate Astroglial and Oligodendroglial Cell-Cultures from Rat Cerebral Tissue, J. Cell Biol., 85 (1980) 890-902.

[292] Basu,A., Krady,J.K., Enterline,J.R., Levison,S.W., Transforming growth factor beta 1 prevents IL-1 beta-induced microglial activation, whereas TNF alpha- and IL-6-stimulated activation are not antagonized, Glia, 40 (2002) 109-120.

[293] Passaquin,A.C., Schreier,W.A., Devellis,J., Gene-Expression in Astrocytes Is Affected by Subculture, Int. J. Dev. Neurosci., 12 (1994) 363-372.

[294] Wu,X.F., Chen,P.S., Dallas,S., Wilson,B., Block,M.L., Wang,C.C., Kinyamu,H., Lu,N., Gao,X., Leng,Y., Chuang,D.M., Zhang,W., Zhao,J., Hong,J.S. Histone Deacetylase (HDAC) Inhibitors are Neurotrophic and Protective on Dopaminergic neurons: Role of Histone Acetylation on BDNF and GDNF Gene Transcription in Astrocytes. 2008.
Ref Type: Unpublished Work

[295] Guenard,V., Frisch,G., Wood,P.M., Effects of axonal injury on astrocyte proliferation and morphology in vitro: Implications for astrogliosis, Exp. Neurol., 137 (1996) 175-190.

[296] Hirsch,S., Bahr,M., Immunocytochemical characterization of reactive optic nerve astrocytes and meningeal cells, Glia, 26 (1999) 36-46.

[297] Wang,T.G., Liu,B., Qin,L.Y., Wilson,B., Hong,J.S., Protective effect of the SOD/catalase mimetic MnTMPyP on inflammation-mediated dopaminergic neurodegeneration in mesencephalic neuronal-glial cultures, J. Neuroimmunol., 147 (2004) 68-72.

[298] Qin,L.Y., Li,G.R., Qian,X., Liu,Y.X., Wu,X.F., Liu,B., Hong,J.S., Block,M.L., Interactive role of the toll-like receptor 4 and reactive oxygen species in LPS-induced microglia activation, Glia, 52 (2005) 78-84.

[299] Mcmillian,M.K., Pennypacker,K.R., Thai,L., Wu,G.C., Suh,H.H., Simmons,K.L., Hudson,P.M., Sawin,S.B.M., Hong,J.S., Dexamethasone and forskolin synergistically increase [Met(5)]enkephalin accumulation in mixed brain cell cultures, Brain Res., 730 (1996) 67-74.

[300] Kim,W.G., Mohney,R.P., Wilson,B., Jeohn,G.H., Liu,B., Hong,J.S., Regional difference in susceptibility to lipopolysaccharide-induced neurotoxicity in the rat brain: Role of microglia, J. Neurosci., 20 (2000) 6309-6316.

[301] Koeneman,B.A., Lee,K.K., Singh,A., He,J.P., Raupp,G.B., Panitch,A., Capco,D.G., An ex vivo method for evaluating the biocompatibility of neural electrodes in rat brain slice cultures, J. Neurosci. Methods, 137 (2004) 257-263.

[302] Noraberg,J., Poulsen FR, Blaabjerg M, Kristensen,B.W., Bonde C, Montero M, Meyer M, Gramsbergen JB, Zimmer,J., Organotypic hippocampal slice cultures for studies of brain damage, neuroprotection and neurorepair., Current Drug Therapies-CNS & Neurological Disorders, 4 (2005) 435-452.

[303] Bjornsson,C.S., Oh,S.J., Al Kofahi,Y.A., Lim,Y.J., Smith,K.L., Turner,J.N., De,S., Roysam,B., Shain,W., Kim,S.J., Effects of insertion conditions on tissue strain and vascular damage during neuroprosthetic device insertion, Journal of Neural Engineering, 3 (2006) 196-207.

# Biography

## Vadim Steven Polikov

**Education**

**Ph.D., Biomedical Engineering, June 2009**

**Duke University**, Durham, NC. GPA: A Avg.
Center for Biomolecular and Tissue Engineering Certificate

**B.S.E., Biomedical Engineering, May 2003**
**Duke University**, Durham, NC.GPA: 4.0/4.0, 1st in Graduating Class

**Publications**

**Polikov,V.S.**, Hong,J.S., Reichert,W.M., bFGF, Serum, and Inflammatory Cytokines Increase Glial Scarring In Vitro. *(manuscript in preparation).*

**Polikov,V.S.**, Su,E.C., Ball,M.A., Hong,J.S., Reichert,W.M., Control protocol for robust in vitro glial scar formation around microwires: Essential roles of bFGF and serum in gliosis, *Journal of Neuroscience. Methods*, (accepted) (2009).

**Polikov,V.S.,** Block,M.L., Zhang,C., Reichert,W.M., Hong,J.S., In Vitro Models for Neuroelectrodes: A Paradigm for Studying Tissue-materials Interactions in the Brain. In Reichert,WM (Ed.), *Indwelling Neural Implants: Strategies for Contending with the In Vivo Environment* CRC Press, Boca Raton, FL, 2008, pp. 89-115.

**Polikov, V.S.,** Block, M.L., Fellous, J.M., Hong, J.S., Reichert, W.M. (2006) "In vitro model of glial scarring around neuroelectrodes chronically implanted in the CNS." *Biomaterials* 27 (31): 5368-5376

**Polikov VS,** Tresco PA, Reichert WM. (2005) **"**Response of brain tissue to chronically implanted neural electrodes" *Journal of Neuroscience Methods* 148 (1): 1-18

**Honors**

NSF Graduate Student Fellowship, Phi Beta Kappa, Tau Beta Pi Award, Leonardo da Vinci Award, Tau Beta Pi Chapter President, National Merit Scholar, 2nd Place Winner Duke Startup Challenge

**Affiliations**

Duke University, Center for Biomolecular and Tissue Engineering
Biomedical Engineering Society (BMES) – Student Member